

Attachment A

Analysis of Spectrum Sharing Between MSS and Terrestrial Wireless Services

**Dr. Jay Padgett, Senior Research Scientist
Telcordia Technologies
(May 10, 2002)**

Analysis of Spectrum Sharing Between MSS and Terrestrial Wireless Services

*Dr. Jay Padgett
Senior Research Scientist
Telcordia Technologies
May 10, 2002*

Executive Summary

The purpose of this paper is to provide a technical analysis of the prospects for sharing spectrum between Mobile Satellite Services (MSS) and an “ancillary terrestrial component” (ATC), which is nominally intended to provide coverage enhancement for MSS subscribers in areas that are not visible to the MSS spacecraft (SC), such as inside buildings and in urban “canyons” with heavy shadowing. Four interference cases are analyzed in detail: (1) ATC terminal to MSS uplink; (2) MSS terminal to ATC uplink; (3) ATC base to MSS downlink; and (4) MSS SC to ATC downlink. Of these, the first is the most serious obstacle to sharing. The other three are confined to areas near MSS-ATC coverage boundaries and appear to be manageable using fairly straightforward engineering practices such as power-balancing between MSS and ATC.

The problem with interference from ATC terminals to MSS uplinks is that the total power radiated by all ATC terminals transmitting within the footprint of an MSS beam is captured by the SC receiver, so there is an interference aggregation effect. Contributions of ATC terminals that are shadowed from the SC (as might often be expected, since the purported role of ATC is to provide fill-in coverage) will be reduced, but terminals near the coverage boundaries may have paths to the SC with little excess attenuation. Further, if the role of ATC grows beyond the bounds of mere coverage fill-in, it is likely that there will be significant numbers of ATC terminals within the MSS beam with strong paths to the SC.

There is a tradeoff between the total EIRP (effective isotropic radiated power) radiated into the sky by the ATC terminals within an MSS beam footprint, and the resulting uplink capacity degradation to the MSS system. Given some limit on acceptable MSS capacity degradation, there is a corresponding limit on the aggregate ATC terminal EIRP. Calculations given here, as well as those of MSS operators, suggest that this limit corresponds to no more than several tens of outdoor terminals per beam footprint with each terminal transmitting 100 milliwatts. Various calculations can be used to translate this number into a total subscriber base by applying factors that account for excess terminal-to-SC path loss, power control, voice activity, and usage activity (fraction of the time the average subscriber is actually using the terminal). However, the end result is that the MSS uplink can tolerate only a small number of active cochannel ATC terminals with line-of-sight paths to the satellite, within a beam footprint. A beam footprint covers

a very large area (on the order of one million square kilometers). Unless the ATC system design can ensure that ATC terminals have heavily-attenuated paths to the SC, the allowable ATC terminal density is extremely low, in the cochannel sharing case.

MSS operators have proposed dynamic coordination mechanisms to prevent MSS and ATC systems from using the same frequencies within an MSS beam. Such measures will reduce the effect of the ATC uplink interference but will not eliminate it. The in-beam interference will become adjacent-channel interference rather than cochannel interference, and the cochannel interference will be limited to adjacent (non-covering) beams, and will therefore be attenuated by the beam antenna pattern rolloff. Therefore, there will still be a limit on the total ATC uplink EIRP per MSS beam, although it will be higher than the limit in the cochannel case.

Results provided by Globalstar and ICO suggest the degree to which dynamic coordination will allow the ATC uplink EIRP limit to be increased. ICO states that a 50% increase is possible, based on its simulations. Globalstar is less specific, and does not disclose the assumptions or calculations that were used, but Globalstar's stated results suggest an increase of roughly a factor of four.

It is clear from these results, provided by MSS operators, that the increase in allowable ATC terminal deployment per beam footprint afforded by dynamic coordination is extremely modest, and that there will still be a limit on the order of several watts on the total EIRP radiated by ATC terminals within a beam footprint. This represents several tens of ATC terminals with a line-of-sight path to the SC within an area of roughly a million square kilometers, which is an extremely limiting requirement.

The conclusion is clear: for any significant terrestrial deployment, the terrestrial system must operate in spectrum separate from that used by the MSS system, with guard bands and out-of-band emission requirements that are adequate to protect the MSS uplink from the ATC terminal emissions. With stand-alone terrestrial systems, the terminal density is limited only by the density of cells that are deployed. It is therefore spectrally inefficient for MSS operators to use more spectrum than is needed to support MSS-only operations, in order to be able to support "shared" terrestrial operations. A better approach would be to build terrestrial networks on dedicated spectrum. Not only would this be more efficient from a spectrum-usage perspective, it would eliminate the need for any coordination of MSS and ATC frequency usage.

Given the above, the question of whether ATC and MSS can be effectively "severed" (managed by different operators) does not seem to be the most important issue. As discussed in more detail in this paper, it appears that severing operations is quite feasible, even with dynamic frequency coordination. However, given the severe limitations imposed on terrestrial deployment densities, even with dynamic coordination, MSS/ATC spectrum sharing is technically unsound.

Contents

Introduction.....	5
Technical Overview	6
Downlink Interference	6
Uplink Interference to ATC from MSS Terminals	7
Uplink Interference to MSS from ATC Terminals	8
Dynamic Frequency Coordination.....	10
Feasibility of Different MSS/ATC Spectrum Sharing Scenarios	11
Completely Unrestricted Terrestrial Operation.....	11
Limited Co-channel ATC.....	11
Dynamic Frequency Assignment	11
Segmented Spectrum.....	12
Integrated vs. Separate Operators	12
Summary	12
Spectrum Management Considerations	13
Analysis of the CDMA Uplink	13
SINR and Jamming Margin	14
Basic Uplink Capacity Relationships.....	14
Uplink Capacity Reduction due to External Interference	17
ATC Terminal Interference to MSS Uplink	18
Average ATC Terminal Transmit Power.....	18
Total ATC Uplink Interference to the Spacecraft.....	21
MSS Uplink Capacity Degradation vs. Number of ATC Terminals within Beam Footprint.....	22
MSS Uplink Capacity Degradation vs. Number of ATC Cells or Sectors within Beam Footprint	23
MSS Uplink Capacity Degradation vs. Total ATC Terminal EIRP within Beam Footprint.....	26
MSS Terminal Interference to ATC Uplink	27
ATC Uplink Capacity Degradation vs. MSS Terminal Distance to ATC Cell	27
Average Interference to ATC Base from MSS Terminals	29
Cumulative Distribution Function of the ATC Uplink Capacity Degradation.....	32
Single-Interferer vs. Multiple Interferer Models	34
Notes on Worst-Case Assumptions	35
Analysis of the CDMA Downlink	36
Modeling the CDMA Downlink	36
Downlink Capacity	39
Overhead Channel Power Allocation.....	40
Downlink Pole Capacity	42
Modeling MSS/ATC Downlink Interference.....	46
Effect of Interference on MSS and ATC Downlink Coverage	48
ATC Cluster Outer-Cell Overhead Channel Power Allocation Requirements.....	53

Effect of Adjusting the ATC Outer Cell Pilot Power	55
FDMA/TDMA	61
Frequency Reuse and Capacity: Basic Relationships	61
Effect of Thermal Noise on Reuse	64
Cellular Examples.....	65
Frequency Reuse with MSS Systems	65
Dynamic Channel Assignment	66
MSS-ATC Interference with FDMA/TDMA	67
Dynamic Frequency Coordination Between MSS and ATC	70
Spectrum Efficiency.....	73
ATC/MSS Coexistence with CDMA: Conclusions	76
Summary of Results.....	76
Dynamic Coordination with Separate MSS and ATC Operators	77
Annex A: The Distribution of Combined Interference from Multiple Randomly- Distributed Transmitters	80
The Model.....	80
The Characteristic Function of the Aggregate Interference.....	80
The PDF and CDF of the Aggregate Interference	82
Closed-Form Expressions for Fourth-Power Propagation.....	83
The Single-Interferer Case	85
Annex B: Computation of Downlink Other-Cell Interference for a Terrestrial Cell Cluster	87
References	90

Introduction

In a *Public Notice* released March 6, 2002 (“*Notice*”) [1], the Federal Communications Commission (FCC) raised a number of questions relating to the potential for spectrum-sharing, from a technical viewpoint, between mobile satellite services (MSS) and terrestrial wireless services. The *Notice* is the most recent step in a proceeding (IB Docket 01-185) in which MSS operators have requested that the FCC allow them to provide an “ancillary terrestrial component” (ATC) to provide coverage in areas that do not have a clear signal path to the satellite (e.g., inside office buildings, in urban “canyons” between tall buildings). It has been argued by some MSS operators that MSS and ATC cannot effectively be managed by separate operators; rather, they must be integrated and both must be owned and managed by the MSS operator.

The questions in the *Notice* pertain to the technical feasibility of “severing” ATC and MSS operations; that is, having ATC and MSS infrastructures owned and managed by separate operators. Obviously, severance can be achieved by dividing the MSS bands into separate MSS and ATC sub-bands, but the questions raised in the *Notice* are directed toward the feasibility of allowing severed terrestrial and MSS operations in the same band, the viability of which is not obvious. The purpose of this paper is to develop a detailed technical analysis that can be used to help answer the questions in the *Notice*, and to address the issue of MSS/ATC sharing in general.

The fundamental technical issue is interference. “Forward” band sharing is assumed here; that is, the MSS spacecraft and the ATC base stations transmit in the downlink band, and the MSS and ATC terminals transmit in the uplink band.¹ This leads to four interference cases that must be considered: (1) ATC terminals to spacecraft; (2) MSS terminals to ATC base; (3) ATC bases to MSS terminal; and (4) spacecraft to ATC terminal. Mathematical models are developed to quantify the interference impact for these four cases. The air interface used for the initial analysis is code-division multiple access (CDMA). Much of the modeling is equally applicable to MSS/ATC sharing using frequency-division multiple access and time-division multiple access (FDMA/TDMA), which is discussed following the CDMA analysis.

The approach taken is to initially assume that MSS and ATC CDMA systems operate co-channel. That is, an MSS beam and an ATC cell cluster within the beam footprint use the same frequency. The analysis is used to determine the limitations of such sharing, by quantifying the capacity and coverage impact of each system on the other. The benefits of dynamic coordination between the MSS and ATC networks are then assessed, using results provided by Globalstar [2] and ICO [3].

¹ This is the logical arrangement from an equipment design perspective, simplifying the architecture of terminals that can access both the MSS and ATC systems.

Technical Overview

This overview provides a high-level qualitative summary of ATC-MSS interference effects and to their impact on the potential for ATC/MSS spectrum sharing. The mathematical models to follow give a detailed quantitative account.

Figure 1 shows an idealized illustration of the MSS/ATC sharing scenario, in which a cluster of terrestrial cells lies within the footprint of the MSS beam. In reality, the beam edges are not sharply defined as suggested by Figure 1, and there may be overlapping beams. However, the idealization shown is adequate for the initial discussion.

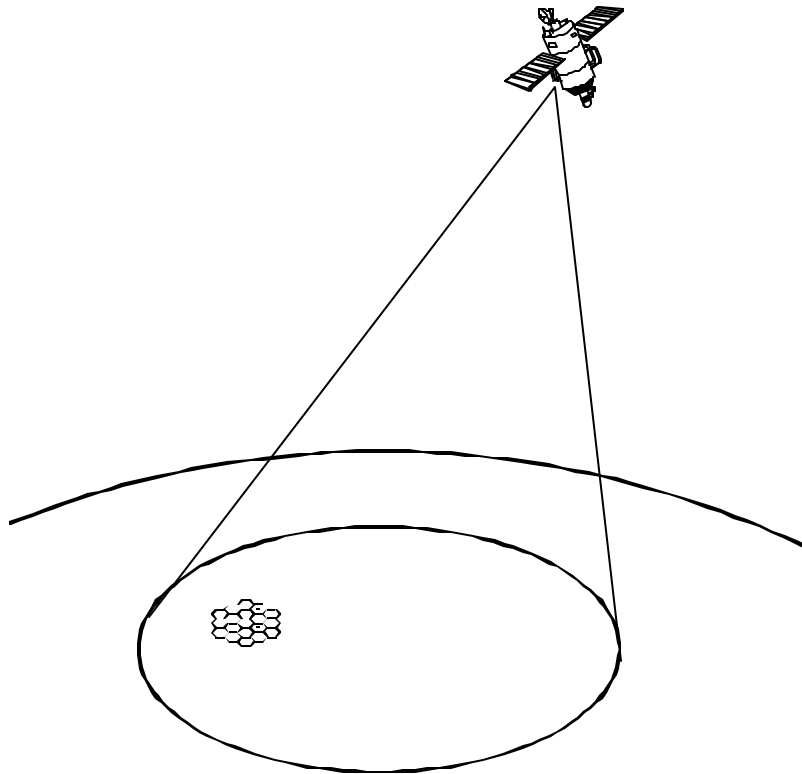


Figure 1: *MSS/ATC spectrum sharing concept*

In questions of spectrum sharing among different services, the main concern is often interference and its effect on measures such as performance and capacity. With MSS/ATC sharing, there are four interference cases of interest; MSS to ATC and ATC to MSS, on both uplink and downlink.

Downlink Interference

A terminal on the surface of the Earth will receive signal power from both the spacecraft and the ATC base stations. For illustrative purposes, the MSS downlink power can be assumed relatively constant over the area surrounding an ATC cell cluster (neglecting

blockage to the SC), while the ATC downlink power will be highly dependent on the distance between the terminal and the ATC base station, as illustrated in Figure 2 (a single ATC cell has been assumed here for simplicity). Near the ATC base, the ATC downlink power overwhelms that from the SC, and a terminal will be unable to maintain a link with the SC on a channel used by the ATC base. If the terminal is sufficiently far away from the ATC base, the ATC downlink power is negligible and the MSS downlink is essentially unaffected by the ATC downlink. There is a transition region where the ATC and MSS downlink power levels are nearly equal, and each represents a significant interference level to the other; i.e., a low carrier-to-interference ratio (CIR) for both. However, as is discussed in the detailed analysis, this transition region can be managed for both the CDMA and FDMA/TDMA cases, although in different ways.

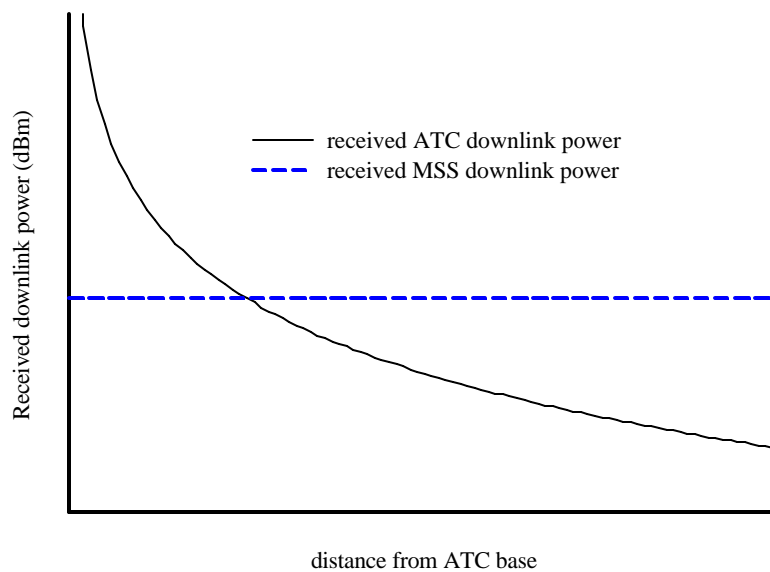


Figure 2: *Received downlink power vs. distance of terminal from ATC base*

Uplink Interference to ATC from MSS Terminals

The two uplink interference cases (MSS to ATC and the reverse) need to be considered separately. In the former case, the uplink interference received by the ATC base station from an MSS terminal will depend on the distance between the MSS terminal and the ATC base, and will follow a curve similar to that shown in Figure 2 for the ATC downlink power. The proximity of an MSS terminal to the ATC base is limited by the relationship between the MSS and ATC downlinks; as the MSS terminal moves toward the ATC base, there will come a point at which either (1) the link to the SC will be lost due to ATC downlink interference, or (2) the terminal switches to ATC mode. In either case, the proximity of an MSS terminal to the ATC base will be limited to approximately the ATC coverage boundary, assuming cochannel operation.

The MSS terminal typically will be transmitting at higher power than an ATC terminal due to the high path loss to the SC. If an MSS terminal is near the ATC coverage boundary, it can cause significant uplink interference to the ATC base station. The effect of this interference depends on the air interface used by the ATC system. With CDMA, the interference from the MSS terminal will cause a significant capacity reduction to the ATC uplink on the CDMA frequency band affected by the interference. With TDMA, the frequency/timeslot channels impacted by the MSS terminal interference will become unusable by the ATC base station, except for ATC terminals that are very near the ATC base station. Again, the lost channel translates into lost capacity for the ATC system.

The spatial density of MSS terminals (active terminals per square km) tends to be extremely low by terrestrial standards, because the coverage area of MSS beams is large, and there is a limit on the number of MSS terminals per beam that can be supported. As an example, assume that the MSS beam has a nominal coverage pattern that is circular with a diameter of 800 km and a capacity of 50 actively-transmitting terminals. The beam area is about $500,000 \text{ km}^2$ and the MSS terminal density is 0.0001 terminals per km^2 . A terrestrial cell with a 4-km radius has a nominal coverage area of 50 km^2 , so on average, there is an active MSS terminal for every 200 such ATC cells. If MSS terminals are randomly-distributed over area, the probability that an MSS terminal is within one ATC cell radius of the edge of a given ATC cell is very low; in this example, less than 2%. Therefore: (1) MSS-to-ATC uplink interference is an infrequent event; and (2) when it does occur, the effect on the ATC is noticeable but not debilitating. Only if MSS-linked terminals are systematically clustered near ATC coverage boundaries does MSS-to-ATC uplink interference become a significant issue.

Uplink Interference to MSS from ATC Terminals

The net result of the above is that the effects of downlink interference in both directions (MSS to ATC and ATC to MSS), as well as MSS uplink interference to ATC, tend to be confined to areas near the ATC-MSS coverage boundaries.

ATC to MSS uplink interference is another matter. The problem is that the receiver on the SC associated with a particular beam will “see” any cochannel transmissions that are captured by the beam antenna pattern. The ATC uplink interference is therefore the sum of the power levels received from all in-beam, cochannel ATC terminals. The result is an effective rise in the noise floor of the MSS SC receiver in the affected frequency bands. If the MSS uses CDMA, this translates into an MSS uplink capacity reduction. With FDMA/TDMA, any given channel becomes unusable if the interference is high enough to cause the CIR to drop below its minimum (threshold) level, and again, the end result is a capacity reduction.

The interference power received by the SC from an individual ATC terminal will depend on the transmit power of the ATC terminal, the path loss to the SC, the SC uplink antenna gain, and any excess blockage or attenuation between the ATC terminal and the SC. ATC terminal transmit power may vary due to power control (tight uplink power control is used in CDMA systems), and excess blockage will depend on the ATC terminal

location. The free-space path loss to the SC and the SC uplink antenna gain will be relatively constant for a given SC and ATC deployment location.

It is useful to represent the effect of ATC uplink interference in terms of the total (aggregate) effective isotropic radiated power (EIRP) from the ATC terminals within an MSS beam footprint. The EIRP accounts for the actual ATC terminal transmit power and antenna gain in the direction of the SC as well as excess attenuation due to blockage. As an example, Figure 3 shows the uplink capacity for a CDMA MSS system vs. the aggregate ATC EIRP within the CDMA band. As can be seen, an EIRP of only 0 dBW (1 watt) reduces the MSS uplink capacity by more than 10%.

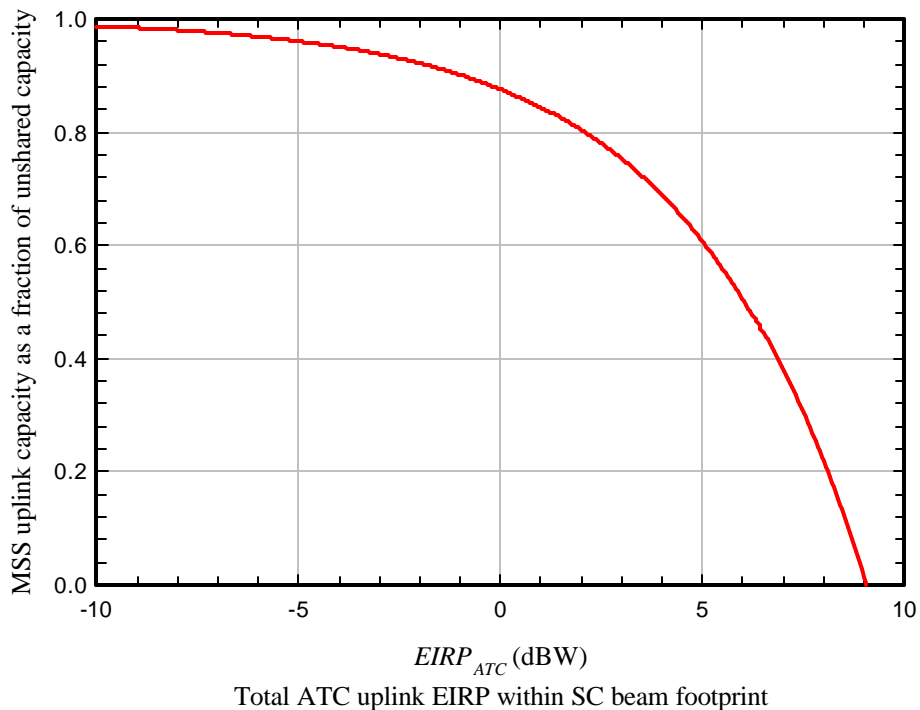


Figure 3: MSS uplink capacity (CDMA) vs. aggregate ATC terminal EIRP

To carry the example further, an EIRP of 1 watt corresponds to 10 ATC terminals, each transmitting 100 mW and with a line-of-sight, unobstructed path to the SC. Given the large area covered by the SC beam, this is a very severe effect. In rough terms, each unobstructed ATC terminal transmitting at full power (assumed 100 mW) reduces the MSS CDMA uplink capacity by about 1.25%.² Thus, the maximum tolerable MSS capacity degradation places a limit on the allowable ATC terminal density. A similar tradeoff applies for MSS systems using FDMA/TDMA. Calculation of the exact limit on the number of ATC terminals within an MSS beam will depend on assumptions about blockage and power control, as shown in the detailed analyses.

² Therefore, 80 ATC terminals transmitting 100 mW outdoors with unobstructed paths to the satellite would completely shut down the MSS uplink of the affected beam.

It should be noted that the ATC uplink interference effect is *not* confined to areas near the ATC-MSS coverage boundaries; it will reduce the MSS uplink capacity available to MSS terminals served by the affected beam whether or not they are near an ATC deployment. It appears that this interference could only be controlled by ensuring that the paths from all ATC terminals to all SC are heavily blocked. Since the ability of a terminal to link to an ATC cell depends on the downlink coverage of the ATC base station, this requirement would mean confining the ATC downlink signal to areas blocked to the SC. On the surface, this degree of control over radio signal coverage seems impractical.

Dynamic Frequency Coordination

MSS operators have suggested that mutual interference between ATC and MSS can be mitigated using “dynamic frequency coordination,” whereby real-time control signaling between the MSS and ATC networks would be used to manage the interference by preventing a terrestrial system within a beam footprint from operating on frequencies being used by that beam. Frequency usage would be assigned dynamically by a control process based on the current load requirements of the MSS beam and ATC cells within the beam footprint.

The effect of such an approach would be to prevent cochannel “in-beam” interference. This would reduce the interference problem but not eliminate it, for two reasons. First, the beam antenna patterns do not have sharp boundaries as might be inferred from idealized diagrams such as Figure 1. The SC uplink antenna will still capture power that is “outside” the nominal beam footprint, although the received power will be reduced according to the rolloff of the beam antenna pattern,³ and ATC terminals farther away from the nominal beam coverage edge will contribute less interference than those nearby. However, adjacent-beam cochannel ATC terminals will still cause interference to the MSS uplink.

Second, although the ATC terminals operating within the nominal beam footprint are no longer cochannel, they may still cause adjacent-channel interference to the MSS uplink, the degree of which will depend on the isolation between adjacent frequency channels. It is likely that adjacent-channel interference is less significant than adjacent-beam interference.⁴

³ This is the reason that an FDMA/TDMA system such as that used by ICO must divide the available frequencies into groups (four in the case of ICO), and assign the frequency groups to beams in a reuse pattern, similar to the way in which terrestrial FDMA/TDMA system employ frequency reuse patterns. This ensures that adjacent beams do not use the same frequencies, to avoid adjacent-beam cochannel interference. CDMA systems such as Globalstar’s can use the same frequency in each beam as can CDMA terrestrial systems, because CDMA can operate with very low carrier-to-interference ratios. In fact, CDMA systems, both terrestrial and MSS, are designed to exploit cochannel cell or beam overlap to provide diversity, which is implemented in the RAKE receiver by combining power from multiple signal paths.

⁴ Adjacent-channel isolation depends on the spectral rolloff of the transmitted signal (i.e., the power spectral density mask), and the adjacent-channel rejection of the intermediate frequency (IF) filtering in the receiver.

A detailed quantitative analysis of ATC uplink interference due to these two factors requires knowledge of the SC antenna patterns and MSS adjacent-channel isolation requirements. Both Globalstar and ICO, who have detailed knowledge of these parameters for their respective systems, have provided results that indicate the degree to which the tolerable ATC interference could be increased using dynamic frequency coordination. ICO states that the ATC terminal density could be increased by 50% compared to the uncoordinated (cochannel, in-beam) cases [3]. Globalstar's results suggest that the ATC terminal density could be increased by roughly a factor of four using dynamic frequency coordination [2]. These results are discussed more fully below. However, for purposes of this overview, the main point is that both the ICO and Globalstar results show that even in the best case, with an integrated ATC/MSS network under control of a single operator and using dynamic frequency coordination, there is still an extremely low threshold on the density of active ATC terminals that can be tolerated within an SC beam footprint.

Feasibility of Different MSS/ATC Spectrum Sharing Scenarios

There are several different possible sharing scenarios. To minimize confusion over terminology, each scenario is described here and a feasibility assessment is provided, based on the technical results summarized above.

Completely Unrestricted Terrestrial Operation

One possibility would be to permit terrestrial systems within the MSS spectrum with no coordination of interference with MSS systems. This does not seem to be workable as a practical matter. The simultaneous operation of a relatively small number of ATC mobile terminals within a spot beam would consume all MSS uplink capacity, rendering the satellite incapable of providing any service with that beam. This arrangement would effectively result in the *de facto* reallocation of the spectrum from MSS to terrestrial mobile services within that beam.

Limited Co-channel ATC

A second possibility is to limit ATC networks so that they do not degrade SC capacity and the ability of the MSS operator to provide MSS services on demand. This would enable the provision of services in areas where MSS is not available today, such as indoors and in urban canyons. ATC uplink interference to MSS is still a concern, and the ATC network would necessarily be very limited in terms of the total allowable EIRP. This would effectively translate into a limit on ATC terminal density (and a very low limit).

Dynamic Frequency Assignment

To reduce the effect of ATC terminal uplink interference, the frequency assignments of the SC beams and ATC networks would be managed such that no beam uses the same frequencies as an ATC system within the beam footprint. As shown by the calculations of ICO [3] and Globalstar [2], this reduces the ATC uplink interference problem slightly. However, even with this approach, only a very limited terrestrial terminal density could be tolerated by the MSS system. Moreover, there are some low-level technical feasibility questions associated with dynamic frequency assignment. In the case of an

FDMA/TDMA MSS system, entire ATC cell clusters may be forced to change frequencies fairly often in response to the movement of spot beam coverage across the surface of the earth. With a CDMA ATC system (as assumed by both ICO and Globalstar in their analyses), this may disrupt communications, since CDMA air interfaces are not designed for routine system-wide frequency switching. A change in frequency would require re-acquisition of the pilot and other overhead channels by every terminal, and re-establishment of power control parameters. These processes could require several seconds. It therefore seems questionable at this point whether ATC service quality could be preserved, if the ATC networks were to be routinely required to change frequencies at the behest of the MSS network.

Segmented Spectrum

If the MSS and terrestrial operations operate in separate spectrum, then the terrestrial terminal density is no longer limited, there is no need for any dynamic frequency management, and the terrestrial network will not degrade the coverage of the MSS network. As is demonstrated quantitatively below, segmentation is also more spectrum-efficient. It should be noted that from an engineering viewpoint, the optimum dynamic frequency management algorithm would be one that effectively segments the terrestrial and MSS spectrum.

Integrated vs. Separate Operators

There does not seem to be any compelling technical argument for either separate operators or an integrated MSS/ATC operator. In either case, separating terrestrial spectrum from MSS spectrum is by far the best solution. However, either cochannel sharing or dynamic frequency assignment could be implemented with either integrated or separate operators. The basic limitations on sharing would be the same, and the questions about the physical-layer impact of abruptly changing the operating frequency of an entire CDMA ATC network remain the same, although the signaling and information exchange necessary to do so are the same for separate operators as for an integrated operators. Functionally, there seems to be no difference.

Summary

It is clear that even with the ideal dynamic frequency assignment cases envisioned by the MSS operators, terrestrial capacity will be extremely limited, if degradation to the MSS uplink is to be avoided. Further, there are unanswered physical-layer feasibility questions about the use of dynamic frequency assignment with CDMA ATC systems. These conclusions apply equally whether there are separate MSS and ATC operators, or a single integrated operator.

Overall, the technical conclusion is clear: if the intent is to provide any significant volume of terrestrial service, terrestrial systems should operate in spectrum separate from that used by MSS systems, regardless of whether they are operated by different entities or a single entity. Terrestrial systems which are truly sharing spectrum with MSS systems

are inherently subject to a very restrictive limit on total terminal density. Such a limit does not exist for stand-alone terrestrial systems. This leads to the conclusion that MSS operators with excess spectrum, once allowed to use that spectrum for terrestrial networks, will tend to manage the frequencies in a way that keeps MSS and terrestrial spectrum separated. It would be very straightforward to design a “dynamic frequency assignment” protocol that effectively segments the spectrum, and that would in fact be the optimum engineering solution and would result in the most efficient spectrum use.

Spectrum Management Considerations

It is worthwhile to consider the implications of these technical results with respect to spectrum management. From a spectrum management perspective, the notion of exploiting “unused” capacity in the MSS spectrum to support complementary terrestrial coverage is undeniably attractive, and suggests that the overall efficiency with which spectrum is used can be increased. In fact, trading off MSS capacity for terrestrial capacity seems efficient in terms of such measures as total (MSS plus ATC) Erlangs/km² or kbps/km², simply because terrestrial systems use spectrum more efficiently than satellite systems due to their much smaller cells. However, this is not the case. As shown below, spectrum efficiency is actually increased by segmenting the spectrum.

If the spectrum currently allocated to MSS is just adequate to meet projected MSS capacity needs, then the operation of any significant terrestrial infrastructure within that spectrum will lead to an MSS capacity shortfall in the future, even though there may be excess MSS spectrum at present. In that case, ATC should not be operated within the MSS spectrum. On the other hand, if the MSS spectrum exceeds the projected steady-state future requirement, then it would be logical to dedicate the spectrum not needed by MSS to other services, which could include ATC. Again, sharing MSS spectrum with terrestrial operations is not the best course of action.

Realistically, the future capacity requirements of MSS are unknown. In the face of an unknown future MSS spectrum requirement, it seems hard to justify deploying ATC systems in the MSS spectrum. In that case, either the future available MSS capacity will be reduced, or the ATC systems will need to be relocated as MSS demand grows. Neither seems to be a desirable result.

Analysis of the CDMA Uplink

To understand the effect of ATC terminal interference on the MSS uplink, and the effect of MSS terminal interference on the ATC uplink, a CDMA uplink capacity model is needed. This subsection develops that model. In the context of this model, the term “receiver” can represent either the receiver at the ATC base station or that at the spacecraft (SC). A “cell” is the coverage area of a single receiver. In the terrestrial case, this may be an actual cell or a cell sector. In the MSS case, it is the footprint of a satellite beam.

SINR and Jamming Margin

If E_b is the received energy per bit on a particular uplink channel, and N_0 and I_0 are the power spectral density (watts/Hz) of the thermal noise and total interference, respectively, then the signal to interference plus noise ratio (SINR) is $E_b/(N_0 + I_0)$, which must meet or exceed some threshold Γ for the channel to meet its frame error rate (FER) objective. That is,

$$\frac{E_b}{N_0 + I_0} \geq \Gamma, \quad (1)$$

where the threshold Γ in general depends on a number of factors, including the multipath delay spread (which determines the RAKE diversity combining gain), interleaving depth, fade rate, type of channel coding, target FER, and the accuracy of the closed-loop (fast) power control.

If the channel intermediate-frequency (IF) channel bandwidth is W Hz and the data rate is R bps, the “spreading gain” or “processing gain” is W/R . Letting C represent the received carrier (desired signal) power, and N and I represent the noise and interference power, respectively, at the receiver, the relationships $E_b = C/R$, $N = WN_0$, and $I = WI_0$ lead to the identity:

$$\frac{E_b}{N_0 + I_0} = \frac{W}{R} \frac{C}{N + I}. \quad (2)$$

Defining the “jamming margin” as

$$M = \frac{W/R}{\Gamma} \quad (3)$$

and combining (1) and (2) gives:

$$\frac{C}{N + I} \geq \frac{1}{M}. \quad (4)$$

Basic Uplink Capacity Relationships

There are assumed to be J terminals in the cell transmitting on the uplink. The desired signal power received from the j^{th} terminal is denoted C_j . The total power received from these J terminals is

$$I_{in} = \sum_{j=1}^J C_j \quad (5)$$

In addition, the receiver sees interference power from other cells of the same system, denoted I_{oc} as well as its own thermal noise power N . In the case of MSS/ATC sharing, each uplink receiver also sees interference power from the other system, denoted I_{os} . The total noise plus interference at the receiver therefore is

$$I_{TOT} = N + I_{in} + I_{oc} + I_{os} \quad (6)$$

The interference plus noise seen by the receiver component associated with the j^{th} terminal is $I_{TOT} - C_j$. Therefore, from (4),

$$\frac{C_j}{I_{TOT} - C_j} \geq \frac{1}{M_j} \quad (7)$$

where $M_j = \frac{W/R_j}{\Gamma_j}$ is the jamming margin for the j^{th} terminal, and R_j and Γ_j are the associated data rate and minimum SINR, respectively. Rearranging (7) gives:

$$C_j = \frac{I_{TOT}}{M_j + 1} \quad (8)$$

Hence,

$$I_{in} = \sum_j C_j = I_{TOT} \sum_j \frac{1}{M_j + 1} \quad (9)$$

To simplify notation in the analysis that follows, it is useful to define

$$\begin{aligned} \Lambda_j &= \frac{1}{M_j + 1} \\ \Lambda &\equiv \sum_j \Lambda_j \end{aligned} \quad (10)$$

so

$$I_{in} = \Lambda I_{TOT} \quad (11)$$

The parameter Λ is a good measure of the total load carried by the uplink. To see this, assume that $M_j \gg 1, \forall j$ (true for low-rate services such as speech; for IS-95 rate set 1, the spreading gain is 21 dB and the required SINR is about 7 dB, giving a jamming margin on the order of 14 dB, or a factor of 25), in which case

$$\Lambda \cong \sum_j \frac{1}{M_j} = \frac{1}{W} \sum_j R_j \Gamma_j \quad (12)$$

If $\Gamma_j = \Gamma, \forall j$, then

$$\Lambda \cong \frac{\Gamma}{W} \sum_j R_j = \frac{\Gamma}{W} R_{TOT} \quad (13)$$

where $R_{TOT} = \sum_j R_j$ is the total uplink throughput for the cell. Therefore, Λ will be referred to as the “load” carried by the cell uplink. The larger Λ is, the greater the total throughput, given the bandwidth W and the SINR thresholds $\{\Gamma_j\}$ (which in general are not equal). Maximizing Λ corresponds to maximizing uplink cell capacity.

In a uniformly-loaded system, the other-cell interference is proportional to the in-cell interference; that is $I_{oc} = \mathbf{m} I_{in}$. For terrestrial systems, \mathbf{m} is typically on the order of 0.4 to 0.6, depending on propagation. Using this relationship, along with (6) and (11) results in:

$$\frac{I_{TOT}}{N} = 1 + \Lambda \frac{I_{TOT}}{N} (1 + \mathbf{m}) + \frac{I_{os}}{N} \quad (14)$$

or

$$\frac{I_{TOT}}{N} = \frac{1}{1 - \Lambda(1 + \mathbf{m})} \left(1 + \frac{I_{os}}{N} \right) \quad (15)$$

For a terrestrial cellular or PCS system with an exclusive allocation, $I_{os} = 0$, and (15) leads to the well-known CDMA load curve, shown in Figure 4.

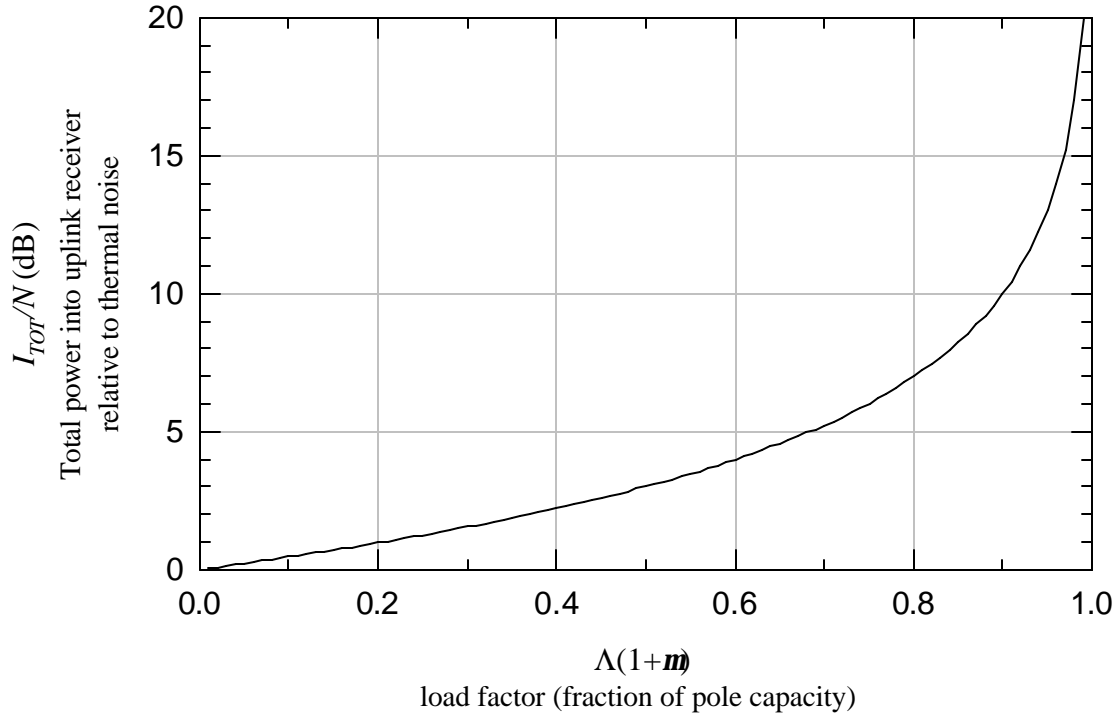


Figure 4: *CDMA uplink load curve*

The “pole capacity” corresponds to $\Lambda(1 + \mathbf{m})=1$, at which point I_{TOT}/N is unbounded. CDMA systems impose an upper bound on I_{TOT}/N to limit the required dynamic range on the uplink receiver as well as the required terminal transmit power. A reasonable limit would be on the order of 6 dB, corresponding to $\Lambda(1 + \mathbf{m})=0.75$. This limit is enforced by the admission control mechanism, and determines the maximum capacity of the uplink.

Uplink Capacity Reduction due to External Interference

The addition of the other-system interference I_{os} clearly reduces the available uplink capacity. To quantify the capacity reduction, assume that $\Phi = (I_{TOT}/N)_{\max}$ is the system-specified upper limit. Without the other-system interference, the uplink capacity is

$$\Lambda_0 = \frac{1}{1 + \mathbf{m}} \left(1 - \frac{1}{\Phi} \right). \quad (16)$$

Adding the other-system interference reduces the capacity to

$$\Lambda = \frac{1}{1+m} \left[1 - \frac{1}{\Phi} \left(1 + \frac{I_{os}}{N} \right) \right], \quad (17)$$

and the capacity reduction is

$$\Delta\Lambda = \Lambda_0 - \Lambda = \frac{1}{1+m} \frac{1}{\Phi} \frac{I_{os}}{N}. \quad (18)$$

As a fraction of the stand-alone capacity, the reduction is

$$\frac{\Delta\Lambda}{\Lambda_0} = \frac{I_{os}/N}{\Phi - 1}. \quad (19)$$

These relationships can be used to calculate the uplink interference impact of MSS/ATC sharing to both systems.

The interference threshold used in Globalstar's calculations is $\Delta T/T = 0.06$ [2]. This corresponds to $I_{os}/N = 0.06$, which for $\Phi = 4$, gives a 2% uplink capacity reduction.

ATC Terminal Interference to MSS Uplink

Average ATC Terminal Transmit Power

Let $P_{ATC \max}$ represent the maximum transmit power of an ATC terminal. As is well-known, CDMA systems use tight closed-loop control of the terminal transmit power so that the power received at the base station from a given terminal is just high enough to maintain the required FER for that terminal. The actual power transmitted by each ATC terminal therefore will depend on the path loss to its base station, its uplink data rate, and a number of other factors. For purposes of this analysis, the average ATC terminal transmit power will be calculated using the following simple model.

Assume the ATC cell is hexagonal with radius r_{ATC} . Terminals at the cell edge transmit the maximum power $P_{ATC \max}$. The path loss between the base station and a terminal separated by a distance d is assumed to be $k \cdot d^g$, where k is a constant that depends on frequency, base station antenna elevation, the propagation environment, and the gains of the terminal and base station antennas. The path loss exponent g is typically between 3 and 4 for terrestrial mobile/portable environments, and depends mildly on the elevation of the base station antenna (g decreases as antenna elevation increases).

For the received uplink power to remain constant for different values of d , the transmit power must vary with the path loss. Hence,

$$\frac{P_{ATC}(d)}{P_{ATC \max}} = \frac{L(d)}{L_{\max}} = \left(\frac{d}{r_{ATC}} \right)^{\beta}, \quad (20)$$

where $L(d)$ is the path loss at distance d and $L_{\max} = L(r_{ATC})$. The average transmit power therefore is $\overline{P_{ATC}} = P_{ATC \max} \cdot \overline{L}/L_{\max} = \left\langle (d/r_{ATC})^{\beta} \right\rangle$.

The distance d must be modeled as a random variable. If ATC terminals are uniformly-distributed over a hexagonal cell, the probability density function (PDF) of d/r_{ATC} is:

$$f_{d/r_{ATC}}(\mathbf{x}) = \begin{cases} \frac{4\mathbf{p}\mathbf{x}}{3\sqrt{3}} & \mathbf{x} \leq \frac{\sqrt{3}}{2} \\ \frac{8\mathbf{x}}{\sqrt{3}} \left(\frac{\mathbf{p}}{6} - \cos^{-1} \frac{\sqrt{3}}{2\mathbf{x}} \right) & \frac{\sqrt{3}}{2} \leq \mathbf{x} \leq 1 \end{cases} \quad (21)$$

Figure 5 shows $f_{d/r_{ATC}}(\mathbf{x})$.

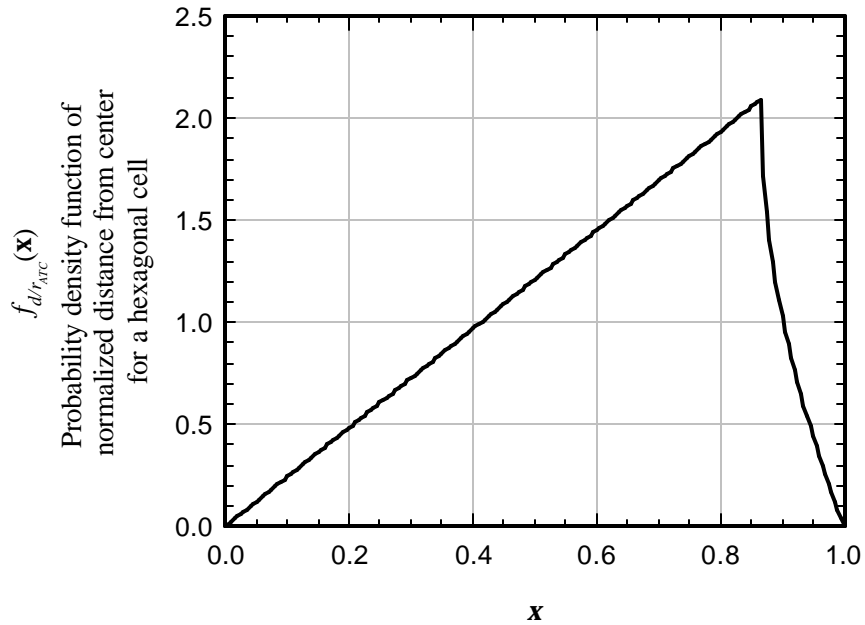


Figure 5: PDF of normalized distance from center for terminals uniformly-distributed over a hexagonal cell

The average ATC terminal transmit power therefore is

$$\left\langle \frac{L}{L_{\max}} \right\rangle = \int_0^1 \mathbf{x}^g f_{d/r_{ATC}}(\mathbf{x}) d\mathbf{x}. \quad (22)$$

For a circular area (instead of a hexagon), $f_{d/r_{ATC}}(\mathbf{x}) = 2\mathbf{x}$, $0 \leq \mathbf{x} \leq 1$, and $\langle L/L_{\max} \rangle = 2/(\mathbf{g} + 2)$. For a hexagon, $\langle L/L_{\max} \rangle$ is easily found numerically and can be closely approximated by

$$\left\langle \frac{L}{L_{\max}} \right\rangle \cong \frac{2}{\mathbf{g} + 2} \left(\frac{1.5\sqrt{3}}{\mathbf{p}} \right)^{\mathbf{g}/2} \quad (23)$$

This approximation relates to the fact that for a circle and a hexagon with the same radius, the area of the hexagon is $1.5\sqrt{3}/\mathbf{p} \cong 2.6/\mathbf{p}$ times the area of the circle.

Figure 6 shows $\langle L/L_{\max} \rangle$ vs. \mathbf{g} for circular and hexagonal cells, and the approximation of (23) for hexagonal cells.

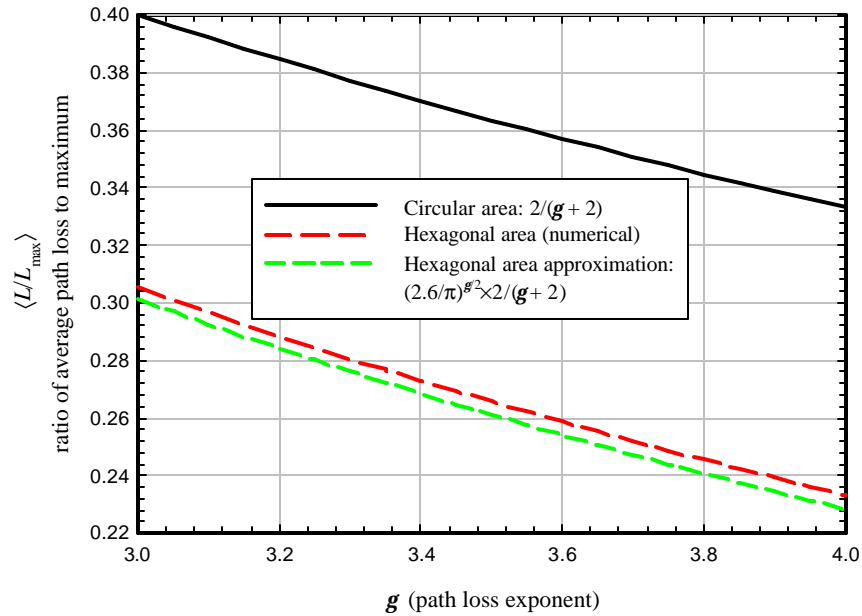


Figure 6: Average path loss relative to maximum for hexagonal and circular cells

Assuming $\mathbf{g} = 3.5$, $\overline{P_{ATC}} \cong 0.26 P_{ATC \max}$; that is, the average ATC terminal transmit power is about 6 dB below the maximum. This must be taken into account when calculating the interference, because the interference into the MSS uplink is the sum of contributions from multiple ATC terminals.

A second factor that must be taken into account in calculating the average ATC terminal transmit power is the speech activity factor. With CDMA, transmit power is significantly reduced unless the terminal has data to transmit. For example, with speech the activity factor is on average slightly less than 0.5 (each user in a conversation is actually speaking roughly half the time, and there is some “idle time” for pauses). For a large number of ATC terminals, slightly less than half of them would actually be transmitting digitized speech at any given time. When not transmitting speech, the terminal transmits a low-power, low data rate signal to maintain the link with the base station. This signal is on the order of 9 dB below the active speech signal level.

Total ATC Uplink Interference to the Spacecraft

Assuming that there are K_{ATC} active ATC terminals within the footprint of an MSS spot beam, the total interference received by the SC is:

$$I_{os} = P_{ATC \max} - F_{PC} - F_{TA} + G_{ATC} - L_{FS} - L_{EX} + G_{SC} + 10 \log K_{ATC} \text{ dBm} \quad (24)$$

where F_{PC} is the power control factor, F_{TA} is the ATC terminal transmit activity factor, G_{ATC} and G_{SC} are the ATC terminal and spacecraft antenna gains, respectively, L_{FS} is the free-space path loss, and L_{EX} is the excess loss due to building penetration, blockage and shadowing. Following the Globalstar analysis [2], it will be assumed for this example that $P_{ATC \max} = 100 \text{ mW}$ (20 dBm), $G_{ATC} = 0 \text{ dB}$, $L_{FS} = 159.6 \text{ dB}$ (corresponding to a spacecraft altitude of 1414 km), and $G_{SC} = 14.7 \text{ dBi}$.

With these values, I_{os} is:

$$\begin{aligned} I_{os} \text{ (dBm)} &= 20 + 0 - 159.6 + 14.7 + 10 \log K_{ATC} - F_{PC} - F_{TA} - L_{EX} \\ &= -124.9 + 10 \log K_{ATC} - F_{PC} - F_{TA} - L_{EX} \end{aligned} \quad (25)$$

According to Globalstar [2], the effective noise temperature seen by the spacecraft receiver is 500°K , so the thermal noise power in a 1.25-MHz band is -110.6 dBm . From (25),

$$\frac{I_{os}}{N} = -14.3 + 10 \log K_{ATC} - F_{PC} - F_{TA} - L_{EX} \text{ dB} \quad (26)$$

or as a ratio,

$$\frac{I_{os}}{N} = \frac{K_{ATC}}{26.9} \cdot \frac{1}{F_{PC} F_{TA} L_{EX}} \quad (27)$$

MSS Uplink Capacity Degradation vs. Number of ATC Terminals within Beam Footprint

Combining (19) and (27) gives the fractional capacity reduction to the MSS uplink as:

$$\frac{\Delta\Lambda}{\Lambda_0} = \frac{1}{\Phi - 1} \cdot \frac{K_{ATC}}{26.9} \cdot \frac{1}{F_{PC} F_{TA} L_{EX}} \quad (28)$$

If $\Phi = 4$ (i.e., $(I_{TOT}/N)_{\max} = 6$ dB), then

$$\frac{\Delta\Lambda}{\Lambda_0} = \frac{K_{ATC}}{80.7} \cdot \frac{1}{F_{PC} F_{TA} L_{EX}} \quad (29)$$

Clearly, the number of ATC terminals corresponding to a given MSS uplink capacity degradation is sensitive to the excess attenuation between the MSS terminals and the SC. If all terminals are unblocked with respect to the SC, then $L_{EX} = 1$ (0 dB). Using an activity factor of 0.5, giving $F_{TA} = 3$ dB, and $F_{PC} = 6$ dB (a factor of 4) gives the result shown in Figure 7.

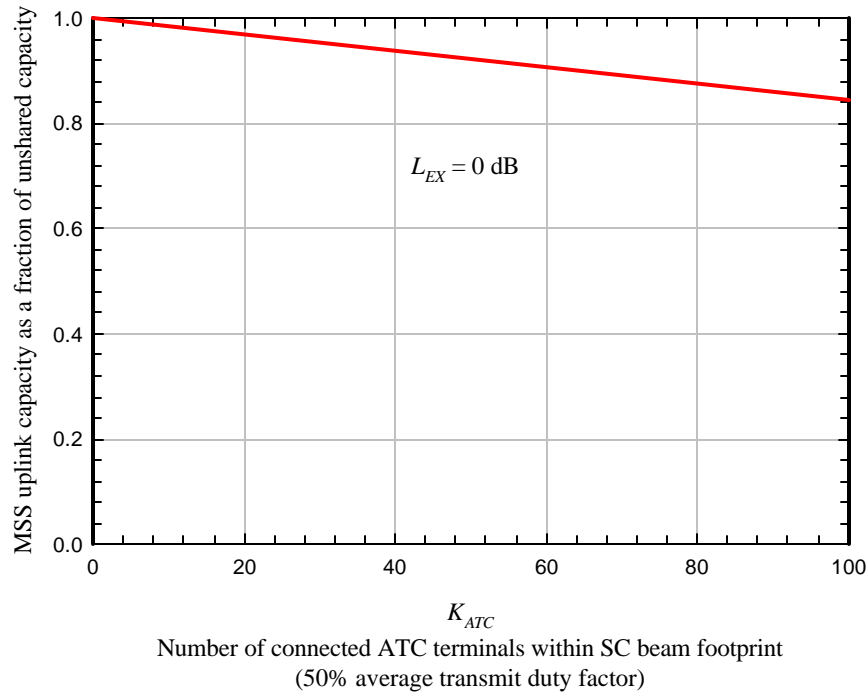


Figure 7: *MSS uplink capacity loss vs. number of ATC terminals with no excess attenuation*

On the other hand, if $L_{EX} = 15$ dB, the relationship between MSS capacity and K_{ATC} is as shown in Figure 8.

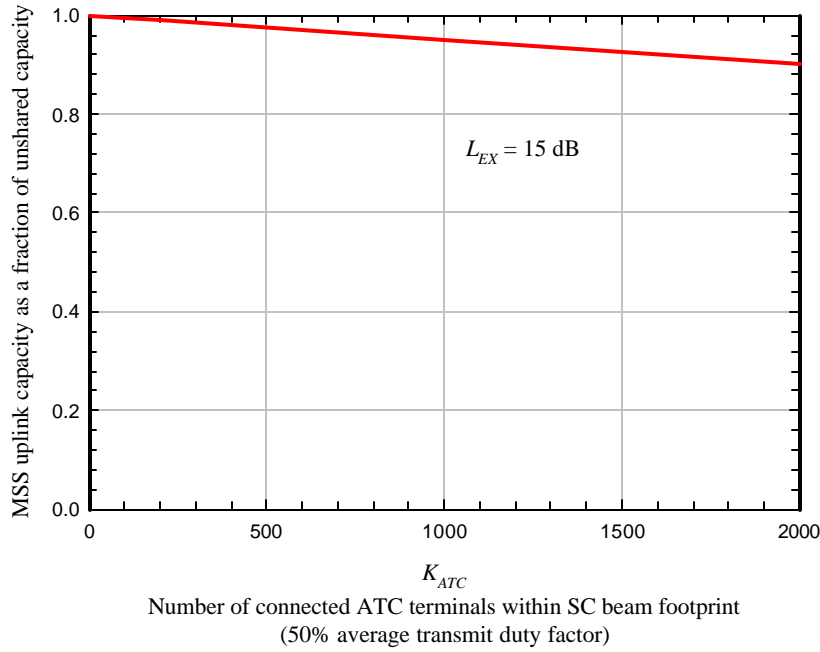


Figure 8: MSS uplink capacity vs. number of active ATC terminals within SC beam

MSS Uplink Capacity Degradation vs. Number of ATC Cells or Sectors within Beam Footprint

It is worthwhile to calculate the number of ATC cells corresponding to a given number of active ATC terminals. Assuming $\Phi = 4$ and $m = 0.5$, (16) gives $\Lambda_0 = 0.5$ for the ATC cells. If all terminals are engaged in voice communications at 9.6 kb/s, and $\Gamma = 7$ dB, then the jamming margin is $M = 1.25 \times 10^6 \div (5 \times 9.6 \times 10^3) = 26$. From (10),

$$\Lambda = K_{TX} \cdot \frac{1}{M+1} = \frac{K_{TX}}{27}, \quad (30)$$

where K_{TX} is the number terminals actually transmitting. Since Λ_0 is the maximum allowable load per cell, the maximum number of terminals that can simultaneously transmit is $K_{TX \max} = \lfloor 27\Lambda_0 \rfloor = 13$. If there are K_C terminals with connections (admitted to the cell and assigned a channel), then the number of terminals actually transmitting is a binomial random variable with an average value of $\overline{K_{TX}} = pK_C$, where p is the probability that a terminal is transmitting, and is assumed 0.5 for speech. The probability that k terminals are transmitting at a given time is

$$\Pr(K_{TX} = k) = \binom{K_C}{k} p^k (1-p)^{K_C-k} \quad (31)$$

where $\binom{K_C}{k} = \frac{K_C!}{k!(K_C-k)!}$ is the binomial coefficient. Given K_C connections, the probability that K_{TX} exceeds the maximum allowed value is:

$$\Pr(K_{TX} > K_{TX \max}) = \sum_{k=K_{TX \max}+1}^{K_C} \Pr(K_{TX} = k) \quad (32)$$

Figure 9 shows $\Pr(K_{TX} > K_{TX \max})$ as a function of the number of connections K_C for $K_{TX \max} = 13$.

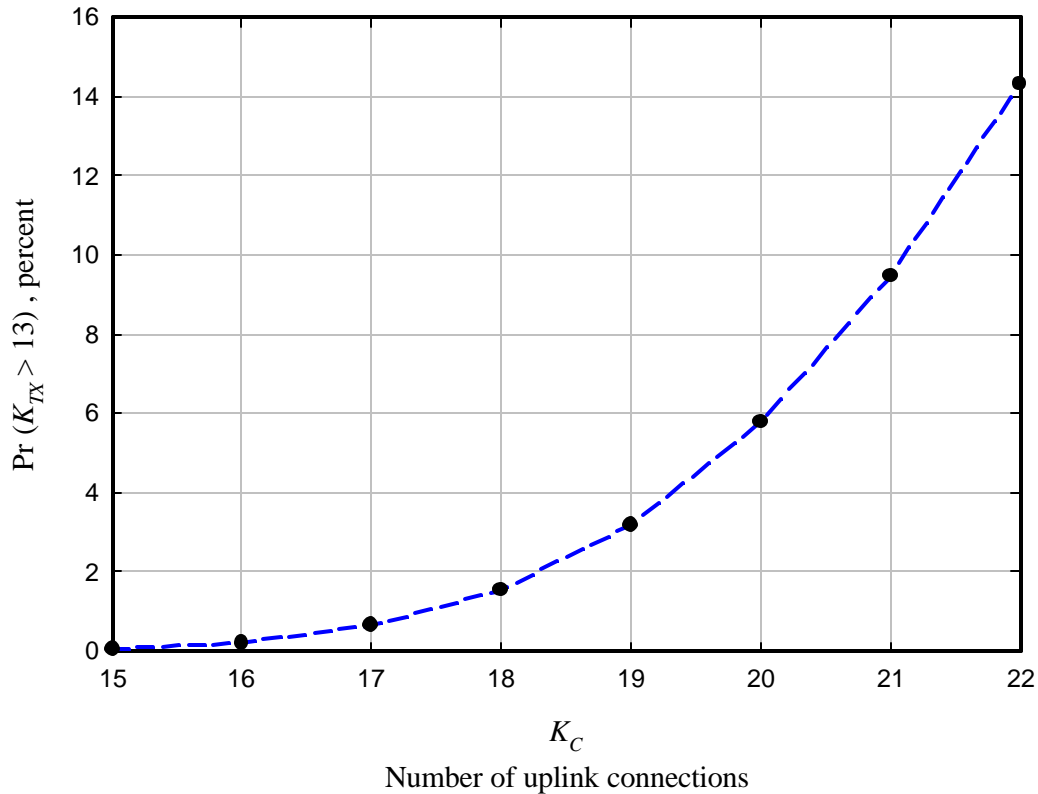


Figure 9: Probability (percent) that number of transmitting terminals exceeds the load limit vs. the number of connections, for terrestrial CDMA uplink.

Given that a maximum of $K_{C \max}$ connections are admitted per cell, the average number of connections can be computed using conventional teletraffic engineering blocking formulas. The Erlang B formula, corresponding to a “blocked calls cleared” queue

discipline, is often used for such calculations. For $K_{C_{\max}}$ servers and an average offered load of a Erlangs, the Erlang B blocking formula gives the blocking probability (the probability that a new connection attempt finds all servers busy) as:

$$P_B = \Pr(K_C = K_{C_{\max}}) = \frac{a^{K_{C_{\max}}} / K_{C_{\max}}!}{\sum_{k=0}^{K_{C_{\max}}} a^k / k!} \quad (33)$$

The average carried load (traffic that is served) is

$$a_C = a(1 - P_B) \quad (34)$$

Figure 10 shows the average carried load a_C vs. the blocking probability for $K_{C_{\max}} = 20$, 21, and 22. Assuming the network is engineered for a blocking probability of 2% and a 20-connection maximum admission limit, the average carried load is about 12.9 Erlangs per cell.⁵ This means there are an average of 12.9 active connections per cell or sector. With a speech activity factor of 0.5, the average number of ATC terminals per cell actually transmitting at any given time would be 6.45.

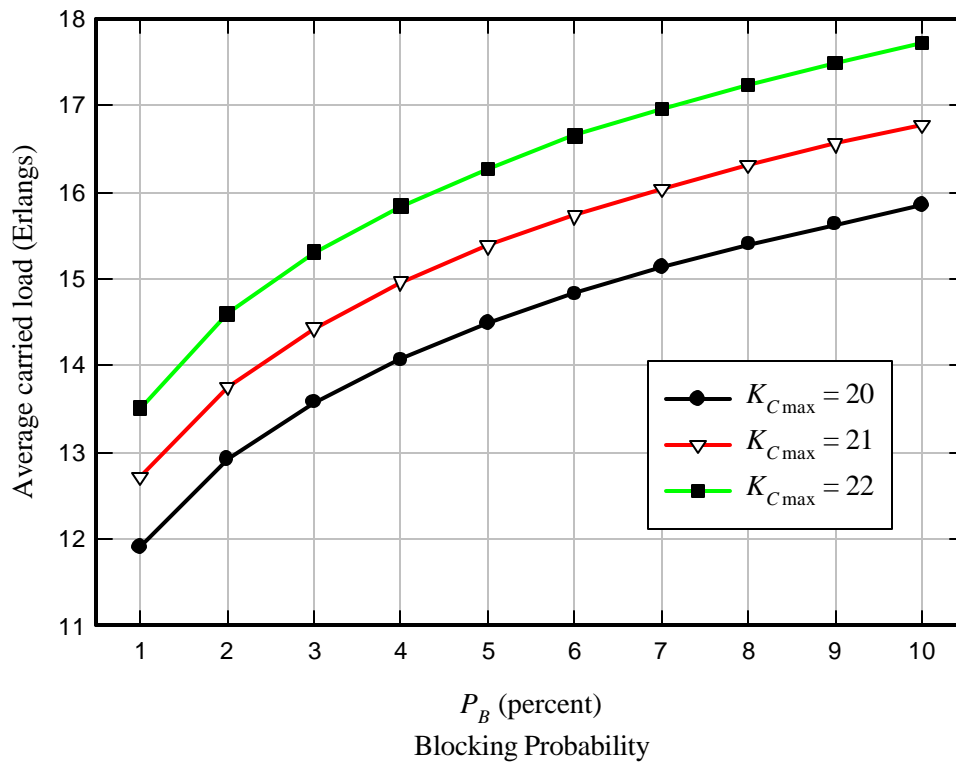


Figure 10: Carried load vs. blocking probability for different connection limits

⁵ If sectorized cells are used, the load would be 12.9 Erlangs per sector.

The MSS capacity reduction now can be expressed in terms of the number of ATC cells within the spacecraft beam footprint by simply dividing the denominator in (29) by 12.9, since the speech activity factor has already been taken into account. Using $F_{TA} = 3$ dB and $F_{PC} = 6$ dB as before gives:

$$\frac{\Delta\Lambda}{\Lambda_0} = \frac{K_{CELL,ATC}}{50L_{EX}} \quad (35)$$

Figure 11 shows the result for different values of L_{EX} . Note that this assumes that every ATC cell or sector is fully-loaded; i.e., operating at offered load corresponding to 2% blocking.

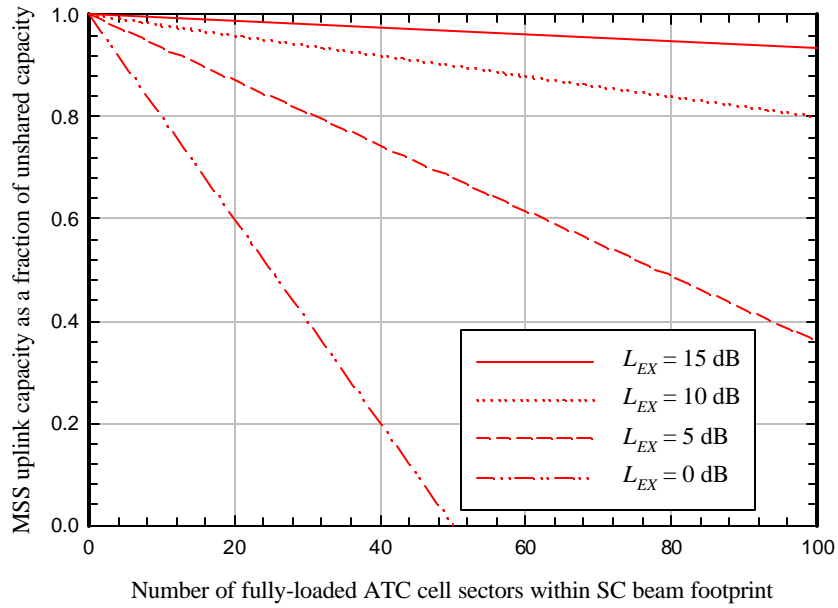


Figure 11: MSS uplink capacity reduction vs. number of ATC sectors in beam footprint

MSS Uplink Capacity Degradation vs. Total ATC Terminal EIRP within Beam Footprint

It is also useful to express the MSS uplink capacity reduction in terms of the total effective isotropic radiated power (EIRP) from the ATC terminals in the beam footprint, which is simply:

$$\frac{\Delta\Lambda}{\Lambda_0} = 0.124 \times EIRP_{ATC} \quad (36)$$

where $EIRP_{ATC}$ is the total EIRP in watts from all ATC terminals within the SC beam footprint. Figure 12 shows the result.

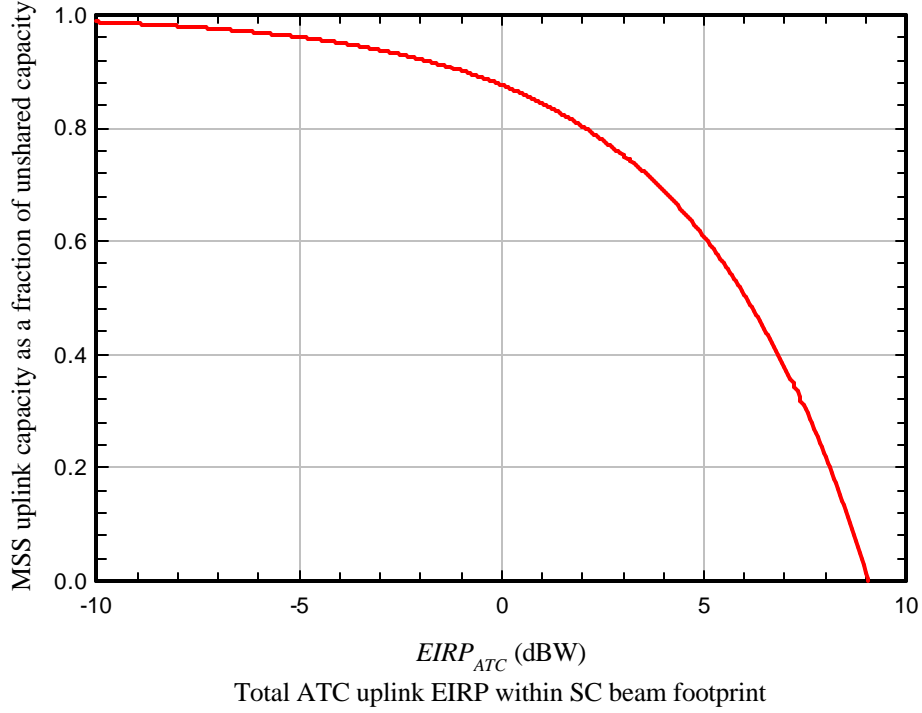


Figure 12: Effect of aggregate ATC terminal EIRP on MSS uplink capacity

MSS Terminal Interference to ATC Uplink

ATC Uplink Capacity Degradation vs. MSS Terminal Distance to ATC Cell

Consider an MSS terminal at the edge of an ATC cell (a distance r_{ATC} from the base station, where r_{ATC} is the ATC cell radius), transmitting a power of $P_{TX,MSS}$. If

$I_{TOT}/N = \Phi$ at the ATC base receiver (the noise rise is at its maximum level), the power received from each ATC terminal is $\Lambda_{ATC} \Phi$, where $\Lambda_{ATC} = 1/(M_{ATC} + 1)$ as above, with M_{ATC} representing the jamming margin for each of the ATC terminals (assumed to have identical data rates and SINR requirements for purposes of this discussion). A proper ATC system design will allow a terminal at the cell edge to communicate if it transmits the maximum power $P_{ATC \max}$ when $I_{TOT}/N = \Phi$. The interference power received from the MSS terminal by the ATC base station therefore is

$$\frac{I_{os}}{N}(0) = \frac{P_{TX,MSS}}{P_{ATC \max}} \Lambda_{ATC} \Phi \quad (37)$$

If the MSS terminal is some distance d_{MSS} from the ATC cell edge, then

$$\frac{I_{os}}{N}(d_{MSS}) = \frac{P_{TX,MSS}}{P_{ATC \max}} \left(\frac{r_{ATC}}{d_{MSS} + r_{ATC}} \right)^g \Lambda_{ATC} \Phi \quad (38)$$

Therefore, from (19), the fractional capacity reduction suffered by the ATC cell is

$$\frac{\Delta\Lambda}{\Lambda_0}(d_{MSS}) = \frac{P_{TX,MSS}}{P_{ATC \max}} \left(\frac{r_{ATC}}{d_{MSS} + r_{ATC}} \right)^g \Lambda_{ATC} \frac{\Phi}{\Phi - 1} \quad (39)$$

To apply (39), the MSS terminal transmit power must be computed. As noted above, the spacecraft receiver noise floor is assume to be -110.6 dBm, based on information in the Globalstar analysis [2]. Assuming $(I_{TOT}/N)_{\max} = 6$ dB for the MSS uplink,

$I_{TOT,MSS} = -104.6$ dBm. With a jamming margin of $M = 26$ (assuming a 9.6 kb/s data rate and a 7-dB SINR requirement), the load factor is $\Lambda = 1/(M + 1) = 1/27$, or -14.3 dB. The signal power that must be received by the spacecraft is then $C = -104.6 - 14.3 = -118.9$ dBm. With a free-space path loss of 159.6 dB, a spacecraft antenna gain of 14.7 dBi, and an MSS terminal antenna gain of 0 dBi, the required transmit power is $P_{TX,MSS} = -118.9 - 14.7 + 159.6 = 26$ dBm, or 400 mW. This number clearly will vary somewhat depending on the path loss to the spacecraft, the MSS terminal antenna gain, diversity combining gain, and the assumed data rate and SINR requirement, but 400 mW is roughly consistent with the assertion in the Globalstar analysis that an MSS terminal is equivalent to 5 ATC terminals in terms of transmit power [2].

Using $P_{TX,MSS}/P_{ATC \max} = 4$, $\Lambda_{ATC} = 0.037$ (-14.3 dB), and $\Phi = 4$, (39) becomes:

$$\frac{\Delta\Lambda}{\Lambda_0}(d_{MSS}) = 0.2 \left(\frac{r_{ATC}}{d_{MSS} + r_{ATC}} \right)^g \quad (40)$$

In other words, a single MSS terminal at the ATC cell edge will reduce the maximum capacity of the ATC cell by 20%. However, the reduction is highly distance-dependent, as shown in Figure 13. Unless the MSS terminal is within a few ATC cell radii of the ATC cell edge, the interference impact is very small. For example, even if the MSS terminal is only 2 ATC cell radii from the ATC cell edge ($d_{MSS} = 2r_{ATC}$), the capacity reduction is less than 1% for all values of g shown. At $d_{MSS} = 3r_{ATC}$, the reduction is about 0.3% for $g = 3$, and less than 0.2% and 0.1% for $g = 3.5$ and $g = 4$, respectively.

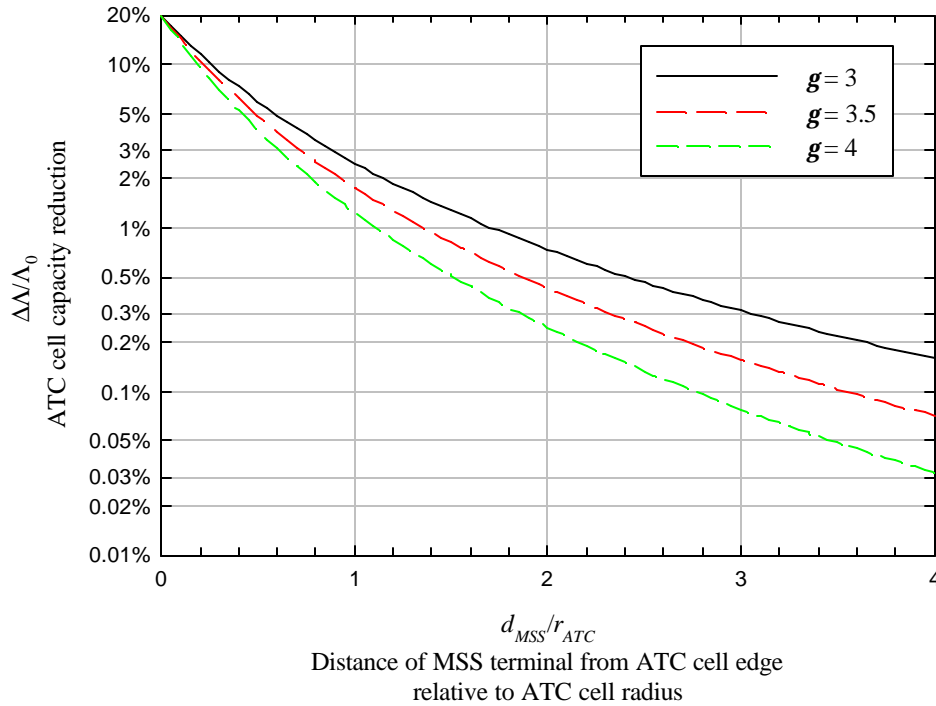


Figure 13: ATC uplink capacity reduction due to MSS terminal interference

Average Interference to ATC Base from MSS Terminals

If MSS terminals are randomly-distributed over area throughout the MSS beam footprint, cumulative interference effects are not significant; any significant interference impact will be dominated by the single nearest MSS terminal. This principal can be illustrated using the geometry shown in Figure 14. The ATC cell is represented by the inner circle of radius r_{ATC} . The outer circle has a radius of D and is centered on the ATC base station. MSS terminals are assumed to be randomly-distributed over the shaded area between the two circles, which has an area of $\pi(D^2 - r_{ATC}^2)$.

If an MSS terminal is a distance d_{MSS} from the ATC cell edge, its distance from the ATC base is $d = d_{MSS} + r_{ATC}$. For a uniform random distribution of MSS terminals over the shaded area, the probability density function (PDF) of d is:

$$f_d(\mathbf{x}) = \frac{2\mathbf{x}}{D^2 - r_{ATC}^2} \quad r_{ATC} \leq \mathbf{x} \leq D \quad (41)$$

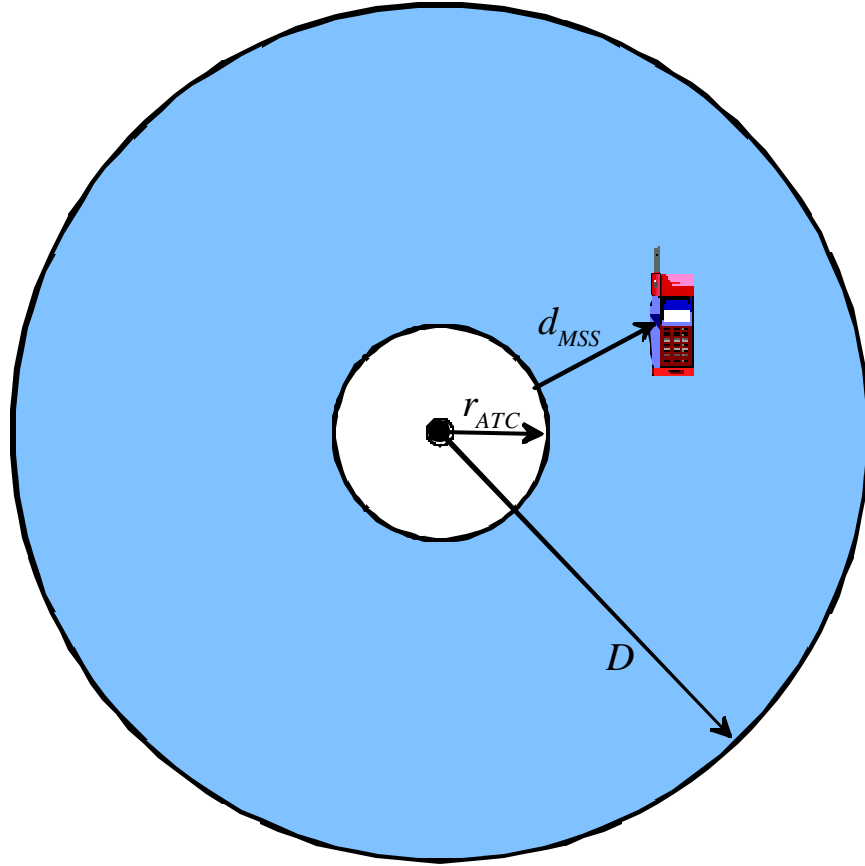


Figure 14: Geometry for interference from MSS terminals to ATC uplink

The interference from the ATC terminal is $I(d) = I_{\max} (d/r_{ATC})^{-g}$, where I_{\max} is the interference that would be received from an MSS terminal with $d = r_{ATC}$.

The average interference power from a single MSS terminal randomly-located in the shaded region therefore is:

$$\bar{I}_1 = I_{\max} \int_{r_{ATC}}^D \left(\frac{\mathbf{x}}{r_{ATC}} \right)^{-g} f_d(\mathbf{x}) d\mathbf{x} = \frac{I_{\max}}{g/2-1} \cdot \frac{1}{D^2 - r_{ATC}^2} \cdot \left[r_{ATC}^2 - D^2 \left(\frac{r_{ATC}}{D} \right)^g \right]. \quad (42)$$

If the average density of active MSS terminals using the same frequency as the ATC base station receiver is \mathbf{r}_{MSS} , then the average number of MSS terminals in the shaded area is $\mathbf{p}\mathbf{r}_{MSS}(D^2 - r_{ATC}^2)$, and the mean interference from ATC terminals in the shaded area is:

$$\bar{I} = \frac{\mathbf{p}\mathbf{r}_{MSS} I_{\max}}{g/2-1} \left[r_{ATC}^2 - D^2 \left(\frac{r_{ATC}}{D} \right)^g \right]. \quad (43)$$

For $D \gg r_{ATC}$, the right hand term of the expression in the brackets is negligible for \mathbf{g} in the range of interest here. Since the coverage of an MSS spot beam generally will extend far beyond the ATC cell, it is reasonable to use the upper bound:

$$\bar{I} < I_{\max} \frac{\mathbf{p} r_{ATC}^2 \mathbf{r}_{MSS}}{\mathbf{g}/2 - 1} = \frac{I_{\max}}{\mathbf{g}/2 - 1} \frac{A_{ATC} K_{MSS}}{A_{MSS}} \quad (44)$$

where $A_{ATC} = \mathbf{p} r_{ATC}^2$ is the area of the ATC cell, A_{MSS} is the coverage area of the MSS beam, and $K_{MSS} = A_{MSS} \mathbf{r}_{MSS}$ is the average number of transmitting MSS terminals served by the beam.

The standard deviation of the MSS interference also is of interest. The mean-square interference from a single source is

$$\begin{aligned} \overline{I_1^2} &= I_{\max}^2 \int_{r_{ATC}}^D \left(\frac{\mathbf{x}}{r_{ATC}} \right)^{-2\mathbf{g}} f_d(\mathbf{x}) d\mathbf{x} = \frac{I_{\max}^2}{\mathbf{g} - 1} \cdot \frac{1}{D^2 - r_{ATC}^2} \cdot \left[r_{ATC}^2 - D^2 \left(\frac{r_{ATC}}{D} \right)^{2\mathbf{g}} \right] \\ &< \frac{I_{\max}^2}{\mathbf{g} - 1} \cdot \frac{r_{ATC}^2}{D^2 - r_{ATC}^2} \end{aligned} \quad (45)$$

The variance of the interference due to a single MSS terminal is $\mathbf{s}_I^2 = \overline{I_1^2} - (\bar{I}_1)^2$. For $D \gg r_{ATC}$, $(\bar{I}_1)^2 \ll \overline{I_1^2}$, so the variance of the interference from mobiles in the shaded area is tightly bounded by

$$\mathbf{s}_I^2 < \frac{\mathbf{p} \mathbf{r}_{MSS} r_{ATC}^2 I_{\max}^2}{\mathbf{g} - 1}, \quad (46)$$

and

$$\begin{aligned} \frac{\mathbf{s}_I}{\bar{I}} &\cong \frac{\mathbf{g}/2 - 1}{\sqrt{\mathbf{g} - 1}} \frac{1}{\sqrt{\mathbf{p} r_{ATC}^2 \mathbf{r}_{MSS}}} \\ &= \frac{\mathbf{g}/2 - 1}{\sqrt{\mathbf{g} - 1}} \frac{1}{\sqrt{K_{MSS} A_{ATC} / A_{MSS}}} \end{aligned} \quad (47)$$

Cumulative Distribution Function of the ATC Uplink Capacity Degradation

Since $A_{ATC}/A_{MSS} \ll 1$, $\mathbf{s}_I/\bar{I} \gg 1$, so the average MSS uplink interference is not a very useful measure of the interference impact. A much more useful statistic is the probability that the interference exceeds some specified level; i.e., the cumulative distribution function (CDF) of the interference. The CDF is fairly straightforward to derive if the total interference is approximated as the interference from the MSS terminal nearest the ATC base. Accounting for the aggregate power from all MSS terminal is more complicated. However, as will be demonstrated, the single-source CDF is adequate for the present purpose.

Consistent with the assumption of a uniform planar distribution of MSS terminals, the terminal locations are modeled using a Poisson point process. The average number of MSS terminals within some region of total area A is

$$\overline{K}_A = \mathbf{r}_{MSS} A \quad (48)$$

The probability that the region does not contain an MSS terminal therefore is:

$$P_0 = e^{-\overline{K}_A} \quad (49)$$

The area of the ring bounded on the outside by a circle of radius d and on the inside by a circle of radius r_{ATC} , both centered on the ATC base station, is $A = \mathbf{p}(d^2 - r_{ATC}^2)$.

Therefore, the probability that there are no MSS terminals within a distance d of the ATC base station is

$$P_0(d) = e^{-\mathbf{p}\mathbf{r}_{MSS}(d^2 - r_{ATC}^2)} = \frac{e^{-\mathbf{p}\mathbf{r}_{MSS}d^2}}{e^{-\mathbf{p}\mathbf{r}_{MSS}r_{ATC}^2}} \quad d \geq r_{ATC} \quad (50)$$

Since the interference from an MSS terminal at distance d is $I(d) = I_{\max} (d/r_{ATC})^{-g}$,

$P_0(d) = \Pr\{I_{MSS} < I(d)\}$, giving the desired CDF:

$$\Pr(I_{MSS} < I) = \exp\left\{-\mathbf{p}\mathbf{r}_{MSS}r_{ATC}^2 \left((I/I_{\max})^{-2/g} - 1\right)\right\} \quad I \leq I_{\max} \quad (51)$$

It is useful to normalize the interference using

$$Z \equiv \left(\mathbf{p}\mathbf{r}_{MSS}r_{ATC}^2\right)^{-g/2} \frac{I_{MSS}}{I_{\max}}. \quad (52)$$

Clearly, $Z_{\max} = (\mathbf{p}\mathbf{r}_{MSS}r_{ATC}^2)^{-g/2}$, and the CDF in (51) can be written as

$$\Pr(I_{MSS} < I) = \Pr(Z < z) = e^{-z^{2/g}} e^{-z^{-2/g}} \quad z \leq Z_{\max} . \quad (53)$$

Also,

$$\Pr(Z < z) = \Pr\left(\frac{I_{MSS}}{I_{\max}} < z(\mathbf{p}\mathbf{r}_{MSS}r_{ATC}^2)^{g/2}\right) \quad (54)$$

and from (38),

$$\frac{\Delta\Lambda}{\Lambda_0} = \frac{P_{TX,MSS}}{P_{ATC\max}} \Lambda_{ATC} \frac{\Phi}{\Phi-1} \cdot \frac{I_{MSS}}{I_{\max}} \quad (55)$$

Therefore,

$$\Pr\left(\frac{\Delta\Lambda}{\Lambda_0} < I\right) = \Pr\left(\frac{I_{MSS}}{I_{\max}} < \mathbf{k}I\right) = \Pr\left\{Z < \mathbf{k}I(\mathbf{p}\mathbf{r}_{MSS}r_{ATC}^2)^{-g/2}\right\} \quad (56)$$

where $\mathbf{k} = \frac{P_{ATC\max}}{P_{TX,MSS}} \frac{1}{\Lambda_{ATC}} \frac{\Phi-1}{\Phi}$. From the calculations above, $\mathbf{k} = 5$.

The quantity $\mathbf{p}\mathbf{r}_{MSS}r_{ATC}^2$ represents the average number of MSS terminals that would be within an area $\mathbf{p}\mathbf{r}_{ATC}^2$ with a uniformly-distributed field of MSS terminals of density \mathbf{r}_{MSS} terminals/km². Assuming an average SC footprint radius of 2000 km (for the Globalstar system), the area of a beam is $\mathbf{p} \cdot 2000^2/16 = 785,400$ km² (there are 16 beams per spacecraft). Assuming that each beam is equipped with 100 speech circuits, an Erlang B calculation at 2% blocking gives an average traffic of about 88 Erlangs (an average of 88 speech connections). In that case, $\mathbf{r}_{MSS} = 0.00011$ active MSS terminal per km². If $r_{ATC} = 5$ km, $\mathbf{p}\mathbf{r}_{MSS}r_{ATC}^2 = 0.0088$ and $e^{-\mathbf{p}\mathbf{r}_{MSS}r_{ATC}^2} = 0.99$. Thus, $\Pr(Z < z) = 0.99e^{-z^{-2/g}}$ with these assumptions, and

$$\Pr\left(\frac{\Delta\Lambda}{\Lambda_0} < I\right) = 1.01 \exp\left(-0.0088 \cdot (\mathbf{k}I)^{-2/g}\right) \quad I \leq 0.2 \quad (57)$$

which is shown in Figure 15. As an example of how to read the graph, for $g = 3.5$ (the middle curve), the probability is 96% that the ATC uplink capacity will be reduced by less than 1% by the MSS terminal interference.

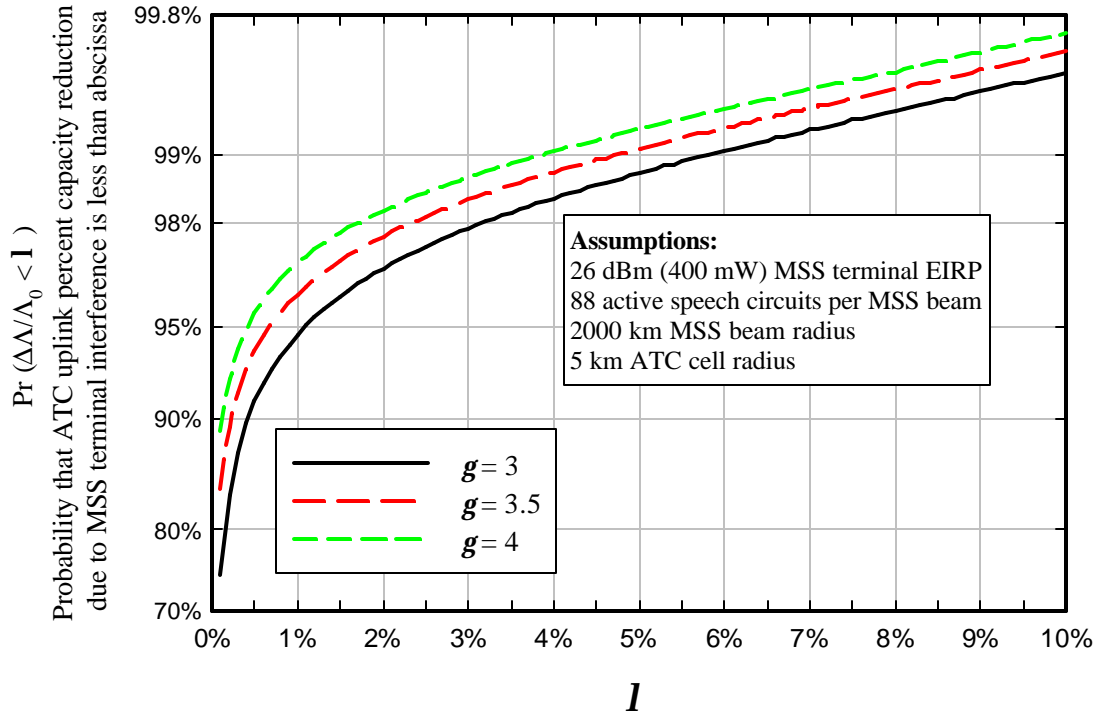


Figure 15: CDF of ATC uplink capacity reduction due to MSS terminal interference

Single-Interferer vs. Multiple Interferer Models

The model used here might be questioned because it was based on the interference from only the nearest MSS terminal, rather than the combined interference from all co-channel MSS terminals. However, at the upper tail of the CDF (high probability values on the ordinate), this “single-interferer” model gives essentially the same results as a model which accounts for the combine interference from multiple sources.

Clearly, the CDF of Z is tightly upper-bounded by

$$\Pr(Z < z) < F_z(z) = e^{-z^{-1/g}} \quad (58)$$

where $F_z(z)$ would be the CDF if MSS terminals were not restricted in the model to the area outside the ATC cell perimeter.

If the total power from all MSS terminals is taken into account, as shown in Annex A, $F_z(z)$ becomes:

$$F_Z(z) = 1 - \frac{1}{p} \sum_{k=1}^{\infty} \frac{\Gamma(kn)}{k!} \left[\frac{\Gamma(1-n)}{z^n} \right]^k \sin kp(1-n), \quad z > 0 \quad (59)$$

where $\Gamma(\cdot)$ is the Gamma function.

Figure 16 shows $F_Z(z)$ for this case, along with the single-interferer model used in the MSS terminal interference calculations. As can be seen, for probability levels greater than 90%, there is no significant difference in the results. The reason is that the upper tail of the CDF corresponds to strong interference, which is dominated by a single strong (nearby) source. At lower levels on the CDF, the combined effect of multiple sources becomes more significant, and the curves diverge.

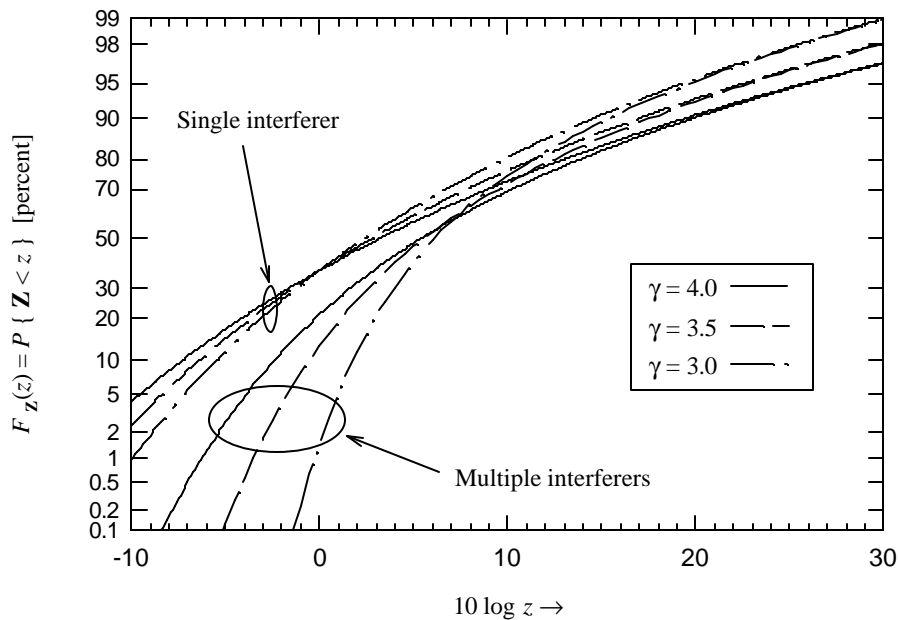


Figure 16: CDF of Z for single-interferer and multiple-interferer models

Notes on Worst-Case Assumptions

It should be noted that the assumptions used to generate Figure 15 are pessimistic, for a number of reasons:

- No blockage or other excess path attenuation was assumed between the MSS terminal and the ATC base station. The model used here is appropriate for outdoor, elevated ATC base stations. If the ATC system is intended to provide fill-in coverage, there may often be excess blockage between an MSS terminal and an ATC base. For example, the ATC base station may be indoors, to provide in-building coverage.
- The only “exclusion zone” (area within which there are no MSS terminals) assumed was the area of a single ATC cell. Typically, the ATC cell would be part of a cluster, and the true exclusion zone would be the area covered by the cluster. Cells inside the

cluster would be protected by the outer cells in the cluster. Each outer cell would be protected on one side by other cells as well.

- The MSS EIRP was assumed to be 400 mW, based on the calculations shown above. This was based on an assumed SINR requirement of 7 dB, which is probably more appropriate for a terrestrial system that requires some margin to account for multipath fading. With a 5-dB SINR requirement, the MSS terminal EIRP would be 250 mW using the same free-space path loss (159.6 dB). Of course, the path loss may be greater, depending on the position of the spacecraft. In an actual system, the MSS terminal transmit power will vary, depending on the free-space path loss as well as the speech rate (which may be as low as 2.4 kbps), blockage between the terminal and the spacecraft, and the traffic load of the spacecraft receiver, which determines I_{TOT}/N .
- A heavily-loaded beam uplink was assumed (88 connections, consistent with 100 speech circuits with 2% blocking with the Erlang B formula), which gives a correspondingly high density of MSS terminals.
- Full-sized outdoor terrestrial cells were assumed. If ATC is used primarily to fill in weak coverage areas for the MSS system, the ATC cells are likely to be smaller (e.g., microcells). The use of smaller ATC cells in the analysis would make the interference problem even less severe.

Overall, the analysis shows that uplink interference from MSS terminals to ATC base stations is a low-probability event, and any significant effects are confined to MSS terminals near the ATC cell.

Analysis of the CDMA Downlink

As with the uplink, it is first necessary to develop a basic downlink capacity model to understand interference effects from MSS satellites to ATC terminals, and from ATC base stations to MSS terminals. With CDMA, the downlink model is quite different from the uplink model. The same general model applies to both MSS and ATC systems, although there are some parameter differences as will be explained.

Modeling the CDMA Downlink

In the following discussion, a “base station” can be either an actual terrestrial base station or an MSS satellite. The downlink originates from a transmitter at the base station, and there is a fixed limit on the total downlink power. That power is shared (allocated) among the traffic channels and the overhead channels (e.g., pilot, sync, and paging for IS-95, plus additional common channels for 3G systems). At the transmitter, the codes assigned to the different traffic and overhead channels are orthogonal. With an ideal free-space propagation channel, this orthogonality is maintained at the receiver, so there is no interference among the different channels (codes) transmitted from the same base station. This might often be the case for MSS. However, in a terrestrial system, the delay spread introduced by multipath in the propagation channel compromises the

orthogonality, resulting in interference among different codes transmitted from the same base station.

As for the uplink, the SINR at the receiver of the j^{th} terminal is

$$\left(\frac{E_b}{N_0 + I_0} \right)_j = \frac{W}{R_j} \frac{C_j}{N + I_j} \quad (60)$$

The total downlink power received by the j^{th} terminal from its associated base station is $P_{rx,j}$, which clearly depends on the path loss between the base station and the terminal, which in turn depends on the distance d_j between the base and terminal. If \mathbf{a}_j is the fraction of the total downlink power which is allocated to the j^{th} terminal, then the desired signal power is $C_j = \mathbf{a}_j P_{rx,j}$. The power received by terminal j that is allocated to all other transmissions is $(1 - \mathbf{a}_j) P_{rx,j}$. As noted above, in a terrestrial system, these transmissions generally are not completely orthogonal to the desired signal due to multipath, and the terminal will see some fraction \mathbf{b}_j of the in-cell downlink power. Figure 17 shows the geometry for a terrestrial system.

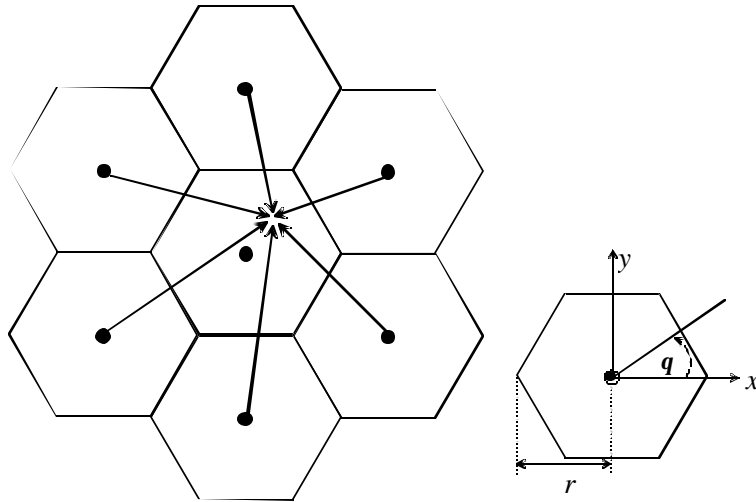


Figure 17: Geometry for terrestrial CDMA downlink model.

The received other-cell interference also depends on the location of the terminal (both the distance d_j and the azimuth angle \mathbf{q}_j), and is denoted here by $I_{oc,j}$.

Accounting for all these factors gives the SINR as:

$$\left(\frac{E_b}{N_0 + I_0} \right)_j = \frac{W}{R_j} \frac{\mathbf{a}_j P_{rx,j}}{N + \mathbf{b}_j (1 - \mathbf{a}_j) P_{rx,j} + I_{oc,j}} \quad (61)$$

Assuming, as with the uplink, that the SINR is maintained at its threshold Γ_j , and substituting $M_j = W/\Gamma_j R_j$ gives:

$$M_j \mathbf{a}_j P_{rx,j} = N + \mathbf{b}_j (1 - \mathbf{a}_j) P_{rx,j} + I_{oc,j} \quad (62)$$

or

$$\mathbf{a}_j = \frac{1}{M_j + \mathbf{b}_j} \left(\frac{N}{P_{rx,j}} + \mathbf{b}_j + \frac{I_{oc,j}}{P_{rx,j}} \right). \quad (63)$$

The total fraction of the downlink power available for traffic channels is $\mathbf{a}_T = 1 - \mathbf{a}_{oh}$, where \mathbf{a}_{oh} represents the total fraction of the downlink power allocated to the common overhead channels (pilot, sync, control), and is typically fixed (static). Therefore, the downlink power constraint on the traffic channels is $\sum_{j=1}^J \mathbf{a}_j \leq \mathbf{a}_T$. Defining

$\Lambda_j \equiv \frac{1}{M_j + \mathbf{b}_j}$ for notational convenience, the downlink traffic channel capacity limit can be expressed as:

$$\sum_{j=1}^J \Lambda_j \left(\frac{N}{P_{rx,j}} + \mathbf{b}_j + \frac{I_{oc,j}}{P_{rx,j}} \right) \leq \mathbf{a}_T. \quad (64)$$

A more useful form of the limit for capacity calculations is

$$\sum_{j=1}^J \Lambda_j \left(\frac{P_{\min}}{P_{rx,j}} \frac{N}{P_{\min}} + \mathbf{b}_j + \frac{I_{oc,j}}{P_{rx,j}} \right) \leq \mathbf{a}_T \quad (65)$$

where P_{\min} is the minimum received downlink power (i.e., at the cell vertex). The ratio N/P_{\min} defines the cell edge, and as discussed below, determines the power allocation required for the overhead channels.

Downlink Capacity

The downlink power allocation required to support a terminal depends on the location of the terminal in the cell. For a terminal near the cell edge, $P_{rx,j}$ will be lower and $I_{oc,j}$ will be higher than for a terminal nearer the cell center.⁶ Therefore, the downlink capacity for any specific situation clearly depends on the locations of the terminals. To develop a general capacity expression, cell-area averages of the location-dependent terms in (65) can be used, giving

$$\mathbf{a}_T = \left(\left\langle \frac{N}{P_{rx,j}} \right\rangle + \mathbf{b} + \left\langle \frac{I_{oc,j}}{P_{rx,j}} \right\rangle \right) \sum_{j=1}^J \Lambda_j \quad (66)$$

where $\langle \cdot \rangle$ in this case indicates an average taken over area, and it has been assumed that $\mathbf{b}_j = \mathbf{b}, \forall j$. Note that $\langle N/P_{rx} \rangle = \langle P_{\min}/P_{rx,j} \rangle N/P_{\min} = \langle L/L_{\max} \rangle N/P_{\min}$, where L is the path loss between the base station and the mobile, and L_{\max} is its maximum value.

Letting $Y_{oc,j} \equiv I_{oc,j}/P_{rx,j}$ with $\langle Y_{oc} \rangle$ representing its area-average,

$x_p \equiv \langle P_{\min}/P_{rx} \rangle = \langle L/L_{\max} \rangle$, and $\Lambda_T \equiv \sum_{j=1}^J \Lambda_j$ (the traffic channel load, like the load parameter Λ in the uplink case), (66) gives

$$\mathbf{a}_T = \left(x_p \frac{N}{P_{\min}} + \mathbf{b} + \langle Y_{oc} \rangle \right) \Lambda_T \quad (67)$$

Table 1 shows $\langle Y_{oc} \rangle$, $Y_{oc \max}$, and \mathbf{c}_p for different values of \mathbf{g} . The Annex B describes the other-cell interference computations, and \mathbf{c}_p was computed using the calculation of $\langle L/L_{\max} \rangle$ for a hexagonal cell, as described in the analysis of the CDMA uplink; that is, $\langle L/L_{\max} \rangle \cong (2.6/p)^{g/2} \cdot 2/(g+2)$.

Table 1: Parameters for capacity calculations

\mathbf{g}	$\langle Y_{oc} \rangle$	$Y_{oc \max}$	\mathbf{c}_p
3.0	0.81	2.82	0.30
3.5	0.57	2.53	0.26
4.0	0.44	2.34	0.23

⁶ Further, terminals near the cell edge will likely be in soft handoff, thereby using resources from neighboring cells.

Overhead Channel Power Allocation

The coverage of the common downlink overhead channels must extend to the cell edge, where by definition the total received downlink power is at its minimum value P_{\min} . If the required rate and SINR of the k^{th} overhead channel are R_k and Γ_k , respectively, then the corresponding jamming margin is

$$M_k = \frac{W}{\Gamma_k R_k} \quad (68)$$

For IS-95, the downlink overhead channels are pilot, sync, and paging.

Table 2 shows the assumed minimum SINR (Γ), spreading gain (W/R), and jamming margin (M) for these channels, and for the 9.6 kb/s speech traffic channel.⁷

Table 2: Assumed downlink channel jamming margins

	Γ	W/R	M
pilot	-16 dB	0 dB	16 dB
sync	6	30	24
paging	6	24	18
traffic ⁸	6	21	15

Letting $\Lambda_k \equiv 1/(M_k + \mathbf{b})$, the power allocation required to support the k^{th} overhead channel is $\mathbf{a}_k = \Lambda_k (N/P_{\min} + \mathbf{b} + Y_{oc\max})$. If there are K_{oh} overhead channels, the total downlink power allocation necessary to support them is

$$\mathbf{a}_{oh} = \sum_{k=1}^{K_{oh}} \mathbf{a}_k = \left(\frac{N}{P_{\min}} + \mathbf{b} + Y_{oc\max} \right) \sum_{k=1}^{K_{oh}} \Lambda_k. \quad (69)$$

Figure 18 shows \mathbf{a}_{oh} vs. P_{\min}/N (power at the cell edge relative to the thermal noise floor) for different values of \mathbf{b} . Since the curves are fairly flat for $P_{\min}/N > 0$ dB, this suggests that from the perspective of power available for traffic channels, $P_{\min}/N \approx 0$ dB might be a reasonable design choice.

⁷ The required traffic channel SINR for the downlink typically is less than for the uplink because coherent detection is used on the downlink, but not the uplink.

⁸ For rate set 1.

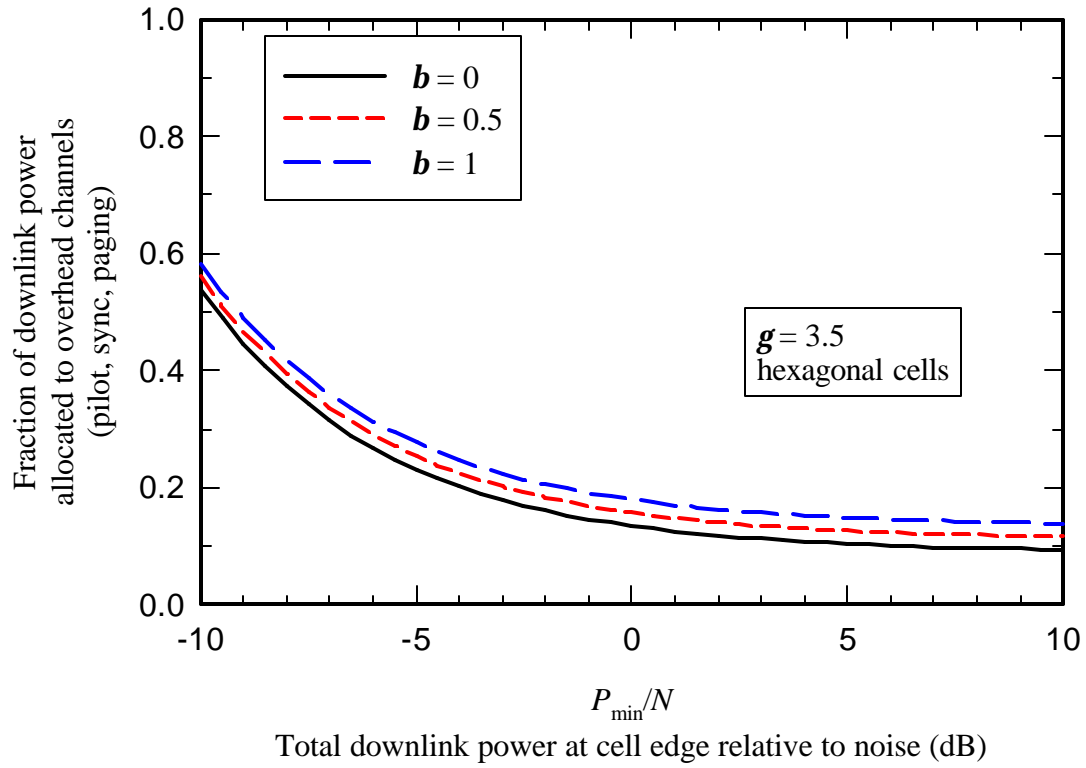


Figure 18: Total overhead power allocation vs. P_{\min}/N for a terrestrial CDMA network.

The received power at the cell edge associated with each overhead channel is $\mathbf{a}_k P_{\min}$, which is shown in Figure 19 for $\mathbf{b} = 0.5$.

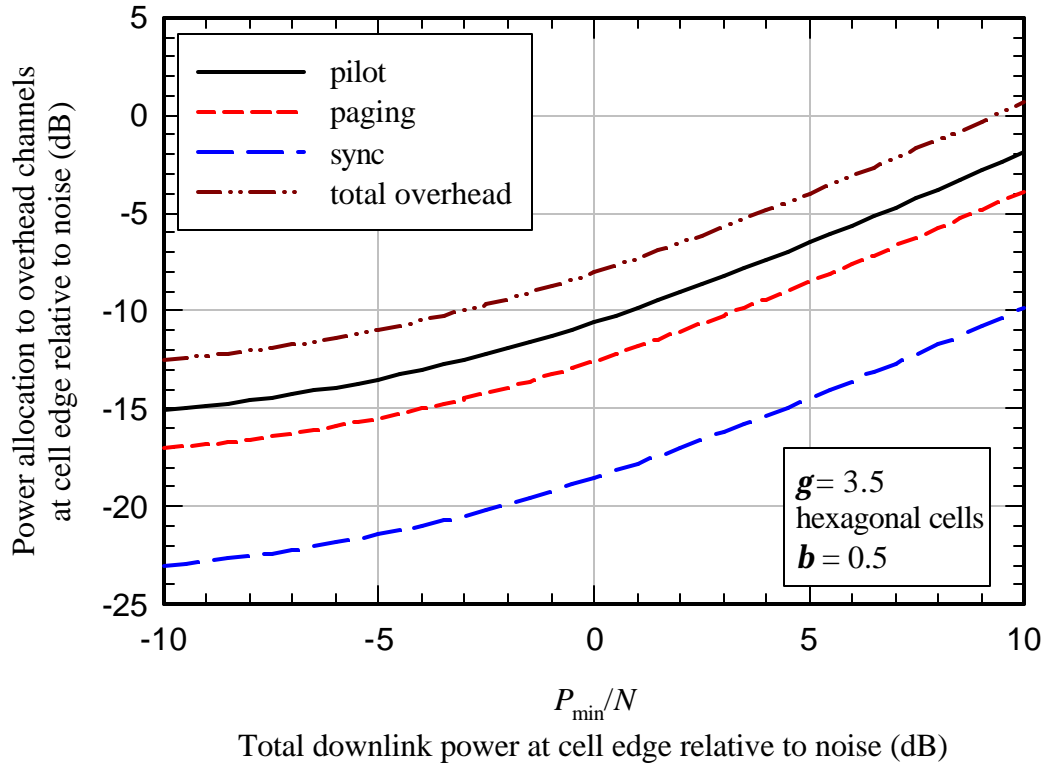


Figure 19: Received power at cell edge for CDMA downlink overhead channels

Downlink Pole Capacity

It is also useful to develop an expression for total capacity per cell as a function of P_{\min}/N . As will be seen, the downlink exhibits a “pole capacity” as does the uplink, although the form is slightly different. At the pole point, thermal noise is insignificant compared to other-cell and in-cell interference.

To develop such an expression, total downlink power allocation limit can be expressed, using $\Lambda_{oh} = \sum_k \Lambda_k$ as

$$\mathbf{a}_{oh} = \left(\frac{N}{P_{\min}} + \mathbf{b} + Y_{oc\max} \right) \Lambda_{oh} = \frac{N}{P_{\min}} \Lambda_{oh} + \mathbf{a}_{oh\min} \quad (70)$$

where $\mathbf{a}_{oh\min} = \Lambda_{oh}(\mathbf{b} + Y_{oc\max})$ is the fraction of downlink power required by the overhead channels for $N/P_{\min} \rightarrow 0$.

Since $\mathbf{a}_{oh} + \mathbf{a}_T = 1$,

$$\frac{N}{P_{\min}} (\Lambda_{oh} + x_p \Lambda_T) = 1 - \mathbf{a}_{oh\min} - \Lambda_T (\mathbf{b} + \langle Y_{oc} \rangle). \quad (71)$$

For $N/P_{\min} \rightarrow 0$, $\mathbf{a}_T \rightarrow \mathbf{a}_{T\max} = 1 - \mathbf{a}_{oh\min}$ and $\Lambda_T \rightarrow \Lambda_{T\max}$. From (67),

$\mathbf{a}_{T\max} = (\mathbf{b} + \langle Y_{oc} \rangle) \Lambda_{T\max}$, so (71) becomes:

$$\frac{P_{\min}}{N} = \frac{\Lambda_{oh} + x_p \Lambda_T}{\mathbf{a}_{T\max} (1 - \Lambda_T / \Lambda_{T\max})}. \quad (72)$$

The minimum value of P_{\min}/N occurs when $\mathbf{a}_{oh} = 1$; that is, all downlink power is allocated to the overhead channels. This corresponds to $\Lambda_T = 0$ (no power is available to support traffic channels), which from (72) gives $(P_{\min}/N)_{\min} = \Lambda_{oh}/\mathbf{a}_{T\max}$. The incremental required power as a function of traffic channel load therefore can be expressed as:

$$\Delta \left(\frac{P_{\min}}{N} \right) = \frac{P_{\min}}{N} - \left(\frac{P_{\min}}{N} \right)_{\min} = \frac{\Lambda_T / \Lambda_{T\max}}{1 - \Lambda_T / \Lambda_{T\max}} \left(\frac{x_p}{\mathbf{b} + \langle Y_{oc} \rangle} + \frac{\Lambda_{oh}}{\mathbf{a}_{T\max}} \right) \quad (73)$$

or

$$\frac{P_{\min}}{N} = \frac{\Lambda_T / \Lambda_{T\max}}{1 - \Lambda_T / \Lambda_{T\max}} \left(\frac{x_p}{\mathbf{b} + \langle Y_{oc} \rangle} + \frac{\Lambda_{oh}}{\mathbf{a}_{T\max}} \right) + \frac{\Lambda_{oh}}{\mathbf{a}_{T\max}} \quad (74)$$

with $\mathbf{a}_{T\max} = 1 - \Lambda_{oh} (\mathbf{b} + Y_{oc\max})$ and $\Lambda_{T\max} = \mathbf{a}_{T\max} / (\mathbf{b} + \langle Y_{oc} \rangle)$.

For a numerical example, values are needed for the parameters. Figure 20 shows $Y_{oc} = I_{oc}/P_{rx}$ vs. d/r , the normalized distance of the terminal from the base station, for $\mathbf{q} = 0$ (Y_{oc} is not very sensitive to \mathbf{q}). It is assumed that $\mathbf{g} = 3.5$ for this example. Thus, from Table 1, $Y_{oc\max} \cong 2.5$ (4 dB), $x_p = \langle P_{\min}/P_{rx} \rangle = 0.26$ and $\langle Y_{oc} \rangle = 0.57$. Using the values in

Table 2, $\Lambda_{oh} \cong 0.04$. This gives $\mathbf{a}_{oh} = 0.18$ (18% of total power allocated to overhead channels) when $P_{\min}/N = 1$ and $\mathbf{b} = 1$, and 0.16 for $\mathbf{b} = 0.5$. Table 3 summarizes these parameters and the derived values $\mathbf{a}_{oh\min}$, $\mathbf{a}_{T\max}$, and $\Lambda_{T\max}$.

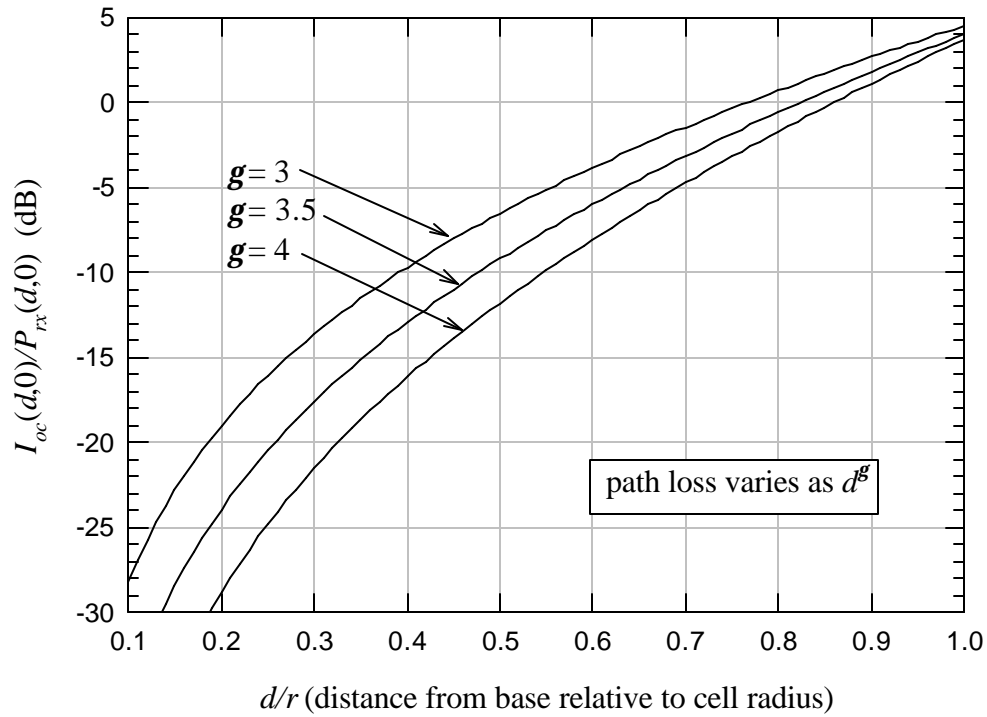


Figure 20: Y_{oc} vs. distance from cell center for $q = 0$.

Table 3: Parameter values for the downlink capacity example

x_p	$Y_{oc \max}$	$\langle Y_{oc} \rangle$	\mathbf{b}	Λ_{oh}	$\mathbf{a}_{oh \min}$	$\mathbf{a}_{T \max}$	$\Lambda_{T \max}$
0.26	2.5	0.57	0.5	0.04	0.12	0.88	0.82

With these values, (74) becomes:

$$\frac{P_{\min}}{N} = 0.288 \frac{\Lambda_T / \Lambda_{T \max}}{1 - \Lambda_T / \Lambda_{T \max}} + 0.045, \quad (75)$$

Figure 21 shows P_{\min}/N vs. $\Lambda/\Lambda_{T \max}$ for $\mathbf{b} = 0, 0.5, \text{ and } 1$. As shown in Figure 18, \mathbf{a}_{oh} is relatively flat for $P_{\min}/N > 0$ dB, so increasing P_{\min}/N beyond that point does not increase the power allocation available for traffic significantly. However, Figure 21 shows significant capacity gains when P_{\min}/N is increased above 0 dB. The reason for the difference can be understood by comparing (67) to (69). In (69), $Y_{oc \max} + \mathbf{b}$ rapidly becomes the dominant term as P_{\min}/N increases above 0 dB, but $(Y_{oc \max} + \mathbf{b})/P_{\min}$ is constant, so the only change in \mathbf{a}_{oh} is due to the decreasing term $\Lambda_{oh}(N/P_{\min})$, which is

only about 0.04 for $P_{\min}/N = 1$. This is the maximum amount that \mathbf{a}_{oh} can decrease as P_{\min}/N increases above 0 dB. For $\mathbf{b} = 0.5$, the other term is $\Lambda_{oh}(Y_{oc\max} + \mathbf{b})/P_{\min} \cong 0.12$, which is the asymptotic value of \mathbf{a}_{oh} as $P_{\min}/N \rightarrow \infty$. Thus, \mathbf{a}_{oh} is reduced by only about 25% as P_{\min}/N increases from 0 dB to a very large value. Further, \mathbf{a}_T increases from 0.84 to 0.88, an increase of less than 5%.

Conversely, referring to (67), the term $x_p N/P_{\min} + \mathbf{b} + \langle Y_{oc} \rangle$ has a value of 1.33 for $P_{\min}/N = 0$ dB (with $\mathbf{b} = 0.5$), but decreases to 1.07 as $P_{\min}/N \rightarrow \infty$, which gives a 24% increase in Λ_T even with \mathbf{a}_T held constant. Combined with the roughly 5% increase in \mathbf{a}_T , the total increase in Λ_T is about 30%. As can be seen from Figure 21, $\Lambda_T/\Lambda_{T\max}$ increases from about 0.77 at $P_{\min}/N = 0$ dB to 1.0 as $P_{\min}/N \rightarrow \infty$ for $\mathbf{b} = 0.5$.

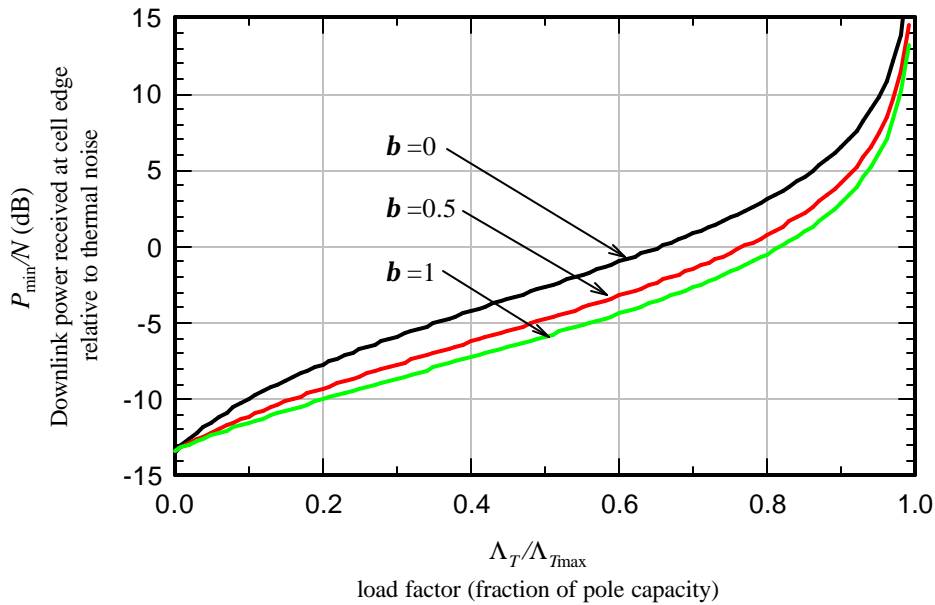


Figure 21: CDMA downlink: cell edge received power vs. traffic load.

Figure 21 seems to suggest a more favorable result as \mathbf{b} increases. However, this is not the case, because $\Lambda_{T\max}$ decreases as \mathbf{b} increases. As with the uplink, the total downlink throughput can be approximated using

$$R_{TOT} \cong \frac{W\Lambda_T}{\Gamma} = \frac{W\Lambda_{T\max}}{\Gamma} \cdot \Lambda_T/\Lambda_{T\max} \cdot \quad (76)$$

The result is shown in Figure 22 for $\Gamma = 6$ dB. As can be seen, increasing \mathbf{b} reduces the throughput. As noted on the graph, this calculation does not include the effect of soft

handoff. While soft handoff is “free” on the uplink from a capacity perspective (it requires no additional transmissions from the mobile), this is not the case on the downlink. Each terminal in soft handoff requires transmissions from multiple base stations. Since the total power allocation available to traffic channels is fixed, soft handoff will reduce the downlink throughput by some factor.

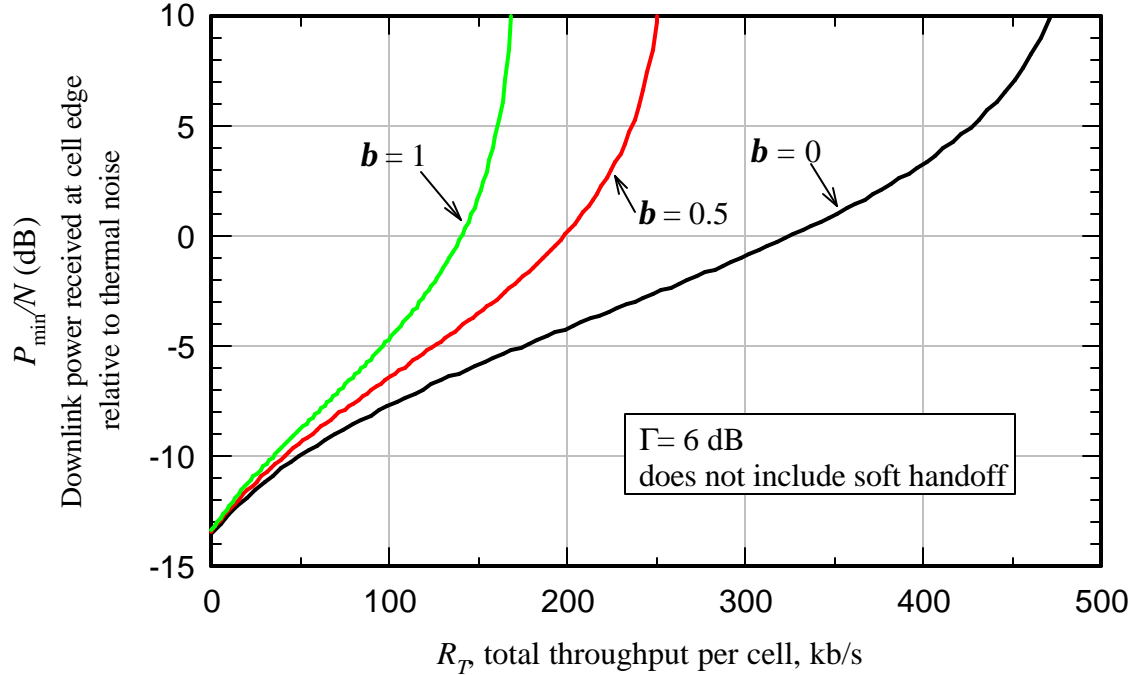


Figure 22: CDMA downlink: cell edge received power vs. total cell throughput.

Modeling MSS/ATC Downlink Interference

The model developed above can be used to understand mutual interference between the MSS and ATC downlinks. If other-system interference is introduced, (64) becomes

$$\sum_{j=1}^J \Lambda_j \left(\frac{N}{P_{rx,j}} + b_j + \frac{I_{oc,j}}{P_{rx,j}} + \frac{I_{os,j}}{P_{rx,j}} \right) \leq a_T \quad (77)$$

so the other-system interference has the same effect as additional other-cell interference and apparently, traffic channel capacity is correspondingly reduced. The effect of $I_{os,j}$ is also the same as an increase in the noise floor N , but the increase may be different for different terminals, depending on the situation. For example, in the case of ATC base station interference to the MSS downlink, MSS terminals will be different distances from the ATC base station, and will experience different levels of other-system interference.

The effect on reception of the overhead channels and the impact on cell coverage must be taken into account. From the discussion above, it is clear that the fraction of the

downlink power allocated to the overhead channels depends on the design value of P_{\min}/N , which corresponds to the edge of coverage, since coverage is determined by the ability of the terminal to decode the overhead channels. This means that for each of the K_{oh} overhead channels, it is necessary that:

$$\frac{N}{P_{rx,j}} + \mathbf{b}_j + \frac{I_{oc,j}}{P_{rx,j}} + \frac{I_{os,j}}{P_{rx,j}} \leq \mathbf{a}_k (M_k + \mathbf{b}_j) \quad (78)$$

If additional interference is added, coverage will be reduced, because terminals that would have been near the cell edge without the interference have little or no margin in their link budget with respect to the overhead channels, and cannot receive the overhead channels in the presence of the additional interference.

If I_{oc} is known in advance, the base station transmit power, overhead channel power allocations, and/or layout can be adjusted to compensate. As an example, consider an idealized case in which there is no shadowing and all ATC terminals have a line-of-sight path to the MSS spacecraft. As related by Globalstar (p. 18), the power flux density (PFD) at the ground is constrained by ITU Radio Regulations by the mask:

$$PFD = \begin{cases} PFD_{low} & \Theta \leq 5^\circ \\ PFD_{low} + 0.05(PFD_{high} - PFD_{low})(\Theta - 5^\circ) & 5^\circ < \Theta \leq 25^\circ \\ PFD_{high} & 25^\circ < \Theta \leq 90^\circ \end{cases} \quad (79)$$

where Θ is the elevation of the spacecraft in degrees and

$$\begin{aligned} PFD_{low} &= -126 \text{ dBW/m}^2/\text{MHz} \\ PFD_{high} &= -113 \text{ dBW/m}^2/\text{MHz} \end{aligned} \quad (80)$$

The power received by a terminal with bandwidth W and antenna gain G_t at wavelength λ is:⁹

$$P = PFD \cdot W \cdot \frac{\lambda^2}{4\pi} \cdot G_t \text{ watts} \quad (81)$$

⁹ For a discussion of the relationship between received power and spatial power density (watts/m²), see e.g. Jordan and Balmain, *Electromagnetic Waves and Radiating Systems*, p. 377, second edition, Prentice-Hall, 1968.

Assuming, as does Globalstar, a 0-dB antenna gain for the ATC terminal, and using $W = 1.25$ MHz and $I = 0.125$ m (corresponding to a frequency of 2.4 GHz), the received power levels are:

$$\begin{aligned} P_{low} &= -124 \text{ dBm} \\ P_{high} &= -111 \text{ dBm} \end{aligned} \quad (82)$$

Note that these levels are 6 dB higher than those calculated by Globalstar (p. 18, Fig. 1-11). The reason for this discrepancy is unclear.

The noise floor of the ATC terminal receiver in dBm is $-114 + 10 \log W_{\text{MHz}} + F = -113 + F$, where F is the receiver noise figure. Terrestrial cellular and PCS terminals typically have noise figures in the range of 6 to 8 dB, giving a thermal noise floor in the range of -107 to -105 dBm. In that case, the power received from the spacecraft causes an increase in the effective noise floor of 1 to 1.5 dB (total effective noise floor of -105.5 to -104 dBm). Because the signal from the spacecraft is fairly weak, the noise figure of the MSS terminal will be lower. If the MSS terminal noise figure is 2 dB, the thermal noise floor would be -111 dBm, which is equal to P_{high} .

Effect of Interference on MSS and ATC Downlink Coverage

To understand downlink interference between MSS and ATC it is worthwhile to illustrate with an idealized case. Figure 23 shows a cluster of 19 ATC cells with base stations arranged in the traditional hexagonal pattern. Without shadowing, the cell boundaries are also hexagonal as shown. The cell radius is r . Of interest is the total power received from the ATC base stations as a function of the distance d from one of the outer cells; that is, beyond the coverage area of the ATC cluster. P_{rx} denotes the power from the base station of the middle cell on the far right, shown as the starting point of the arrow. I_{oc} is the other-cell interference as seen by a terminal connected to that cell, which is the sum of the power from all other base stations. The interference power seen by an MSS terminal outside the cluster is $P_{rx} + I_{oc}$. It is assumed for this idealized case that there is no shadowing, and that the desired signal power for the ATC system at the cell edge is $P_{\min} = P_{rx}(r) = N_{MSS}$, the thermal noise floor of the MSS terminal. With the addition of the ATC interference, the effective MSS terminal noise floor is $N_{MSS,eff}(d) = N_{MSS}(d) + P_{rx}(d) + I_{oc}(d)$. The result is shown in Figure 24, with $d/r = 0$ being the location of the ATC base station.

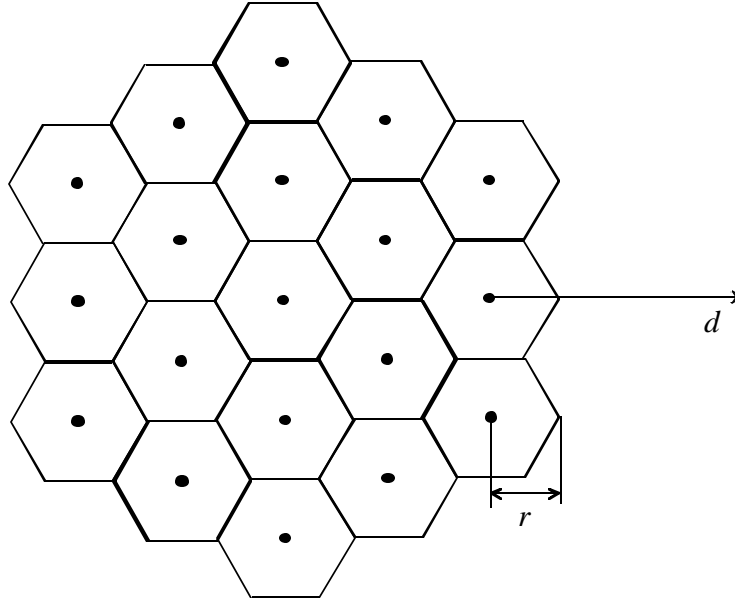


Figure 23: Idealized ATC cell cluster (19 cells)

At the edge of the ATC cluster ($d/r = 1$), $N_{MSS,eff}$ is about 3 dB above N_{MSS} , but one ATC cell radius from the ATC cluster edge ($d/r = 2$), $N_{MSS,eff}$ is only about 0.8 dB above N_{MSS} . At a distance of two cell radii from the cluster edge ($d/r = 3$), the excess is only about 0.3 dB. Obviously, if there is blockage between the nearest ATC base station and the MSS terminal, the interference is reduced.

Figure 25 shows the result if P_{min} is 6 dB above N_{MSS} . This might apply if the ATC terminal noise figure is 6 dB higher than that of the MSS terminal (e.g., 2 dB for the MSS terminal and 8 dB for the ATC terminal), and the ATC system is designed such that $P_{min} = N_{ATC}$. In this case, the excess noise to the MSS receiver is about 1.1 dB two cell radii from the cluster edge, dropping to about 0.6 dB three cell radii away.

It is also useful to consider the effect of the MSS downlink interference on the ATC terminal for the same scenario, as shown in Figure 26. In this case, it was assumed as above that $P_{min} = N_{ATC}$; that is the desired signal power at the ATC cell edge equals the ATC terminal noise floor. It was also assumed that $I_{os} = N_{ATC}$; that is, the MSS downlink interference is equal to the ATC terminal noise floor. Figure 27 shows the result if I_{os} is 6 dB below N_{ATC} .

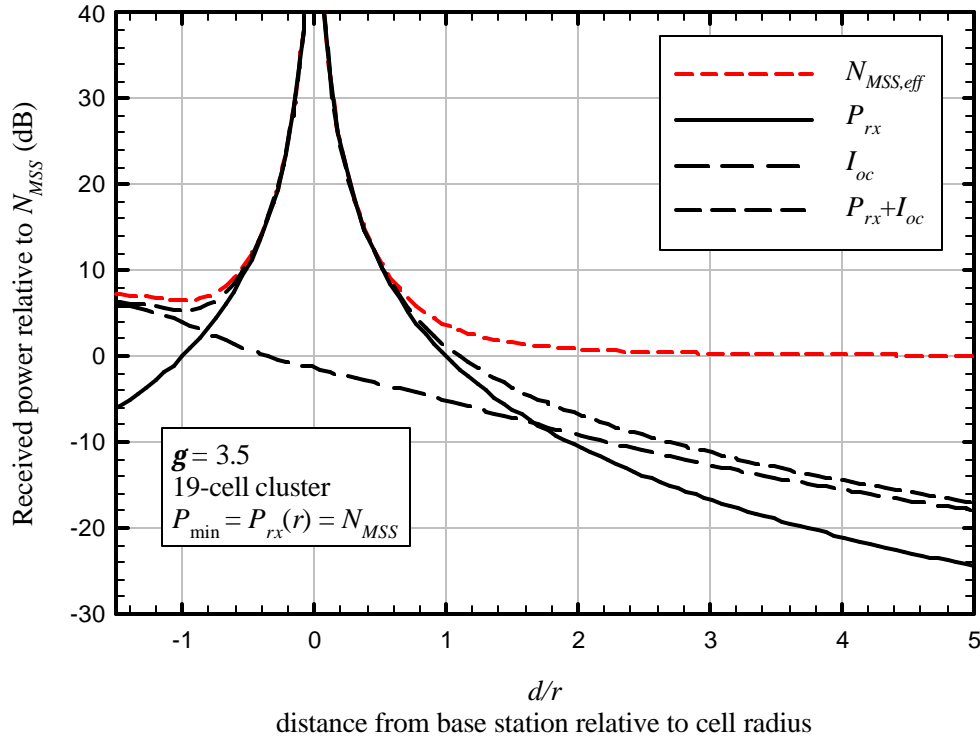


Figure 24: Received ATC downlink power and effective MSS terminal noise floor

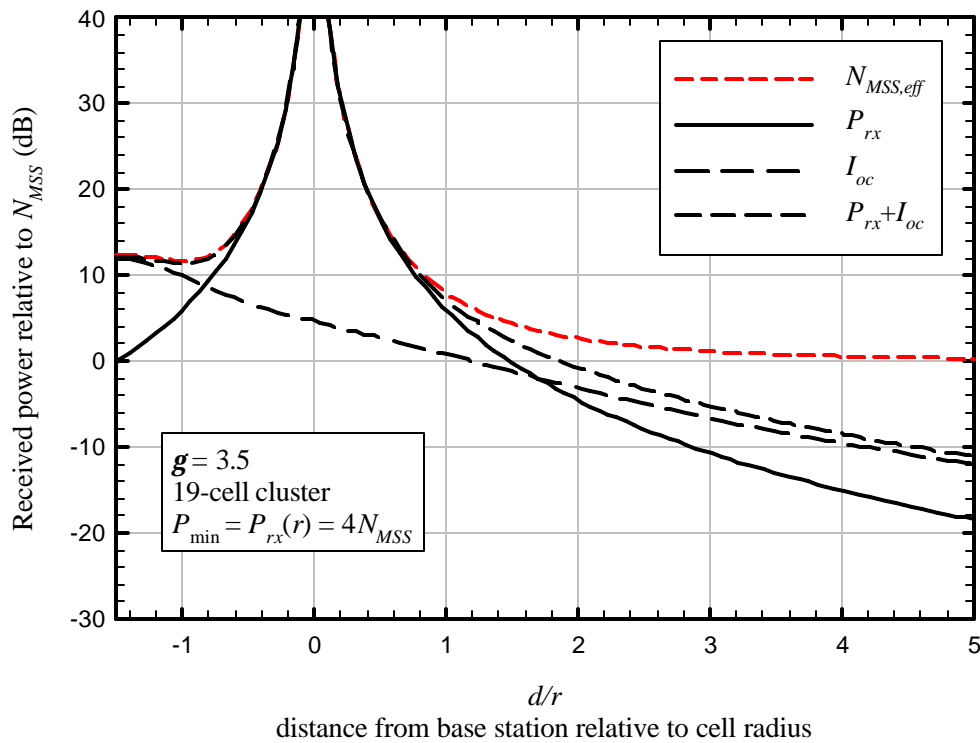


Figure 25: Received ATC downlink power with P_{min} 6 dB above N_{MSS}

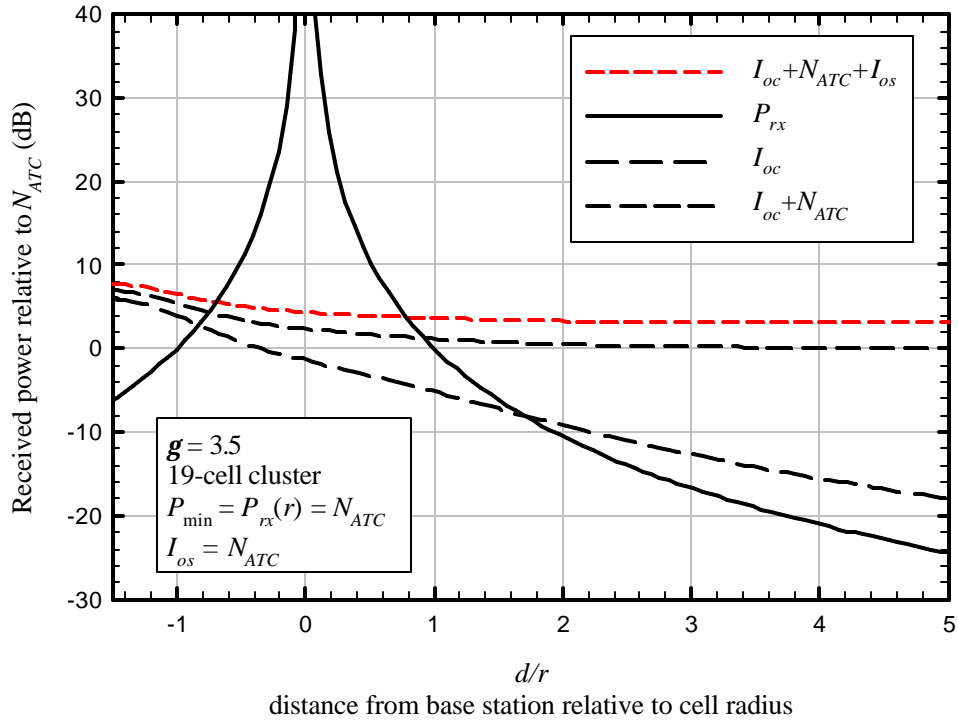


Figure 26: Total noise plus interference to the ATC terminal

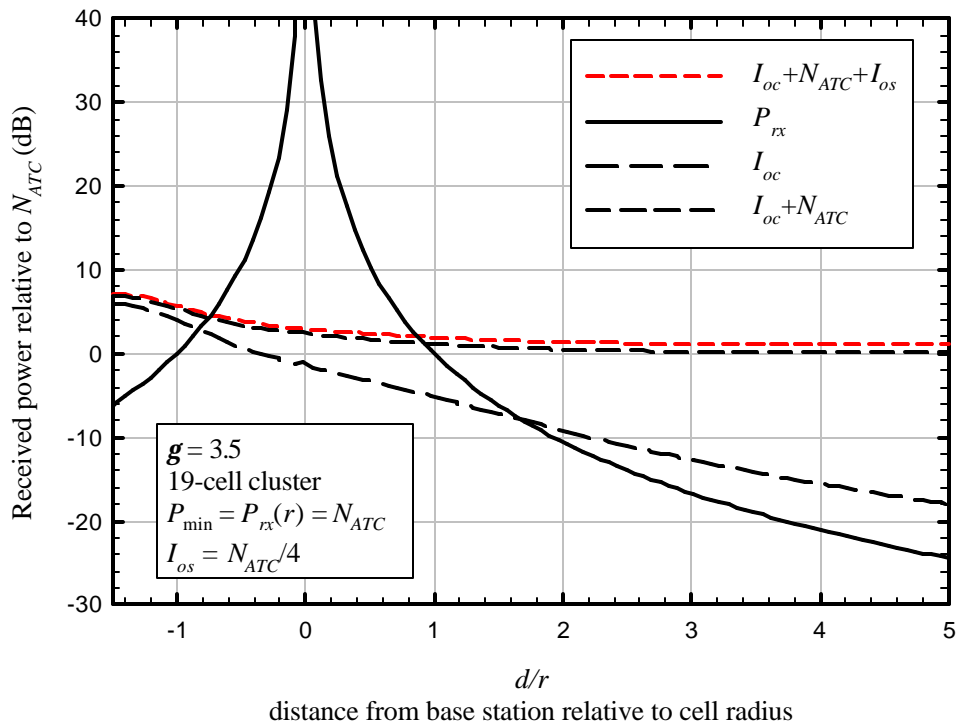


Figure 27: ATC noise and interference with I_{os} 6 dB below the ATC noise floor

The situation can be improved for the MSS terminal if the ATC downlink power at the cell cluster edge is reduced. Figure 28 shows the result if P_{\min} is 6 dB below the MSS terminal noise floor. At the edge of the ATC cell cluster, $N_{MSS,eff}$ is only about 1.1 dB above N_{MSS} , and one cell radius away from the edge, the excess has dropped to about 0.2 dB. However, this improvement is gained at the expense of the ATC system, as shown in Figure 29. In this case, it is assumed that the MSS and ATC terminal noise figures are equal; that is, $N_{ATC} = N_{MSS}$. Again, N_{MSS} is assumed equal to I_{oc} as seen by the ATC terminal (-111 dBm).

Not surprisingly, there seems to be a tradeoff between the impact of the MSS downlink on the ATC terminals, and the ATC downlink on the MSS terminals. However, since the PFD from the spacecraft is limited and the ATC network has yet to be built, it seems reasonable to make this tradeoff in favor of the MSS downlink.

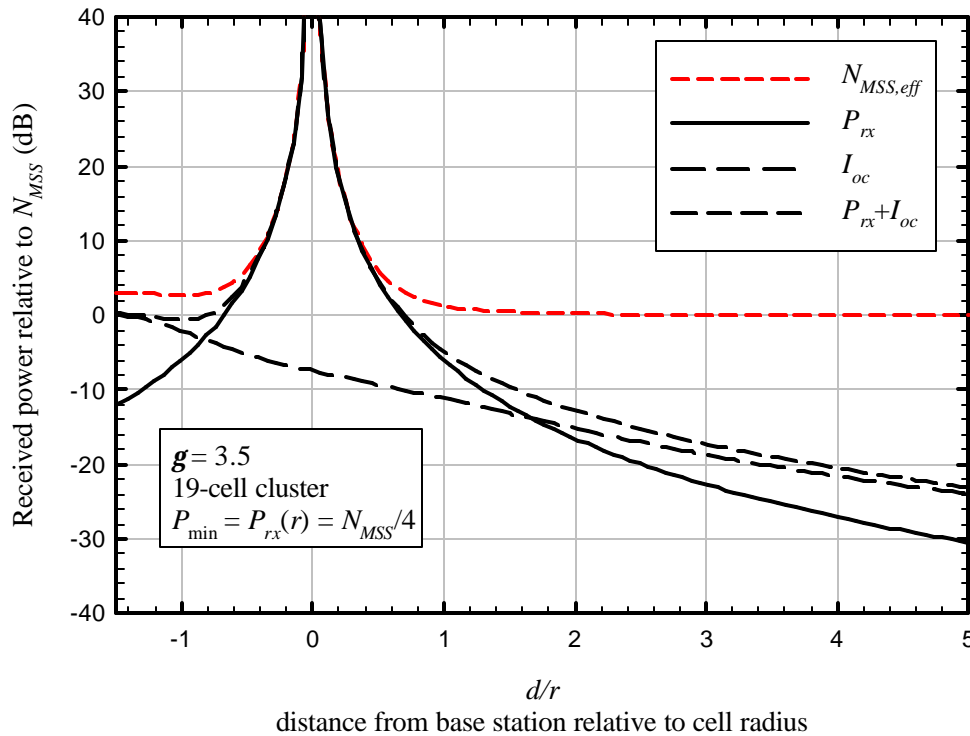


Figure 28: ATC interference to MSS downlink if P_{\min} is 6 dB below N_{MSS}

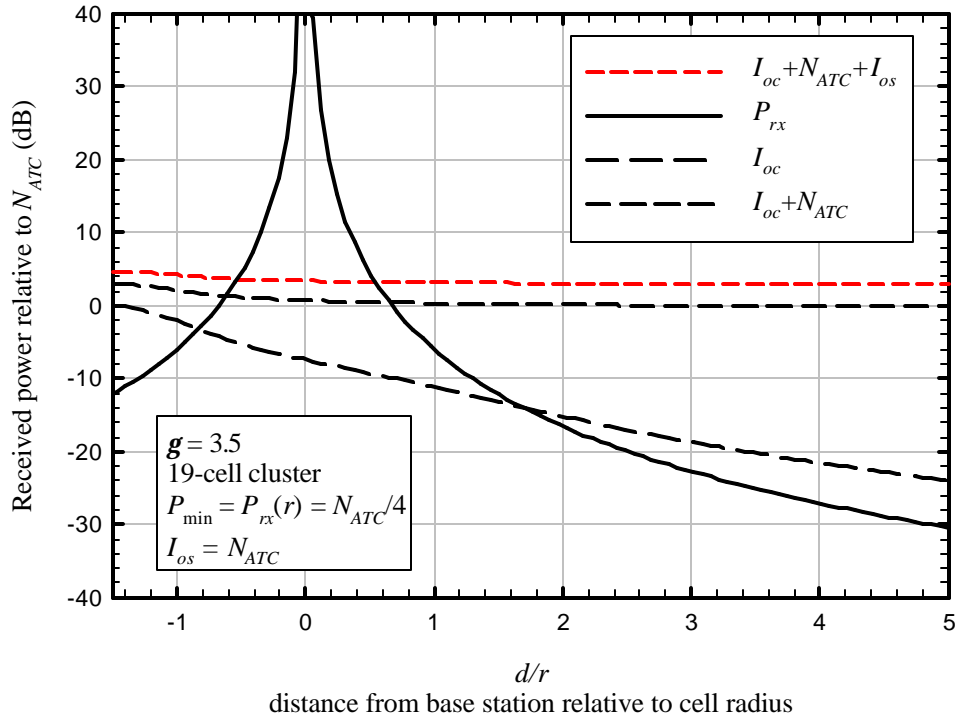


Figure 29: ATC noise and interference with I_{os} and N_{ATC} 6 dB above P_{min}

At this point, it might be observed that the concept of a “cell edge” for the ATC base station is somewhat arbitrary, and the effect of reducing the ATC base station power output is simply to reduce the cell coverage. This would be true if overhead channel allocations and other-cell interference were held constant. For example, reducing the power as shown in Figure 29 would seem to reduce the effective radius to the point at which $P_{rx} = N_{ATC} + I_{os}$, or roughly $d/r \approx 0.5$ for the outer cell edge. However, the other-cell interference is significantly (nearly 10 dB) less on the cell edge on the outside of the cluster ($d/r = 1$) than on the opposite (inside) edge ($d/r = -1$) for obvious reasons. This clearly works to the advantage of the ATC cell. In addition, the overhead channel power allocations can be increased to provide coverage at $d/r = 1$, albeit at the expense of capacity.

ATC Cluster Outer-Cell Overhead Channel Power Allocation Requirements

Figure 30 shows the total downlink overhead channel allocations obtained using $Y_{oc\ max} = 0.3$, the value at $d/r = 1$, and Figure 31 shows the actual received power levels for each of the overhead channels, for $b = 0.5$. Comparing Figure 30 to Figure 18, it is clear that the effect of the reduction in $Y_{oc\ max}$ is the most pronounced at high P_{min}/N , where other-cell and in-cell (for $b > 0$) interference are the dominant impairments. As P_{min}/N , or in the case of Figure 30, $P_{min}/(N + I_{os})$, is reduced, the effect of reducing $Y_{oc\ max}$ decreases. However, even for $P_{min}/(N + I_{os}) \approx -9$ dB as in Figure 29, there is still

some benefit; the reduction in $Y_{oc\ max}$ allows \mathbf{a}_{oh} to be reduced from about 0.47 to 0.38, resulting in a mild (17%) increase in the power available for traffic channels. Nonetheless, there will still be a significant reduction of the traffic capacity of the outer ATC cell, compared to that of a stand-alone terrestrial system. In addition, the total coverage of the cell will shrink as well, because at the inside edge, the other-cell interference is greater, and the overhead channel allocations that are adequate for $d/r = 1$ are too low for $d/r = -1$.

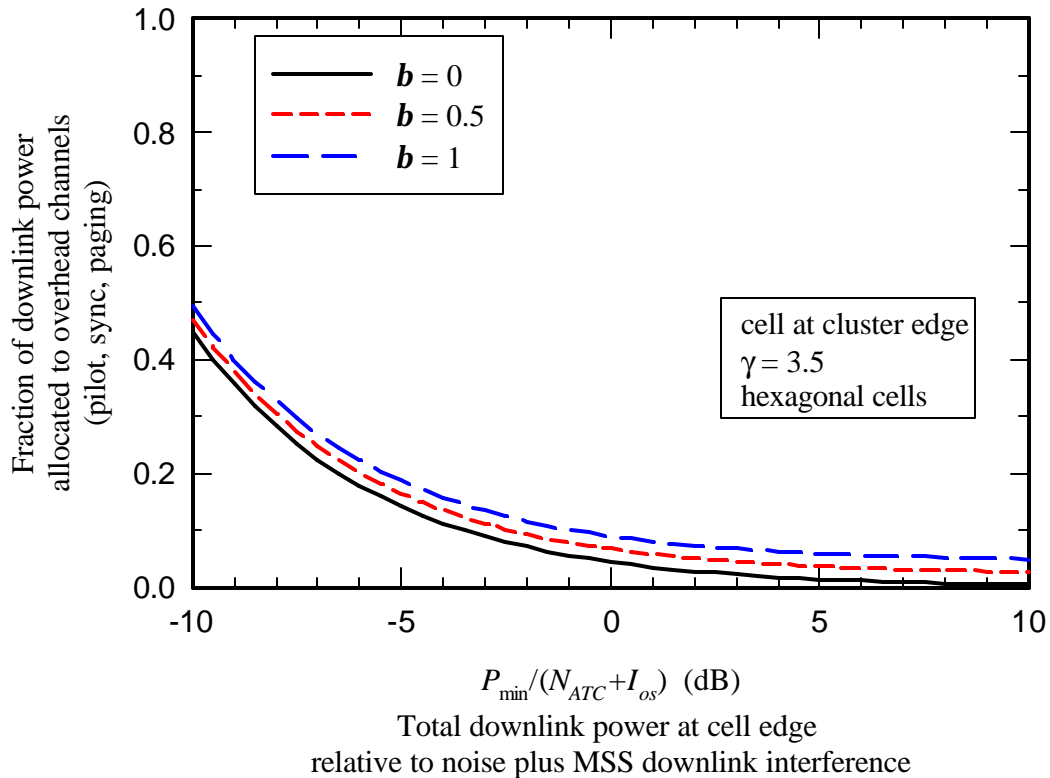


Figure 30: Overhead power allocations for the outside edge of a cluster-edge cell

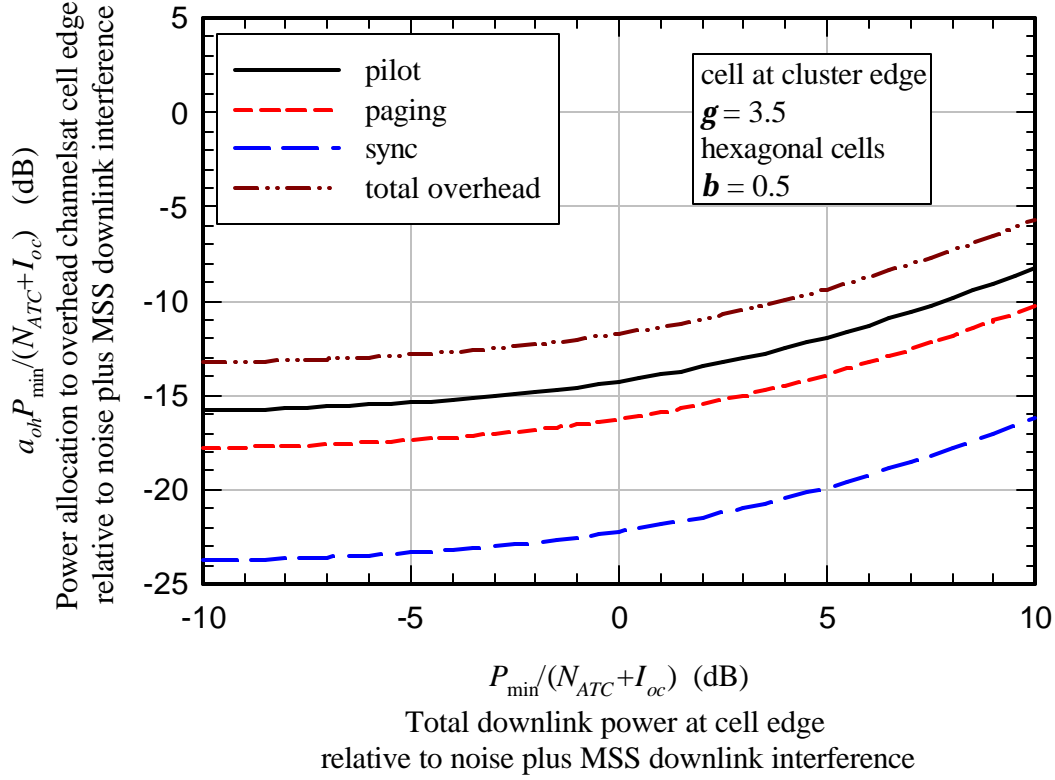


Figure 31: Receiver overhead channel power at cell edge for a cluster-edge cell

Effect of Adjusting the ATC Outer Cell Pilot Power

It is instructive to explore combinations of ATC/MSS power balancing and ATC overhead channel allocations for the outer ATC cells to eliminate coverage gaps between the ATC and MSS systems. For the ATC system, the pilot SINR is

$$\Gamma_{p,ATC} = \frac{\mathbf{a}_{p,ATC} P_{ATC}}{N + \mathbf{b}(1 - \mathbf{a}_{p,ATC}) P_{ATC} + I_{oc,ATC} + I_{MSS}} \quad (83)$$

where $\mathbf{a}_{p,ATC}$ is the fraction of the downlink power allocated to the ATC pilot.

For the MSS system, it is

$$\Gamma_{p,MSS} = \frac{\mathbf{a}_{p,MSS} P_{MSS}}{N + I_{oc,MSS} + I_{ATC}}. \quad (84)$$

Note it has been assumed that $\mathbf{b} = 0$ for the MSS system, and that a new term, $I_{oc,MSS}$, has been introduced to represent the downlink power received from other MSS beams.

Letting $Y_{oc,MSS} = I_{oc,MSS}/P_{MSS}$, with $\Gamma_{p0,MSS}$ representing the pilot SINR with no ATC interference, (84) can be written as:

$$\Gamma_{p,MSS} = \frac{\Gamma_{p0,MSS}}{1 + \frac{I_{ATC}/P_{MSS}}{N/P_{MSS} + Y_{oc,MSS}}} \quad (85)$$

with

$$\Gamma_{p0,MSS} = \frac{\mathbf{a}_{p,MSS}}{N/P_{MSS} + Y_{oc,MSS}} \quad (86)$$

It seems reasonable to assume that $Y_{oc,MSS}$ is on the order of 3 dB (a factor of 2), representing the downlink signals from two interfering beams. Sensitivity to this assumption will be explored.

Figure 32 shows an example of the ATC and MSS pilot SINRs as seen by a terminal with a noise floor N_{MSS} , which in this example is assumed equal to the received MSS (desired signal) power P_{MSS} . ATC power is assumed balanced so that the received ATC downlink at $d = r$ is also equal to the terminal noise floor. Both the ATC and MSS pilot allocations were assumed to be 10%.

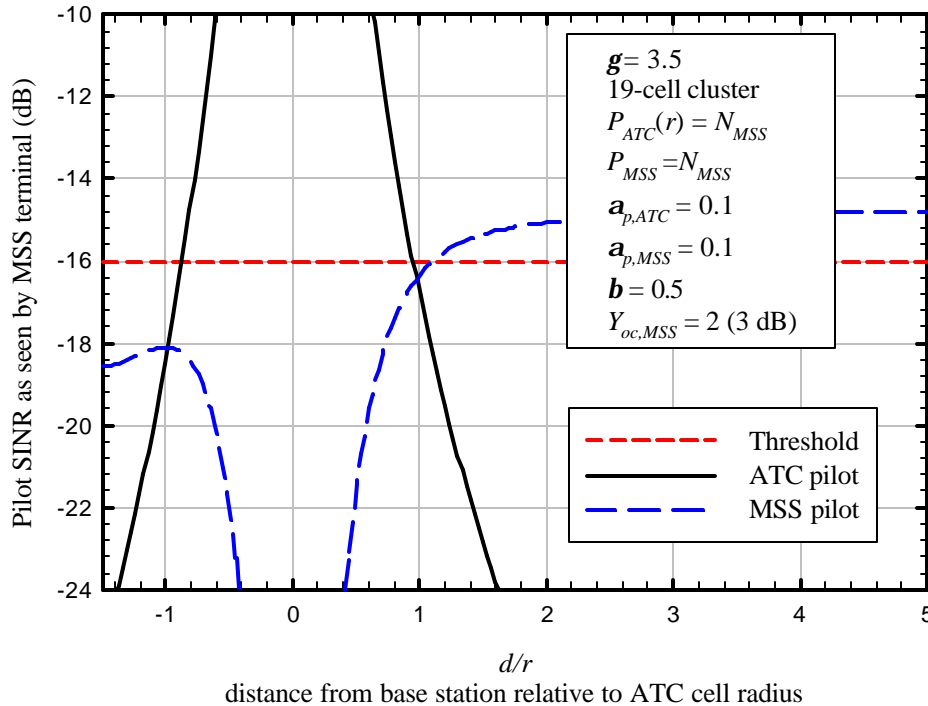


Figure 32: ATC and MSS pilots as seen by an MSS terminal

Also shown in the pilot SINR threshold, assumed to be -16 dB here. This represents the coverage limit. Note that there is a small gap between the ATC and MSS coverage. Also, coverage on the inside of the ATC cell does not extend all the way to the cell boundary ($d/r = -1$). Both problems can be solved by increasing the ATC pilot allocation (and those of the other overhead channels as well), as shown in Figure 33.

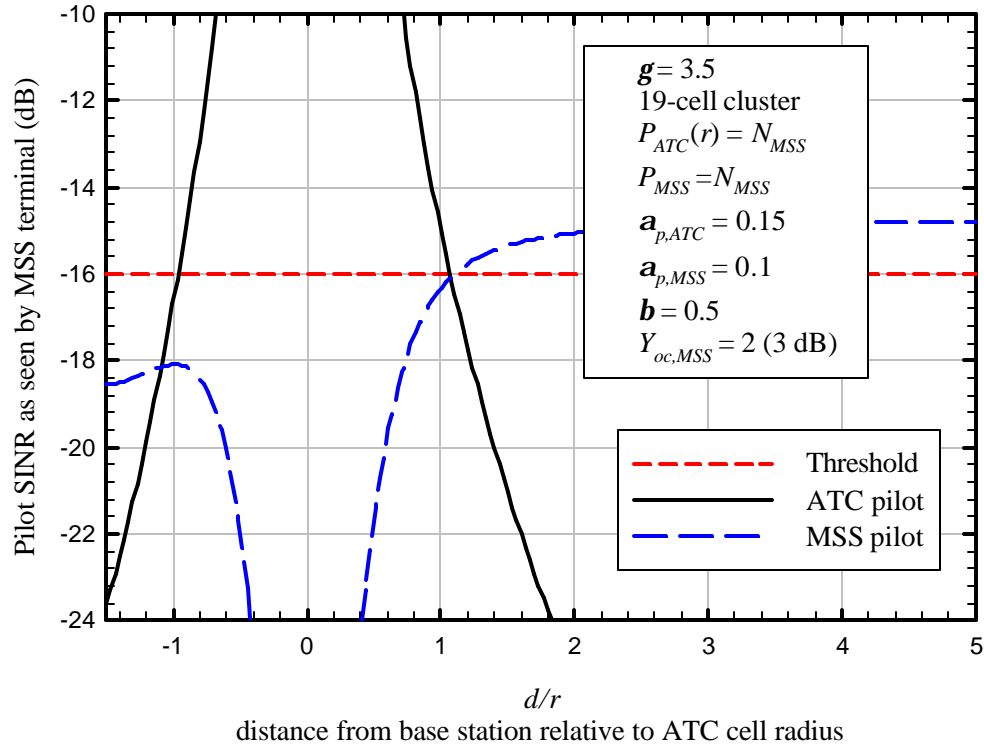


Figure 33: Effect of increasing the ATC pilot power allocation to 15%.

Figure 34 shows the results if $Y_{oc,MSS} = 1$. From (86), it is clear that the effect is to increase $\Gamma_{p0,MSS}$ by a factor of 1.5, or about 1.8 dB, which seems to be the case from comparison with Figure 33 ($\Gamma_{p0,MSS} \rightarrow \Gamma_{p0,MSS}$ for $d/r \gg 1$).

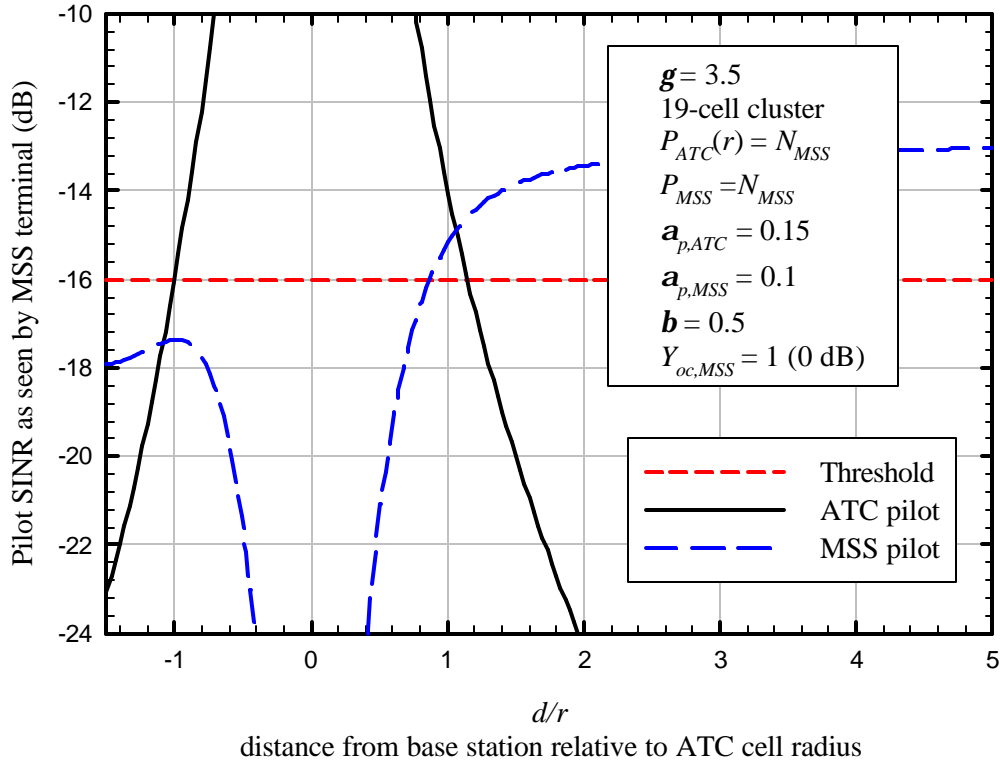


Figure 34: Effect of reducing $Y_{oc,MSS}$

In the MSS system design, $\mathbf{a}_{p,MSS}$ would likely be set to provide adequate pilot SINR for the worst-case value of $Y_{oc,MSS}$, plus a margin. This can be reflected in the analysis by setting the margin instead of $\mathbf{a}_{p,MSS}$. In that way, determination of $\mathbf{a}_{p,MSS}$ is automatic, depending on the assumed worst-case value of $Y_{oc,MSS}$. If $\Gamma_{p\min}$ is the minimum acceptable pilot SINR (assumed -16 dB here), and \mathbf{d}_m is the allowed margin, then $\Gamma_{p0,MSS} = \mathbf{d}_m \Gamma_{p\min}$. Figure 35 shows the effect of using a 2-dB margin; that is $\Delta_{\Gamma,MSS} = 10 \log \mathbf{d}_{\Gamma,MSS} = 2$ dB. In this case, $Y_{oc,MSS} = 2$ and $\mathbf{a}_{p,ATC} = 0.1$. It is clear from (85) that if a fixed margin is used, the effect of the ATC interference decreases as $Y_{oc,MSS}$ increases. To illustrate, Figure 36 shows the result if $Y_{oc,MSS} = 4$ (6 dB). While the MSS and ATC pilot SINRs cross above the threshold in Figure 35 and Figure 36, the ATC pilot still must be increased (above 10%) to provide full coverage on the inside of the cell.

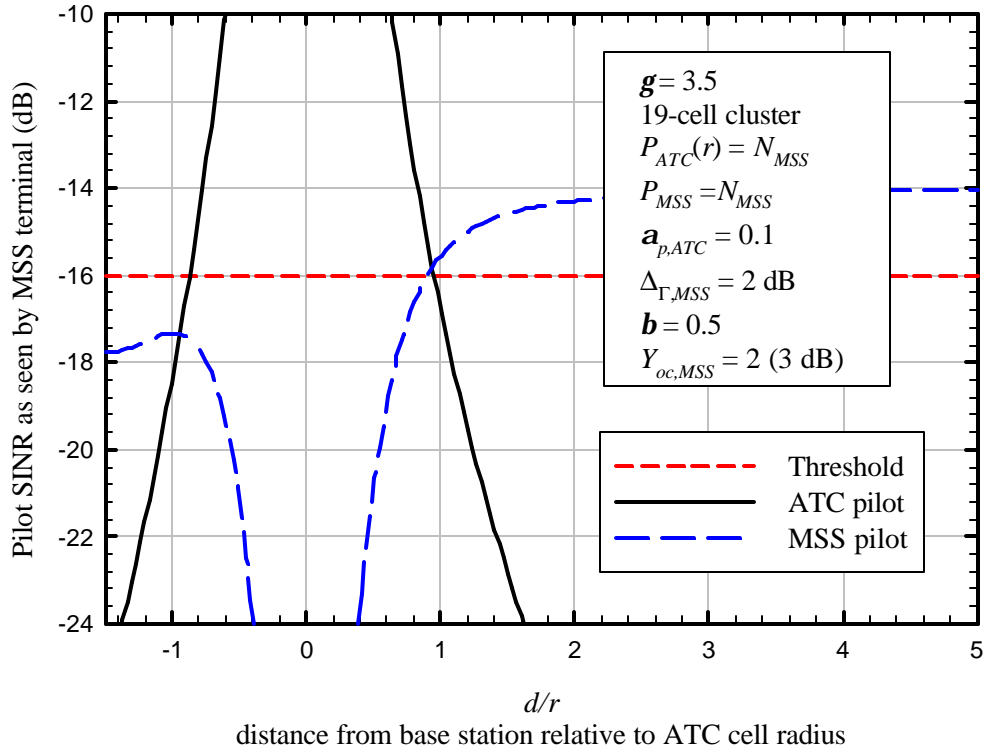


Figure 35: Use of a pilot SINR margin for the MSS downlink

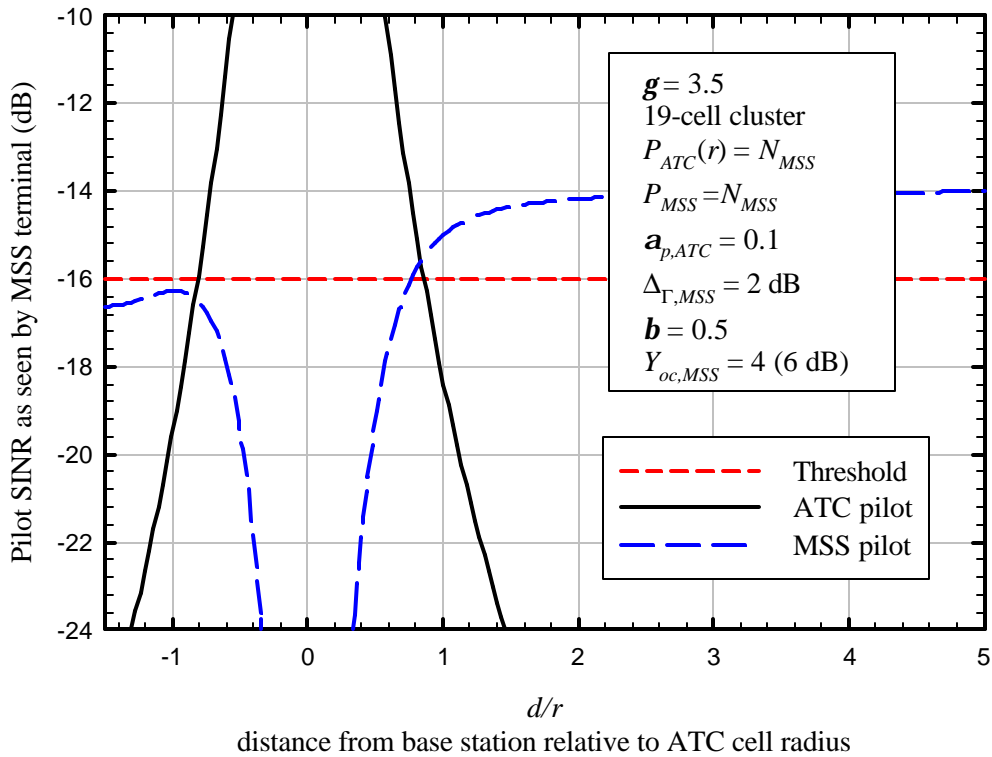


Figure 36: Effect of increasing $Y_{oc,MSS}$ to 6 dB with a 2-dB MSS pilot SINR margin

The assumption that the terminal receiver noise is equal to the received MSS downlink signal (-111 dBm) is consistent with an MSS terminal with a very low-noise front end (e.g., 2 dB noise figure). ATC terminals typically have higher noise figures, in the range of 6-8 dB. Figure 37 shows the results if the terminal noise floor is 6 dB above the ATC downlink power at the cell edge (compare with Figure 33). As can be seen, the coverage of the ATC has shrunk slightly, and the MSS system provides no coverage at all. This suggests that it might be desirable for ATC terminals to use the same low-noise front end as MSS terminals. Of course, it would be possible for terminals to switch between an MSS mode (low noise) and an ATC mode (de-sensed front end), but there seems to be little benefit, and the de-sensed ATC terminals would require higher traffic channel power allocations in the outer regions of the cell, reducing overall capacity.

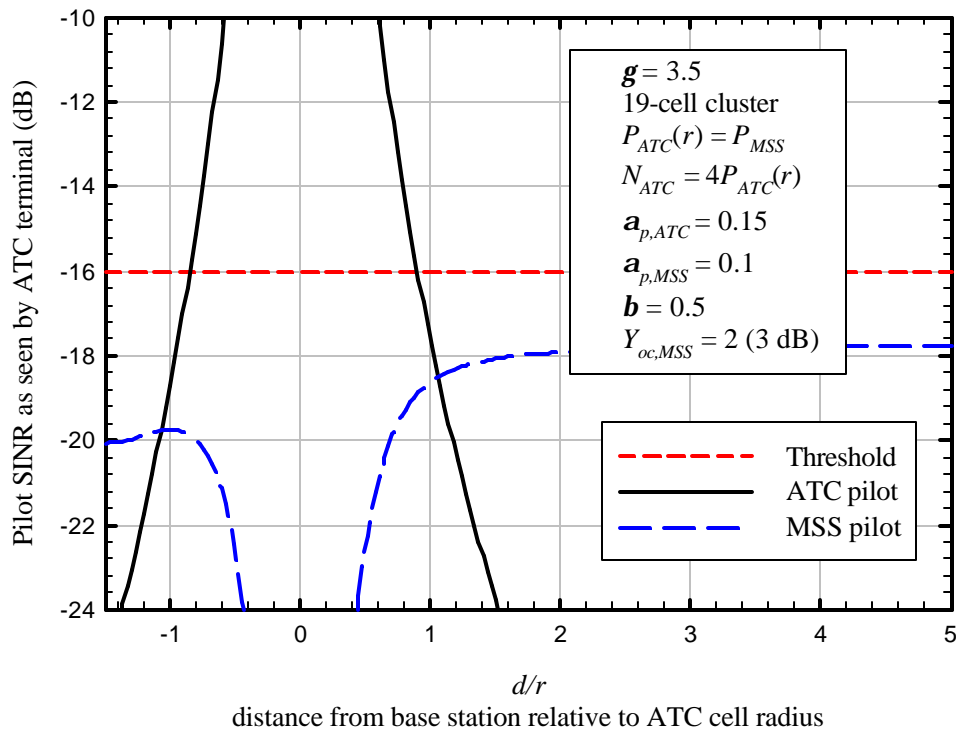


Figure 37: Pilot SINR seen by an ATC terminal with an 8-dB noise figure

There are clearly a large number of parameter combinations that could be explored. However, it seems clear from the examples given here that it is technically feasible to provide continuous coverage at the ATC/MSS boundary, based on available overhead channel power. It may be necessary to increase the overhead channel allocations for the outer cells of the ATC cluster, but the examples given here suggest that the required increase would be modest. If the overhead allocations are increased to 30% total, compared to the 20% typical of stand-alone terrestrial systems, the total allocation available to traffic channels is reduced from 80% to 70%, a 12.5% reduction. The reduction in the traffic capacity might be slightly larger, due to the effect of the MSS interference on ATC terminals near the boundary. However, the ATC downlink power increases rapidly as the distance to the base station decreases, so the traffic channel

power allocation required by terminals not near the boundary will not be affected much by the MSS downlink interference. Further, if the ATC system is deployed to serve weak MSS coverage areas, most of the terminals linked to the ATC cell will be blocked to the spacecraft and the MSS downlink interference will be insignificant. The MSS downlink interference will therefore affect the required ATC traffic channel power allocation only to those terminals near the ATC/MSS boundary.

The capacity impact on the MSS system will be even less. In the case studied here, with equal received downlink power levels from the ATC base and the MSS spacecraft at the ATC cell edge, with $Y_{oc,MSS} = 2$, the ratio of desired to undesired power for the MSS downlink at the ATC cell edge is reduced by only about 1.6 dB compared to its value without the ATC interference (this is evident from the curve for the MSS pilot in Figure 33). This corresponds to an increase of about 44% in the required traffic channel power allocation, compared to the case without ATC interference. Because of the low density of the MSS terminals relative to the ATC cell size, few MSS terminals are likely to be near enough to an ATC cell to require any significant traffic channel power allocation increase as a result of ATC interference.

FDMA/TDMA

Unlike CDMA systems, time-division multiple access (TDMA) and frequency-division multiple access (FDMA) systems use the dimensions of time and frequency to distinguish among different user channels. A “channel” is a specific timeslot on a particular carrier frequency. FDMA/TDMA frequency reuse systems are based on the principle that two terminal/base station pairs can use the same channel if they are sufficiently spatially separated to maintain a high enough carrier-to-interference ratio (C/I). Many of the geometry-dependent results from the CDMA analysis also apply for analysis of FDMA/TDMA systems, but the interference analysis is different (and less complex), and will be explained here. Without loss of generality, FDMA can be assumed.

Frequency Reuse and Capacity: Basic Relationships

Assume that there are M channels available and the bandwidth per channel is W , so the total bandwidth available per direction (uplink/downlink) is MW . In the original cellular systems, the M available frequency channels were divided into K groups. Typically, groups are assigned to cells in a spatial reuse pattern, as shown in Figure 38 for $K = 3$.

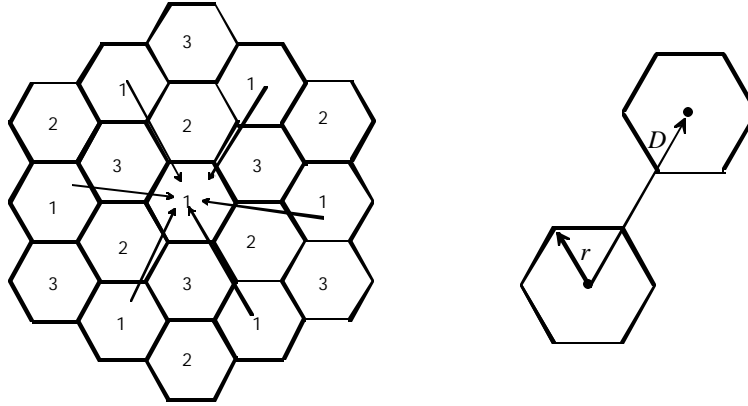


Figure 38: Example of frequency group assignments for $K = 3$

The *reuse factor*, denoted F_r , represents the fraction of cells in which a given RF channel can be simultaneously used. Thus, the maximum number of channels that can be supported per cell is

$$M_{cell} = F_r M \text{ channels/cell} \quad (87)$$

With a fixed 3-cell reuse pattern, $F_r = 1/3$.

If r is the cell radius (center to vertex for hexagonal cells) and D is the distance from a base station to the nearest cochannel base station (i.e., that uses the same frequency group), then the ratio D/r is related to K by the well-known formula [5]:

$$D/r = \sqrt{3K} . \quad (88)$$

Since there are 6 cochannel cells at that distance, if g is the path loss exponent, then the carrier-to-interference ratio at the cell edge is roughly

$$\frac{C}{I} \cong \frac{1}{6} \left(\frac{D}{r} \right)^g = \frac{1}{6} (3K)^{g/2} . \quad (89)$$

This clearly is an approximation, because the mobile at the cell corner will be nearer to some cochannel bases than D , and further away from others. The table below show C/I based on interference from the first tier of cochannel cells (which contributes most of the interference), computed based on the actual distance between each interfering cell and a mobile on a vertex of the center cell, for $g = 3.5$.

K	C/I exact	C/I approx.
3	7.3 dB	8.9 dB
4	10	11.1
7	14.7	15.4
9	16.8	17.3
12	19.1	19.4

In terms of the reuse factor,

$$\frac{C}{I} = \frac{1}{6} \left(\frac{F_r}{3} \right)^{-g/2} \quad (90)$$

For terrestrial frequency-reuse systems, a generalized form of this relationship holds, even for systems that have no fixed frequency assignments (e.g., use some form of dynamic channel assignment):

$$\frac{C}{I} = k F_r^{-g/2}, \quad (91)$$

where k is a constant that depends on g as well as the channel assignment algorithm and other factors that determine the statistics of the interference, such as the discontinuous transmission, power control, and frequency hopping options with GSM. With the fixed frequency assignment example above, $k = 3^{g/2}/6$. With another approach to channel selection, k will be different but the general relationship still holds. It should be noted that (91) applies individually to the forward and reverse links; the one with the lower reuse will be the limiting factor on overall capacity.

The reuse factor should be as large as possible, while still meeting the carrier-to-interference requirements. For adequate signal quality, the carrier-to-interference ratio must meet or exceed some threshold Γ_0 . Thus, the C/I threshold is related to the maximum reuse factor by

$$F_{r\max} = \left(\frac{k}{\Gamma_0} \right)^{2/g}; \quad (92)$$

that is, the lower the necessary carrier-to-interference ratio, the better the reuse (cochannel users can be packed closer together, relative to the cell size). This motivates the use of baseband signal processing techniques such as error-correction coding in second-generation digital wireless systems.

Effect of Thermal Noise on Reuse

If the thermal noise is included, then the requirement is $C/(I + N) \geq \Gamma_0$, where N is the noise power at the receiver. The cochannel interference I is still related to the desired signal power and the reuse factor by (91), that is:

$$I = \frac{CF_r^{g/2}}{k}, \quad (93)$$

so the achievable reuse, including the effect of noise, is reduced to:

$$F_{r,N} = \left[k \left(\frac{1}{\Gamma_0} - \frac{N}{C} \right) \right]^{2/g}. \quad (94)$$

The reduction in reuse due to the noise is

$$\frac{F_{r,N}}{F_{r,\max}} = \left(1 - \frac{1}{\Delta_\Gamma} \right)^{2/g}, \quad (95)$$

where $\Delta_\Gamma = C/\Gamma_0 N$. Figure 39 shows $F_{r,N}/F_{r,\max}$ vs. Δ_Γ .

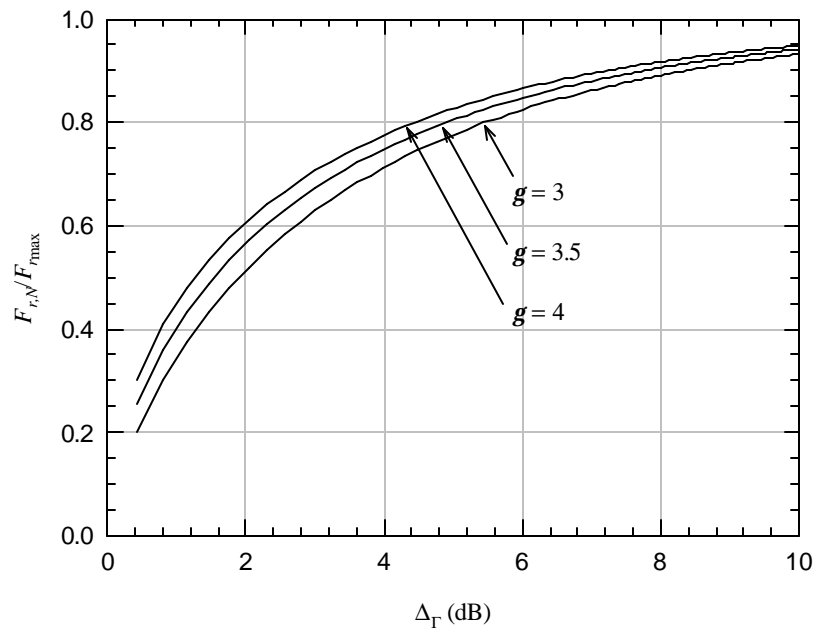


Figure 39: Reuse reduction vs. carrier-to-noise ratio at the cell edge.

Cellular Examples

As an example, assume that a system is designed for $\Delta_{\Gamma} = C/\Gamma_0 N = 6$ dB. For GSM, the channel bandwidth is 200 kHz. With an 8-dB noise figure, $N = -113$ dBm. If $\Gamma_0 = 15$ dB (this is the local mean carrier-to-interference threshold, averaged over the multipath-related variations), then for the downlink, $C = -92$ dBm. Assuming fixed frequency group assignments with 3 sectors per cell, and $g = 3.5$, then $k = 3^{g/2}/2 = 3.45$ (since interference comes mainly from two nearest cochannel sectors rather than 6 nearest cochannel cells), and $F_{r_{\max}} = 0.289$. Since, for $\Delta_{\Gamma} = C/\Gamma_0 N = 6$ dB and $g = 3.5$, $F_{r,N}/F_{r_{\max}} = 0.85$, $F_{r,N} = 0.85 \times 0.289 = 0.246$, and $1/F_{r,N} = 4.07$. Many GSM systems do in fact use a 4-cell, 3-sector frequency assignment pattern.

As a second example, consider an IS-136 system with a 30-kHz bandwidth (so $N = -121.2$ dBm) and $\Gamma_0 = 18$ dB. Assuming as above that $\Delta_{\Gamma} = C/\Gamma_0 N = 6$ dB, $C = -97.2$ dBm at the cell edge for the downlink. Again assuming 3-sector cells and $g = 3.5$, $k = 3.45$ and $F_{r_{\max}} = 0.19$. With $F_{r,N}/F_{r_{\max}} = 0.85$, $F_{r,N} = 0.16$, and $1/F_{r,N} = 6.2$, which rounds up to a 7-cell reuse pattern (allowable reuse pattern values are $K = i^2 + ij + j^2$, where i and j are integers [5], so 7 is the nearest allowed pattern). In fact most AMPS and IS-136 systems use a 7-cell, 3-sector pattern.

These calculations suggest that for the GSM system, a slightly greater value of Δ_{Γ} would be used at the cell edge, so that $1/F_{r,N} \leq 4$, and for the IS-136 system, Δ_{Γ} could be reduced somewhat. Note that for the IS-136 system, even if $\Delta_{\Gamma} \rightarrow \infty$ so that $F_{r,N} \rightarrow F_{r_{\max}}$, the achievable reuse (0.19) is still not large enough to use a 4-cell pattern ($1/0.19 = 5.26$).

In practice, cell design and layout is more complex, but these simple calculations serve to illustrate the basic principles for fixed-frequency terrestrial systems.

Frequency Reuse with MSS Systems

For MSS systems, the achievable reuse will also depend on Γ_0 , the minimum C/I but obviously not on the terrestrial path loss exponent. Instead, it will depend on the discrimination (rolloff) of the antenna beam pattern and beam overlap. ICO has indicated that with its system, the required C/I is 12.8 dB and the effective reuse factor is $1/4$ [3].

The frequency reuse relationships can easily be generalized to apply to systems not governed by terrestrial path loss, using:

$$\frac{C}{I} = G(F_r) \quad (96)$$

where $G(\cdot)$ is a function that depends on the mechanism by which cochannel interference is introduced into a receiver. In the case of a terrestrial system, the mechanism is propagation over the surface of the Earth. With MSS, the mechanism is finite beam antenna pattern rolloff. Therefore, in the MSS case, the function $G(\cdot)$ is determined by the SC service link antenna pattern.

Relationships that are generalized versions of those above that then be expressed as:

$$F_{r\max} = G^{-1}(\Gamma_0) \quad (97)$$

$$I = \frac{C}{G(F_r)} \quad (98)$$

$$F_{r,N} = G^{-1}\left(\frac{\Gamma_0}{1 - 1/\Delta_\Gamma}\right) \quad (99)$$

$$\frac{G(F_{r\max})}{G(F_r)} = 1 - \frac{1}{\Delta_\Gamma} = 1 - \frac{\Gamma_0 N}{C} . \quad (100)$$

Thus, as in the terrestrial case, C/N affects the reuse.

The important point here is that with a fixed frequency-reuse plan, be it for a terrestrial system or an MSS system, there is an upper limit on the additive noise that can be tolerated. This is relevant because the ICO system uses a 4-frequency group reuse pattern to assign frequencies to spot beams, and ATC interference will have an effect similar to that of additive noise.

Dynamic Channel Assignment

Many modern FDMA/TDMA systems use dynamic channel assignment (DCA), whereby each base station has the capability to use any available channel. Upon receiving a connection request, a channel can be selected based on its C/I . A conceptually simple approach is to use the least-interfered channel, or at least a channel with an acceptably low interference level. In fact, Subpart 15D of the FCC Rules (sometimes referred to as the “spectral etiquette”), which applies to unlicensed personal communications services (UPCS), requires the use of these techniques to minimize interference among different systems. With DCA on duplex channels, the interference level must be acceptably low to

both ends of the link. This can be verified by a simple exchange of signaling information over a control channel.

Given Γ_0 , DCA improves frequency reuse compared to fixed-frequency assignment. This is because fixed-frequency reuse patterns are necessarily based on a worst-case situation: the terminal at the cell edge, where the desired signal is weakest. A terminal near the base station can tolerate much more interference, and therefore will be able to use channels that a cell-edge terminal cannot. Alternatively, power control can be used to reduce the transmitted power to a level just adequate to achieve the necessary $C/(N + I)$, thereby reducing interference to other cells. Finally, DCA offers a trunking efficiency advantage, because each cell is not limited to a pre-assigned set of channels. Cells experiencing a heavy traffic load can use as many of the available channels with acceptable C/I as necessary, providing the base station has an adequate number of channel service units.

MSS-ATC Interference with FDMA/TDMA

Interference between MSS and ATC using FDMA/TDMA can best be understood by considering the area near an ATC base station. Figure 40 shows the received ATC downlink power $C_{dl,ATC}$, the received MSS downlink power $C_{dl,MSS}$, the thermal noise floor N , and the ATC other-cell downlink interference $I_{dl,ATC}$. For simplicity in this illustration, Δ_r is assumed the same for both systems, and the noise floor N is assumed to be the same for both the ATC-mode and MSS-mode terminals. Also, this illustration assumes that the MSS downlink signal is unblocked over the coverage of the ATC cell. Finally, the MSS and ATC systems are assumed to use the same air interface.

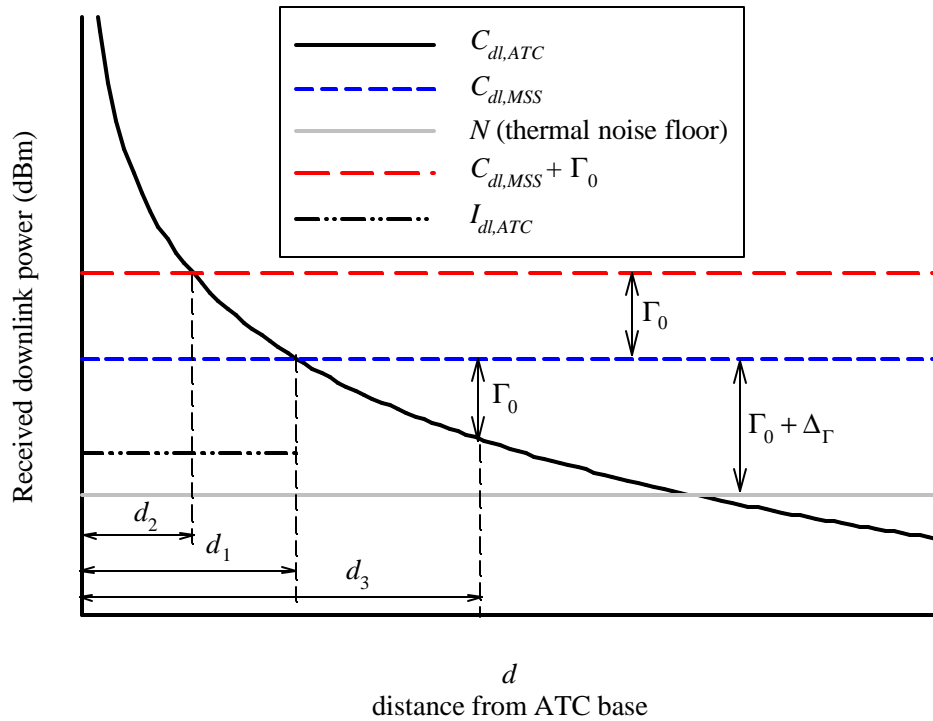


Figure 40: ATC and MSS received downlink power near an ATC base station

For adequate receptions by MSS terminals, the received MSS signal is above the noise floor by $\Gamma_0 + \Delta_\Gamma$ dB on channels being used by the MSS system within the beam of interest. The nominal ATC cell radius, for channels not used by the MSS system in that location, is d_1 , which is assumed here to correspond to the nominal ATC cell edge. For a channel that is used by the MSS system, the received power from the ATC base must exceed the MSS downlink power by at least Γ_0 dB. That is, $C_{dl,ATC,\min} \geq \Gamma_0 C_{dl,MSS}$, resulting in a maximum range of d_2 (the effects of N and $I_{dl,ATC}$ have been ignored here because they are significantly below $C_{dl,MSS}$). As a result, the path loss between the ATC terminal and base has been reduced by Γ_0 dB. Therefore, if the ATC terminals have the capability for high-resolution transmit power control, the ATC terminal transmit power can also be reduced by Γ_0 dB. Regardless of whether this is the case, ATC terminals sharing a channel used by the MSS beam will be restricted to a fraction $\Gamma_0^{-2/g}$ of the ATC cell area. For example, if $\Gamma_0 = 12.8$ dB and $g = 3.5$, coverage will be available for only about the innermost 18.5% of the nominal ATC cell area. If ATC terminals are assumed to be uniformly distributed over this region, and to use transmit power control, the average transmit power would be about 6 dB less than the transmit power required at the edge of the available region (as shown in the CDMA uplink analysis), so the average transmit power would be $\Gamma_0 + 6$ dB less than the transmit power required by an ATC terminal at the nominal ATC cell edge. If the maximum ATC transmit power is assumed to be 20

dBm (100 mW), then the *average* transmit power of an ATC terminal using a channel that is also used by the MSS beam is 1.2 dBm. If the MSS terminal transmit power is 7 dBW (5 watts), as assumed by ICO in its analysis of March 8, 2001, then the average ATC terminal transmit power is 35.8 dB below that of the MSS terminal, and the interference received at the spacecraft is also 35.8 dB below the desired signal from the MSS terminal. Assuming the ATC terminals use transmit power control, the *minimum* C/I would be $P_{ul,MSS} - P_{ul,ATC} + \Gamma_0$ (dB), where $P_{ul,MSS}$ and $P_{ul,ATC}$ transmit power of the MSS terminal and maximum transmit power of the ATC terminal, respectively. In this case, $P_{ul,MSS} - P_{ul,ATC} = 17$ dB.

The net result is that a *new* ATC connection will not cause any significant interference to an *existing* MSS connection. If the ATC terminal is farther away from the ATC base than d_2 , it must use a channel that is unused by the MSS beam. However, existing ATC connections might prevent establishment of a new MSS connection on a channel, so MSS uplink capacity is still affected by the presence of the ATC system. If there are a large number of terminals using a given channel within an MSS beam footprint, that channel may be unavailable to that beam, as is the case with CDMA. The severity of the effect will depend on the number of active ATC terminals and their respective path losses to the SC. If there are a total of J_{ATC} ATC cells within the beam footprint, on average there will be $F_r J_{ATC}$ terminals using a particular channel if cells are all operating at capacity.

For reasons similar to those just discussed for ATC-to-MSS uplink interference, an MSS terminal near the ATC base will not make a new connection on a channel already used by that base, due to the ATC downlink interference. It will instead select a clear channel. As discussed in the CDMA uplink analysis, it is unlikely that an MSS terminal will be near enough to the ATC base to cause significant reduction in the C/I for the ATC uplink. However, even if there is an active MSS terminal near an ATC cell edge, the effect will simply be to make the channel used by the MSS terminal unavailable to the ATC base. Therefore, with FDMA/TDMA, MSS uplink interference will not have a significant effect on the ATC system capacity overall.

Downlink interference effects are fairly obvious from Figure 40. An MSS terminal must be at least distance d_3 from the ATC base to have an adequate downlink C/I on a channel used by the ATC base. If the MSS terminal is farther away from the base than d_3 , and the ATC terminal is closer than d_2 , they can use the same channel from a downlink perspective. Otherwise, they must use different channels.

It is clear from this brief analysis that as with CDMA, ATC-MSS interference effects are confined to areas near the ATC-MSS coverage boundaries, with the exception of ATC terminal interference into the MSS uplink, which does not depend on the location of the MSS terminal, and requires only that the affecting ATC terminals be within the MSS beam footprint. As in the CDMA case, a sufficiently large terrestrial deployment of ATC terminals could significantly impact the capacity of the MSS system.

Dynamic Frequency Coordination Between MSS and ATC

Four interference cases have been analyzed here. Downlink interference impact in both directions (MSS to ATC and ATC to MSS) is confined to areas near MSS-ATC coverage boundaries, and can be managed by proper setting of the ATC downlink power, and in the CDMA case, the overhead channel power allocations for the outer cells of the ATC cluster. MSS-to-ATC uplink interference effects are similarly limited to the area near the coverage boundaries; an MSS terminal must be relatively near the ATC base station to have a significant effect on the ATC uplink, and due to the low density of MSS terminals relative to the ATC cell size, this is a low-probability event. Even in the case of an MSS terminal near an ATC base, the result is the loss of a single channel for an FDMA/TDMA system, and in the CDMA case, a noticeable but tolerable capacity loss in the uplink of the nearest ATC cell. Thus, the effects of downlink cochannel interference in both directions, and MSS-to-ATC uplink interference are modest overall, and appear to be manageable.

The main problem with cochannel MSS-ATC sharing is the effect of ATC interference to the MSS uplink. All ATC terminals within the MSS beam footprint contribute to that interference. The contribution of each ATC terminal depends on its transmit power (which may be subject to power control), and the excess attenuation in the propagation path from the ATC terminal to the spacecraft. This excess attenuation may be large (15 to 20 dB or more) for indoor ATC terminals, but relatively small for ATC terminals near the MSS-ATC coverage boundary; moreover, if outdoor ATC systems are systematically deployed to increase capacity, there could be many ATC terminals with low-blockage paths to the SC. While this might also be viewed as a “boundary” problem, the difference is that the ATC-to-MSS uplink interference is cumulative, affecting the uplinks for all MSS terminals in the beam, while the impacts of the other three interference cases are localized.

This problem can be reduced by arranging the frequency usage of MSS and ATC systems to eliminate cochannel operation of ATC systems and MSS beams with footprints covering the ATC systems. Globalstar terms this approach “dynamic frequency assignment” for the CDMA case. The basic concept is that ATC would be assigned a certain 1.25-MHz frequency uplink/downlink band pair (2.5 MHz total) in an area, and if the total ATC uplink EIRP within a beam footprint is excessive, the beam will not use the ATC frequency. The beam presumably would have other frequencies available, and other beams that do not span the ATC deployment can use the ATC frequency. The ATC uplink interference then becomes in-beam adjacent-channel interference to the covering beam, and out-of-beam cochannel interference to the adjacent non-covering beams. The interference effect is thereby reduced (but not eliminated).

It is incorrect to assume that eliminating cochannel in-beam ATC operation in this way will allow an unlimited number of ATC terminals to operate without affecting MSS capacity. It will not, for two reasons. First, the ATC terminal transmissions will still

affect the covering beam, due to adjacent channel interference, since the isolation between neighboring frequency channels is not perfect.¹⁰ Second, the ATC terminal transmissions will be captured (albeit with attenuation) by other beams, due to imperfect beam antenna pattern discrimination. Due to these factors, there still will be a limit on the total ATC uplink power radiated into the sky. The exact limit will depend on the allowable MSS capacity degradation, as well as the adjacent-channel isolation of the antenna beam pattern sidelobe (out-of-beam) gain suppression (the location of the ATC terminals relative to the beam antenna gain rolloff also plays a roll). While Globalstar has not disclosed these parameters, it does address the net effect, which is the allowable increase in the number of active ATC terminals within a beam:¹¹

In the forward band sharing operation, a fairly small number of “uncoordinated” ATC handsets (tens to hundreds) within a Globalstar satellite return link (L-band) beam can produce unacceptable interference to the MSS spacecraft receiver. However, when coordinated (i.e., the MSS operator is also operating the ATC service), the number of ATC handsets can be between 500 and 1000.

Globalstar does not include the assumptions or calculations that led to the result for dynamic frequency assignment. However, comparing this result with Globalstar’s calculations for the cochannel sharing case (p. 8 of the Globalstar analysis), it appears that the net effect of dynamic frequency assignment is to allow the ATC uplink EIRP to increase by roughly fourfold. Also, it seems likely that Globalstar’s numbers included the effect of a 15-dB excess attenuation (for indoor terminals); on page 8 of its analysis, Globalstar states:

A pessimistic estimate of the average loss due to these effects [shadowing and multipath] is 15 dB, a factor of 30. When this 15 dB is combined with free space loss, the resulting number of terrestrial terminals required to violate the threshold is between 30 and 270 depending upon the range of the terminals to the spacecraft.

Without this 15-dB additional loss factor, the range of 500 to 1000 becomes a range of 17 to 34 terminals.

The main point is that when satellite and terrestrial systems share spectrum, even with frequency coordination to avoid cochannel in-beam interference, there is still a fairly restrictive limit on the total power that ATC terminals within a given beam footprint can be permitted to radiate into the sky. From Globalstar’s most favorable analysis, that limit corresponds to a total of 1000 actively transmitting indoor terminals. As an example to put this limit into perspective, assume that the coverage area of a Globalstar beam is 785,400 km² as in the CDMA uplink analysis, and that the limit is a total of 1000 transmitting ATC terminals within that area. The limit then corresponds an average of a single active terminal every 785 square kilometers. There is no corresponding limit for

¹⁰ Adjacent channel interference arises from two sources: (1) out-of-band emissions from the adjacent channel; and (2) imperfect (non-rectangular) intermediate frequency (IF) filtering, the result of which is that some of the in-band power in adjacent channels is captured, and acts as interference.

¹¹ See [2], pp. 25-26, section 2.2.

spectrum used exclusively for terrestrial systems, in which case the total terminal usage is limited only by the number of cells deployed.

ICO provides a corresponding analysis for a TDMA/FDMA MSS system sharing spectrum with a CDMA ATC system, using a minimum C/I of 12.8 dB for the MSS system [3]. ICO calculates that with uplink cochannel interference from a single outdoor ATC terminal, the C/I at the SC would be 25.4 dB, so 18 such ATC terminals would reduce the C/I to its 12.8 dB threshold. Allowing average reduction factors of 2 dB for speech activity, 2 dB for power control, and 10 dB for indoor terminal blockage (10% of the terminals are outdoors and the others are totally blocked from the SC)¹², this translates the 18 outdoor, full-power transmitting ATC terminals to about 452 terminals per MSS beam per CDMA (1.25 MHz) frequency channel. ICO then assumes 10 CDMA channels, and 6 beams covering CONUS, which gives a total of about 27,120 active ATC terminals. Finally, ICO applies an activity factor of 25 mE per terminal (each terminal is used 2.5% of the time on average), yielding $27,120/0.025$ or about 1,085,000 terminals total.

ICO then reports that by properly arranging the 4-group frequency patterns used by the MSS beams in a way that minimizes the number of CDMA channels that overlap one or more frequencies from each group, a 50% improvement can be gained, raising the total number of allowable ATC terminals to about 1.6 million over CONUS, with 15 MHz of spectrum (in each direction – uplink and downlink, for a total of 30 MHz).

To relate the ICO and Globalstar results, it is necessary to remove the multipliers used by ICO, giving $18 \times 1.5 = 27$ actively transmitting outdoor terminals per beam. With the 15-dB attenuation apparently assumed by Globalstar ([2], p. 8), this becomes $30 \times 27 = 810$ indoor handsets per CDMA channel per beam, which (probably coincidentally) is within the range cited by Globalstar.

¹² ICO's calculations are based on the interference averaged over the variations in instantaneous interference due to speech activity, transmit power control, and indoor vs. outdoor ATC terminal location. ICO's assertions that an integrated MSS/ATC network can "make adjustments in real time" to accommodate changes in these factors does not seem credible. With power control, as assumed by ICO, transmit power varies to compensate for multipath fading. With a frequency of 2 GHz, the fade rate at a normal pedestrian speed (about 3 mph) is roughly 20 fades per second, so the ATC terminal transmit power will be changing quasi-periodically at this rate. Variations in transmit power due to speech activity are somewhat slower, occurring with cycle times on the order of seconds. Even so, from the perspective of a network management process, power fluctuations due to speech activity are rapid.

ICO's claim is that an integrated operator can make real-time adjustments to compensate for these variations in ATC terminal transmit power, but an independent ATC operator cannot, and therefore must allow for a margin to account for the variations in transmit power and blockage. However, it is unclear from ICO's discussion what mechanism would be used by the integrated operator to make the "real-time adjustments" to fast changes in ATC transmit power. Moreover, it is unclear what role these "real time adjustments" play in ICO's subsequent explanation regarding "Harmonization of Frequency Selection," which describes how ATC and MSS frequencies could be arranged to reduce interference. In sum, ICO has not justified its contention that an integrated MSS/ATC operator can design its network based on the average ATC terminal transmit power, without allowing any margin for statistical variations, whereas a separate operator must allow for a margin.

Although neither Globalstar nor ICO explain how the number of allowable ATC terminals per beam with frequency coordination is computed, it is clear from their results that the increase, compared to the cochannel sharing case, is fairly modest, and that even with coordination, there is still a very low limit on the amount of ATC uplink EIRP that can be tolerated by the MSS system.

What this means is that either with or without coordination, MSS systems can share spectrum with only very small deployments of terrestrial systems. However, to provide any significant terrestrial capacity, a separate frequency band is needed in which there is no limit on the total EIRP radiated into the sky by terrestrial terminals.

Spectrum Efficiency

The concept of “spectrum efficiency” is often discussed but seldom defined or analyzed in concrete terms. The purpose of this subsection is to discuss different ways in which spectrum efficiency can be quantified, and the relationship between MSS/ATC spectrum sharing and spectrum efficiency.

From the perspectives of frequency reuse and capacity, MSS systems are subject to the same basic principles as terrestrial wireless systems. To understand these principles, it is useful to introduce the following terms:

A	cell area, km^2
r_s	active subscriber density (per km^2)
R_s	data rate per subscriber (kbps)
r_R	throughput density (kbps/ km^2)
W	bandwidth per RF channel (MHz)
J	number of RF channels per direction (uplink/downlink)
$B = JW$	total bandwidth available per direction (MHz)
h_s	user cell efficiency (users/cell/MHz)
h_R	throughput cell efficiency (kbps/cell/MHz)

The efficiency terms h_s and h_R depend on the air interface used, and inter-cell interference. With basic frequency-division multiple access (FDMA) and time-division multiple access (TDMA) systems, inter-cell interference is controlled by the frequency reuse pattern, which determines the distance separation between cochannel cells. With CDMA, the same frequency channel pair can be used in every cell, and the inter-cell interference determines the per-cell capacity reduction. For terrestrial systems, these factors depend on how rapidly the received signal power decays with distance (i.e., the path loss exponent g). For MSS systems, the inter-cell interference is determined by the discrimination of the spacecraft antenna pattern and beam overlap. In either case, the density of active subscribers that can be served by the system is

$$\mathbf{r}_S = \frac{\mathbf{h}_S B}{A} \text{ active subscribers/km}^2 \quad (101)$$

Similarly, the throughput density is

$$\mathbf{r}_R = \frac{\mathbf{h}_R B}{A} \text{ kbps/km}^2 . \quad (102)$$

Clearly, $\mathbf{h}_S = \mathbf{h}_R / R_S$ so $\mathbf{r}_S = \mathbf{r}_R / R_S$. Whether (101) or (102) is the more useful depends on whether use of the system is predominantly speech, or a mix of speech and data.

Good measures of spectrum efficiency are the subscriber density per unit bandwidth ($\mathbf{r}_S / B = \mathbf{h}_S / A$ active subscribers/km²/MHz) and the throughput density per unit bandwidth ($\mathbf{r}_R / B = \mathbf{h}_R / A$ kbps/km²/MHz). For a given air interface, the spectrum efficiency is inversely proportional to the cell area. For MSS systems, the cells (beam footprints) cover a very large area compared to terrestrial cells, so the spectrum efficiency is very small compared to a terrestrial system with the same air interface and available bandwidth. This is the price paid for the large coverage afforded by MSS.

With MSS, the beam footprint area is determined by the beam antenna pattern and the position of the satellite relative to the earth, so shrinking cell size to increase capacity is not an option. At first, it might seem as though the addition of ATC offers the possibility of increasing total terminal density dramatically, because the ATC cell area is so much smaller than the MSS beam footprint. However, this is not the case, because the impact on MSS uplink capacity depends on the number of ATC terminals operating within the beam footprint, not the number of ATC terminals per ATC cell. Thus, with spectrum sharing, supportable ATC terminal density limits, and hence spectrum efficiency, are inversely proportional to the MSS beam footprint area, not the ATC cell area.

As has been shown, for a CDMA MSS system, the capacity degradation, relative to the stand-alone capacity, is proportional to the number of ATC terminals operating within the MSS beam footprint:

$$\frac{\Delta\Lambda}{\Lambda_0} = k_{CR} K_{ATC1} \quad (103)$$

where K_{ATC1} is the number of ATC handsets operating per beam on a single CDMA carrier pair, and k_{CR} is a capacity reduction factor, the value of which will depend on whether cochannel sharing or dynamic channel assignment is used. With cochannel sharing and 100-mW outdoor ATC handsets sharing spectrum with the Globalstar MSS system, $k_{CR} \cong 0.0125$ (1/80).

Continuing with the CDMA example, let \mathbf{h}_{MSS} represent the number of transmitting MSS terminals per beam per CDMA carrier pair that the MSS uplink can support in the absence of ATC. The stand-alone terminal density that the MSS uplink can support with a single CDMA carrier pair is:

$$\mathbf{r}_{0MSS,1} = \frac{\mathbf{h}_{MSS}}{A_{MSS}} \quad \text{subscriber s/km}^2 \quad (104)$$

where A_{MSS} is the area of the beam footprint. With J carrier pairs, the supportable terminal density is

$$\mathbf{r}_{0MSS,J} = J\mathbf{r}_{0MSS,1} \quad (105)$$

If there are $K_{ATC,j}$ ATC terminals transmitting on the j^{th} uplink carrier within the beam footprint, the capacity degradation to the MSS beam uplink on that carrier is

$$\Delta\mathbf{r}_{MSS,j} = \mathbf{r}_{0MSS,1}k_{CR}K_{ATC,j} \quad (106)$$

and the total capacity degradation for all J carriers is

$$\Delta\mathbf{r}_{MSS} = \sum_{j=1}^J \Delta\mathbf{r}_{MSS,j} = \mathbf{r}_{0MSS,1}k_{CR}K_{ATC} \quad (107)$$

where $K_{ATC} = \sum_{j=1}^J K_{ATC,j}$ is the total number of ATC terminals transmitting within the beam footprint.

The total MSS capacity for the J carriers is

$$\mathbf{r}_{MSS,J} = \mathbf{r}_{0MSS,J} - \Delta\mathbf{r}_{MSS} = \mathbf{r}_{0MSS,1}(J - k_{CR}K_{ATC}) \quad (108)$$

If $K_{ATC} = 1/k_{CR}$, then

$$\mathbf{r}_{MSS,J} = \mathbf{r}_{0MSS,1}(J - 1) = \mathbf{r}_{MSS,J-1} \quad (109)$$

and the ATC interference has reduced the MSS uplink capacity of the beam by the amount supported by a single carrier. At that point, spectrum efficiency can be improved by allocating a single carrier exclusively for ATC operation. The capacity of the MSS system is the same as it would be if J carriers are shared with the ATC system, and the capacity of the ATC system is freed from the limitation on the total number of transmitting terminals. The ATC system can then enjoy capacity that is limited only by the number and size of the ATC cells as with any terrestrial system. Overall, therefore, spectrum efficiency can be greatly increased by segmenting the spectrum.

It is therefore clear that spectrum sharing between MSS and ATC systems is not spectrum-efficient, compared to segmentation.

The fundamental reason is that with sharing, the allowable MSS and ATC terminal densities are both controlled by the very large area of the MSS beam footprint, whereas with segmentation, only the MSS terminal density depends on the beam footprint.

To see this quantitatively, the above relationships can be written in a different form:

$$\begin{aligned} \mathbf{r}_{MSS,J} &= \mathbf{r}_{0MSS,J} \left(1 - k_{CR} \frac{\mathbf{r}_{ATC} A_{MSS}}{J} \right), \\ &= \mathbf{r}_{0MSS,J} - \mathbf{h}_{MSS} k_{CR} \mathbf{r}_{ATC} \end{aligned} \quad (110)$$

which clearly shows the tradeoff between MSS and ATC terminal density (capacity). The total (MSS plus ATC) capacity is

$$\mathbf{r}_{TOT,J} = \mathbf{r}_{0MSS,J} + \mathbf{r}_{ATC} (1 - \mathbf{h}_{MSS} k_{CR}) \quad (111)$$

If $\mathbf{h}_{MSS} k_{CR} > 1$, then not only is MSS capacity reduced by the addition of ATC terminals, but total capacity is reduced as well.

With segmentation, \mathbf{r}_{MSS} is independent of \mathbf{r}_{ATC} :

$$\mathbf{r}_{TOT,J} = \mathbf{r}_{0MSS,J} + \mathbf{r}_{ATC}, \quad (112)$$

and \mathbf{r}_{ATC} can be very large relative to \mathbf{r}_{MSS} , because \mathbf{r}_{ATC} is no longer limited by A_{MSS} .

ATC/MSS Coexistence with CDMA: Conclusions

Summary of Results

Four interference cases have been considered here:

1. ATC terminals to MSS uplink
2. MSS terminals to ATC uplink
3. ATC base stations to MSS downlink
4. MSS spacecraft to ATC downlink

For cases 2, 3, and 4, effects are confined to areas near the MSS/ATC coverage boundaries. In case 2, the low spatial density of the MSS terminal relative to the size of the ATC cell results in a very low probability that there will be a significant impact on the capacity of the ATC uplink, if the MSS terminals are distributed randomly over the coverage area of a beam. In the downlink cases (3 and 4), the main issue for CDMA seems to be coverage, as determined by the available SINR of the overhead channels. As is shown here, it appears quite feasible to provide continuous coverage, perhaps with a mild (e.g., 2 dB) increase in the power allocation to the overhead channels for the outer cells of the ATC cluster. This will reduce the ATC downlink power available for traffic channels on the order of 15%, but any additional capacity reduction due to increases in the power allocation required by traffic channels will be confined to ATC terminals very near the inside of the cell boundary. For FDMA/TDMA, coverage is not an issue. Channels MSS or ATC terminals near a coverage boundary simply will not use channel that are in use by the other system. Overall, the ATC capacity reduction will be modest and will be largely (if not exclusively) confined to the outer cells of the cluster.

In case 1, the interference from ATC terminals to the MSS uplink is the sum of the power levels received from all ATC terminals within the MSS beam footprint. The location of the ATC terminal *per se* is unimportant, although ATC terminals operating in the interior of an ATC cell cluster may be blocked from the spacecraft, reducing the effect of their interference. As was shown, the capacity reduction to the MSS uplink depends directly on the total EIRP radiated by terrestrial terminals within the SC beam footprint. A relatively small number (tens) of unblocked ATC terminals within the beam can significantly degrade MSS uplink capacity. A large number of ATC terminals can be supported only if high blockage to the SC can be ensured.

In the case of a heavily-used ATC deployment that is not limited to areas shielded from the spacecraft, co-channel sharing does not seem feasible under any practical conditions. MSS operators have proposed coordinating MSS and ATC operations to eliminate cochannel operation of ATC systems within an SC beam. However, even with such measures, the total ATC terminal EIRP that can be tolerated by the MSS uplink is very limited. Widespread spectrum sharing between ATC and MSS therefore is not a technically sound solution, compared to operating the terrestrial systems on completely separate frequencies, with appropriate guard bands to control adjacent-channel interference.

Dynamic Coordination with Separate MSS and ATC Operators

In this section, mechanisms are explored to prevent the terrestrial system within an MSS beam footprint from using the same frequencies as the beam. By assumption, there will

typically be areas within ATC coverage that are also within range of MSS spacecraft. This offers the opportunity for the MSS and ATC systems to exchange control information directly over the radio link, and there are several different potential approaches.

One possibility is to use the ATC terminals themselves as conduits. Terminals that are idle (currently do not have an active connection) could periodically scan the frequencies that are not currently used by the ATC system. If an MSS signal is detected, the terminal would decode the control information and if appropriate, relay it to its ATC base station. To minimize battery drain on the terminals, the scanning could be done fairly infrequently. The scan cycles of different terminals would be randomized with respect to one another, so that at any given time, there would usually be one or more terminals searching for MSS signals. The control message header could include a flag indicating whether there is control information that needs to be relayed to the ATC base station. If the flag is cleared, the terminal can stop decoding the control channel (again, to conserve battery power). If the flag is set, the terminal requests a connection from its ATC base station and relays the control information. Upon receiving an acknowledgment from the base, the terminal ends the connection, and then signals the spacecraft on the MSS uplink frequency to confirm that the control information was successfully received by the ATC network. Upon receiving this confirmation, the MSS system clears the flag to prevent other ATC terminals from transmitting the same information to their respective bases.

A variation is to deploy “relay stations,” which would be modified terminals, specifically designed to perform the control relay function. These would be located in places with a clear path to the sky and to at least one ATC base station, and would be line- or solar-powered. Relay stations with multiple radios could provide 2-way communication directly between an ATC base and a spacecraft. This would support information exchange between the ATC and MSS system regarding traffic load, interference levels, etc. The relay station can also directly measure signal levels from the spacecraft and the ATC base, and may be useful in performing monitoring functions in addition to its relay role.

Finally, the control information can be conveyed to the ATC network in a more conventional manner, using landline facilities connecting the MSS network controller and the ATC network.

The control information itself would be a fairly small block of data instructing the ATC network on the frequencies available for ATC use in the near term. These instructions would be generated by the MSS system controller based on its knowledge of the ATC system coordinates, and of course its own spacecraft locations, trajectories, and beam frequency usage. With this approach, the frequency-use instructions to the ATC network are uniquely determined by MSS frequency usage, independent of the load on the ATC system. It is conceivable that an adaptive approach could be used, in which the spacecraft monitor the additional uplink load (effective noise floor increase) due to ATC terminals within each beam. If this load is sufficiently light, the MSS network may elect not to require the ATC system to change frequencies.

In sum, there seems to be no technical reason why spectrum-sharing MSS and ATC systems cannot be provided by separate operators. However, as shown in detail in this paper, MSS/ATC spectrum sharing is problematic and spectrally inefficient whether it is implemented by separate operators or an integrated operator.

Annex A: The Distribution of Combined Interference from Multiple Randomly-Distributed Transmitters

The Model

Assume a normalized distance scale such that the average density of interference sources transmitting within the band of interest at a given time is $1/p$ (interferers per normalized unit area). If the “victim” receiver is at the center of a circle of a normalized radius \sqrt{K} , the expected (average) number of interference sources within the circle is K . Assuming that interfering transmitters are randomly-distributed over area in a uniform fashion, the *actual* number of active interfering transmitters within the circle at a given time can be modeled as a Poisson-distributed random variable \mathbf{J} with discrete probability density function (pdf):

$$P_{\mathbf{J}}(k) = \Pr\{\mathbf{J} = k\} = \frac{e^{-K} K^k}{k!} \quad (1)$$

where the notation $\Pr\{\cdot\}$ represents the probability of the indicated event. The normalized power received at the base station from the k^{th} interfering transmitter a normalized distance s_k away from it is $z_k = s_k^{-g}$. The total power received from interfering transmitters within the circle of normalized radius \sqrt{K} is:

$$Z_K = \sum_{k=1}^J z_k \cdot \quad (2)$$

With interferers that are randomly distributed over area, the pdf of s_k is:

$$f_{s_k}(s) = \frac{2s}{K}, 0 \leq s \leq \sqrt{K}. \quad (3)$$

Hence, the pdf of z_j is:

$$f_{z_j}(z) = \frac{2}{gK} z^{-(g+2)/g}, \quad K^{-g/2} \leq z \leq \infty \quad (4)$$

The Characteristic Function of the Aggregate Interference

The characteristic function of Z_K is:

$$\Phi_{Z_k}(\mathbf{w}) = E[e^{j\mathbf{w}Z_k}] = \int_0^{\infty} f_{Z_k}(z)e^{j\mathbf{w}z} dz, \quad (5)$$

which is the Fourier transform of $f_{Z_k}(z)$. The lower limit is 0 rather than $-\infty$ in this case because Z_k represents power and therefore is non-negative.

Assuming the $\{z_k\}$ are independent and identically-distributed (i.i.d.), (2) and (5) yield:

$$\Phi_{Z_k}(\mathbf{w})|J = E\left[\exp\left(j\mathbf{w}\sum_{k=1}^J z_k\right)\right] = \left(E[e^{j\mathbf{w}z_k}]\right)^J. \quad (6)$$

Taking the expectation over J using (1) gives:

$$\Phi_{Z_k}(\mathbf{w}) = \sum_{n=0}^{\infty} \frac{e^{-K} K^n}{n!} [\Phi_{Z_k}(\mathbf{w})]^n = \exp\left\{K[\Phi_{Z_k}(\mathbf{w}) - 1]\right\}. \quad (7)$$

Thus, Z_k has a compound Poisson distribution [6]. Letting $\mathbf{n} = 2/\mathbf{g}$, (4) gives the characteristic function of z_k as:

$$\Phi_{z_k}(\mathbf{w}) = \int_0^{\infty} f_{z_k}(z)e^{j\mathbf{w}z} dz = \frac{2}{\mathbf{g}K} \int_{K^{-1/\mathbf{n}}}^{\infty} z^{-1-\mathbf{n}} e^{j\mathbf{w}z} dz. \quad (8)$$

The ‘‘second characteristic function’’ of Z_k is defined as the natural logarithm of the characteristic function [7]. Hence,

$$\Psi_{Z_k}(\mathbf{w}) = \ln \Phi_{Z_k}(\mathbf{w}) = K[\Phi_{Z_k}(\mathbf{w}) - 1] = \left(\mathbf{n} \int_{K^{-1/\mathbf{n}}}^{\infty} z^{-1-\mathbf{n}} e^{j\mathbf{w}z} dz\right) - K. \quad (9)$$

Integrating by parts and recalling that $\mathbf{Z} = \lim_{K \rightarrow \infty} \mathbf{Z}_K$ gives:¹³

$$\begin{aligned} \Psi_{\mathbf{Z}}(\mathbf{w}) &= \lim_{K \rightarrow \infty} \Psi_{Z_k}(\mathbf{w}) = j\mathbf{w} \int_0^{\infty} z^{-\mathbf{n}} e^{j\mathbf{w}z} dz \\ &= \begin{cases} -|\mathbf{w}|^{\mathbf{n}} \Gamma(1-\mathbf{n}) e^{-j\mathbf{p}\mathbf{n}/2}, & \mathbf{w} \geq 0 \\ -|\mathbf{w}|^{\mathbf{n}} \Gamma(1-\mathbf{n}) e^{j\mathbf{p}\mathbf{n}/2}, & \mathbf{w} < 0 \end{cases} \end{aligned} \quad (10)$$

where $\Gamma(\cdot)$ is the Gamma function [9].

¹³ See also [8], p. 10, §1.3, #1, and p. 68, §2.3, #1.

The PDF and CDF of the Aggregate Interference

The pdf of \mathbf{Z} is given by the Fourier inversion formula:

$$\begin{aligned} f_{\mathbf{Z}}(z) &= \frac{1}{2p} \int_{-\infty}^{\infty} \Phi_{\mathbf{Z}}(\mathbf{w}) e^{-j\mathbf{w}z} d\mathbf{w} = \frac{1}{2p} \int_{-\infty}^{\infty} e^{\Psi_{\mathbf{Z}}(\mathbf{w})} e^{-j\mathbf{w}z} d\mathbf{w} \\ &= \frac{1}{2p} \sum_{k=0}^{\infty} \int_{-\infty}^{\infty} \frac{[\Psi_{\mathbf{Z}_k}(\mathbf{w})]^k}{k!} e^{-j\mathbf{w}z} d\mathbf{w}. \end{aligned} \quad (11)$$

Letting $x = -\Gamma(1-n)e^{-jp\mathbf{n}/2} = \Gamma(1-n)e^{jp(1-n)/2}$, $\Psi_{\mathbf{Z}}(\mathbf{w}) = \mathbf{w}^n x$ for $\mathbf{w} \geq 0$, and $\Psi_{\mathbf{Z}}(\mathbf{w}) = -\mathbf{w}^n x^*$ for $\mathbf{w} < 0$ (where x^* denotes the complex conjugate of x), and (11) becomes:

$$f_{\mathbf{Z}}(z) = \frac{1}{2p} \sum_{k=0}^{\infty} \frac{1}{k!} \int_0^{\infty} \left[(\mathbf{w}^n x)^k e^{-j\mathbf{w}z} + (\mathbf{w}^n x^*)^k e^{j\mathbf{w}z} \right] d\mathbf{w} \quad (12)$$

The integrals $\int_0^{\infty} \mathbf{w}^{kn} e^{-j\mathbf{w}z} d\mathbf{w}$ and $\int_0^{\infty} \mathbf{w}^{kn} e^{j\mathbf{w}z} d\mathbf{w}$ can be evaluated using a form of Euler's integral for the Gamma function ([9], p. 255):

$$\Gamma(y) = \mathbf{x}^y \int_0^{\infty} \mathbf{w}^{y-1} e^{-\mathbf{w}\mathbf{x}} d\mathbf{w}, \quad \text{Re } y > 0, \quad \text{Re } \mathbf{x} > 0, \quad (13)$$

where $\text{Re}\{\cdot\}$ denotes the real part of the complex argument and the condition on \mathbf{x} is necessary to assure convergence of the integral.

Letting $\mathbf{x} = z - j\mathbf{e}$, where z and \mathbf{e} are real and positive, (13) gives:

$$\begin{aligned} \int_0^{\infty} \mathbf{w}^{kn} e^{-j\mathbf{w}z} d\mathbf{w} &= \lim_{\mathbf{e} \rightarrow 0} \int_0^{\infty} \mathbf{w}^{kn} e^{-j\mathbf{w}\mathbf{x}} d\mathbf{w} = \lim_{\mathbf{e} \rightarrow 0} \frac{\Gamma(k\mathbf{n} + 1)}{(j\mathbf{x})^{k\mathbf{n}+1}} \\ &= \frac{\Gamma(k\mathbf{n} + 1)}{(jz)^{k\mathbf{n}+1}} = \frac{\Gamma(k\mathbf{n} + 1)}{z^{k\mathbf{n}+1} e^{-jp(k\mathbf{n}+1)/2}}, \quad z > 0 \end{aligned} \quad (14a)$$

and

$$\begin{aligned} \int_0^{\infty} \mathbf{w}^{kn} e^{j\mathbf{w}z} d\mathbf{w} &= \lim_{\epsilon \rightarrow 0} \int_0^{\infty} \mathbf{w}^{kn} e^{-j\mathbf{w}x^*} d\mathbf{w} = \lim_{\epsilon \rightarrow 0} \frac{\Gamma(k\mathbf{n} + 1)}{(j\mathbf{x}^*)^{kn+1}} \\ &= \frac{\Gamma(k\mathbf{n} + 1)}{(-jz)^{kn+1}} = \frac{\Gamma(k\mathbf{n} + 1)}{z^{kn+1} e^{j\mathbf{p}(kn+1)/2}}, \quad z > 0 \end{aligned} \quad (14b)$$

Eq. (12) then becomes:

$$\begin{aligned} f_{\mathbf{z}}(z) &= \frac{1}{2\mathbf{p}} \sum_{k=0}^{\infty} \frac{\Gamma(k\mathbf{n} + 1)}{k! z^{kn+1}} \left[x^k e^{-j\mathbf{p}(kn+1)/2} + (x^*)^k e^{j\mathbf{p}(kn+1)/2} \right] \\ &= \frac{1}{\mathbf{p}} \sum_{k=0}^{\infty} \frac{\Gamma(k\mathbf{n} + 1) [\Gamma(1-\mathbf{n})]^k}{k! z^{kn+1}} \cos[k\mathbf{p}(1-\mathbf{n}/2) - \mathbf{p}(kn+1)/2] \\ &= \frac{1}{\mathbf{p}} \sum_{k=0}^{\infty} \frac{\Gamma(k\mathbf{n} + 1) [\Gamma(1-\mathbf{n})]^k}{k! z^{kn+1}} \sin k\mathbf{p}(1-\mathbf{n}), \quad z > 0. \end{aligned} \quad (15)$$

The argument of the sum vanishes for $k = 0$ and (15) can be written as:¹⁴

$$f_{\mathbf{z}}(z) = \frac{1}{\mathbf{p}z} \sum_{k=1}^{\infty} \frac{\Gamma(k\mathbf{n} + 1)}{k!} \left[\frac{\Gamma(1-\mathbf{n})}{z^{\mathbf{n}}} \right]^k \sin k\mathbf{p}(1-\mathbf{n}), \quad z > 0. \quad (16)$$

The CDF is then:

$$F_{\mathbf{z}}(z) = 1 - \int_z^{\infty} f_{\mathbf{z}}(\mathbf{x}) d\mathbf{x} = 1 - \frac{1}{\mathbf{p}} \sum_{k=1}^{\infty} \frac{\Gamma(k\mathbf{n})}{k!} \left[\frac{\Gamma(1-\mathbf{n})}{z^{\mathbf{n}}} \right]^k \sin k\mathbf{p}(1-\mathbf{n}), \quad z > 0. \quad (17)$$

For $z \gg 1$, the first term in the series dominates. Since $\Gamma(\mathbf{n})\Gamma(1-\mathbf{n}) = \mathbf{p} \csc(1-\mathbf{n})$,¹⁵

$F_{\mathbf{z}}(z) \cong 1 - z^{-\mathbf{v}}$ for $z \gg 1$.

Closed-Form Expressions for Fourth-Power Propagation

For the special case of $\mathbf{g} = 4$ ($\mathbf{n} = 1/2$), (16) and (17) can be reduced to closed form.¹⁶

Since $\sin k\mathbf{p}/2$ vanishes for even values of k , and $\Gamma(1/2) = \sqrt{\mathbf{p}}$, (16) becomes:

¹⁴ Expressions equivalent to (16) and (17) are given in [10]. However, the expression given in that paper for the CDF is incorrect and actually represents the complementary distribution.

¹⁵ [9], p. 256, 6.1.17.

¹⁶ This also is noted in [10].

$$f_z(z) = \frac{1}{\mathbf{p}z^{3/2}} \sum_{k=0}^{\infty} \frac{\Gamma(k+3/2)\mathbf{p}^{k+1/2}}{(2k+1)!z^k} (-1)^k, \quad \mathbf{g} = 4, \quad z > 0. \quad (18)$$

With the identity:¹⁷

$$\Gamma[2(k+1)] = \frac{\Gamma(k+1)\Gamma(k+3/2)2^{2k+3/2}}{\sqrt{2\mathbf{p}}} \quad (19)$$

and the fact that $\Gamma[2(k+1)] = \Gamma(2k+2) = (2k+1)!$, (19) yields:

$$\frac{\Gamma(k+3/2)}{(2k+1)!} = \frac{\sqrt{2\mathbf{p}}}{k!2^{2k+3/2}} = \frac{\sqrt{\mathbf{p}}}{2 \cdot k! \cdot 4^k}, \quad (20)$$

and (18) is seen to be:

$$f_z(z) = \frac{1}{2z^{-3/2}} \sum_{k=0}^{\infty} \frac{(-\mathbf{p}/4z)^k}{k!} = \frac{1}{2} z^{-3/2} e^{-\mathbf{p}/4z}, \quad \mathbf{g} = 4, \quad z > 0. \quad (21)$$

In a similar manner, (17) reduces for $\mathbf{g} = 4$ to:

$$F_z(z) = 1 - \frac{1}{\mathbf{p}} \sum_{k=0}^{\infty} \frac{\Gamma(k+1/2)\mathbf{p}^{k+1/2}}{(2k+1)!z^{k+1/2}} (-1)^k, \quad \mathbf{g} = 4, \quad z > 0. \quad (22)$$

With the identity:¹⁸

$$\Gamma(2k) = \frac{\Gamma(k)\Gamma(k+1/2)2^{2k-1/2}}{\sqrt{2\mathbf{p}}} \quad (23)$$

and with $(2k+1)! = (2k-1)! \cdot (2k+1) \cdot 2k$ and $\Gamma(2k) = (2k-1)!$,

$$\frac{\Gamma(k+1/2)}{(2k+1)!} = \frac{2\sqrt{\mathbf{p}}}{k!(2k+1)2^{2k+1}}. \quad (24)$$

Substituting (24) into (22) yields:

¹⁷ See [9], p. 256, 6.1.18.

¹⁸ *Id.*

$$\begin{aligned}
F_{\mathbf{Z}}(z) &= 1 - \frac{2}{\sqrt{\mathbf{p}}} \sum_{k=0}^{\infty} \frac{\mathbf{p}^{k+1/2}}{k!(2k+1)z^{k+1/2}} (-1)^k \\
&= 1 - \frac{2}{\sqrt{\mathbf{p}}} \sum_{k=0}^{\infty} \frac{(\sqrt{\mathbf{p}}/2\sqrt{z})^{2k+1}}{k!(2k+1)} (-1)^k \\
&= \operatorname{erfc}\left(\frac{\sqrt{\mathbf{p}}}{2\sqrt{z}}\right), \quad \mathbf{g} = 4
\end{aligned} \tag{25}$$

where $\operatorname{erfc}(\cdot)$ is the complementary error function, defined as:¹⁹

$$\operatorname{erfc}(x) = \frac{2}{\sqrt{\mathbf{p}}} \int_x^{\infty} e^{-x^2} d\mathbf{x} = 1 - \operatorname{erf}(x) \tag{26a}$$

and $\operatorname{erf}(\cdot)$ is the error function

$$\operatorname{erf}(x) = \frac{2}{\sqrt{\mathbf{p}}} \int_0^x e^{-x^2} d\mathbf{x} = \frac{2}{\sqrt{\mathbf{p}}} \sum_{k=0}^{\infty} \frac{x^{2k+1} (-1)^k}{k!(2k+1)}. \tag{26b}$$

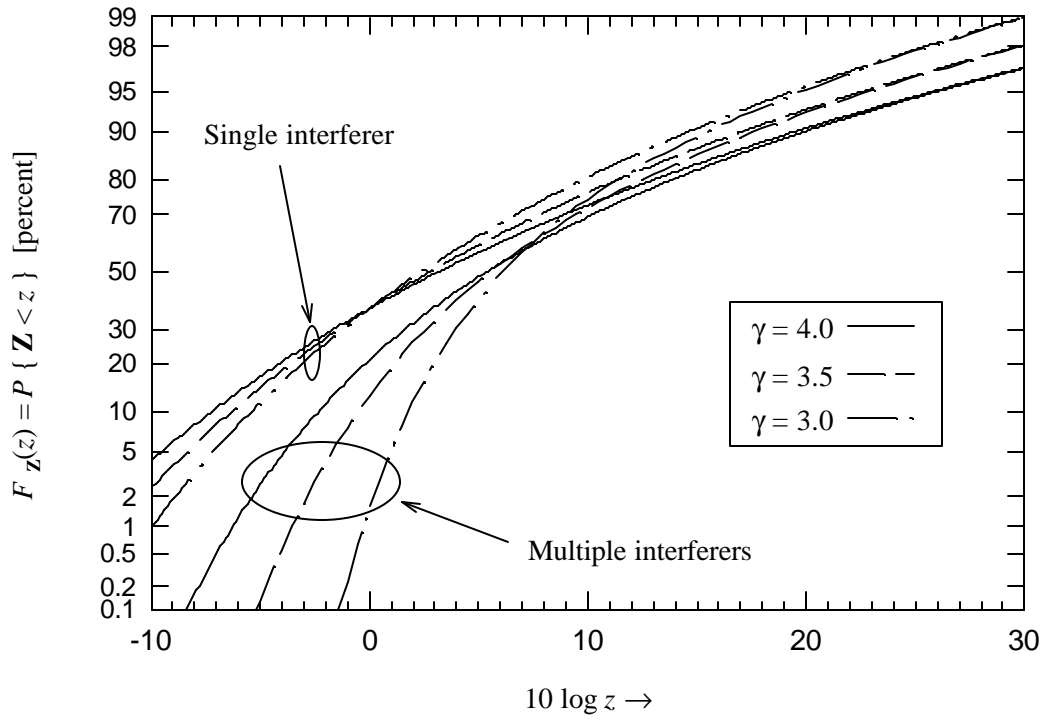
The Single-Interferer Case

In the context of this model, the CDF for the “single-interferer” case is easily derived by recalling that the average interference source density is $1/\mathbf{p}$ active transmitters per unit area, and the normalized interference power from a source a distance s from the receiver is $s^{-\mathbf{g}}$. Since the number of active transmitters within (normalized) distance s of the receiver is a Poisson-distributed random variable with mean value s^2 , the probability that there are *no* active transmitters within that distance of the receiver is e^{-s^2} . Thus, since the normalized interference from a single source at a distance s is $Z = s^{-\mathbf{g}}$, the probability $\Pr\{\mathbf{Z} < z\}$ for the “single-interferer” case is equal to the probability that there are no interfering transmitters within distance $s = z^{-1/\mathbf{g}}$ of the receiver. Hence, for the single-interferer case,

$$F_{\mathbf{Z}}(z) = \exp(-z^{-2/\mathbf{g}}), \quad z \geq 0 \tag{27}$$

The figure below shows $F_{\mathbf{Z}}(z)$ for $\mathbf{g} = 3.0, 3.5,$ and 4.0 , for both the multiple-interferer and single-interferer cases.

¹⁹ See [9], chapter 7.



Annex B: Computation of Downlink Other-Cell Interference for a Terrestrial Cell Cluster

This Annex describes a compact algorithm for generating CDMA downlink other-cell interference. All cells are assumed to be hexagonal, as shown in Figure B-1. Also shown are conventional x - y coordinates along with the directions of the i - j shift indices.

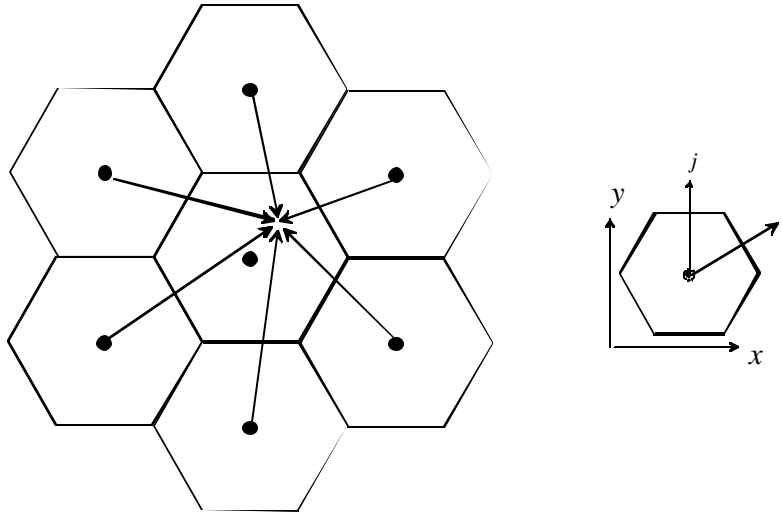


Figure B-1: *Geometry and coordinates for other-cell interference calculation.*

The origin is assumed to be the center of the cell hosting the mobile for which the other-cell interference is to be computed. The indices (i, j) designate the locations of the base stations arranged in a hexagonal grid. As explained in [5], the distance between the origin and a base station at (i, j) is $\sqrt{3} \cdot r \cdot \sqrt{i^2 + ij + j^2}$.

The Cartesian coordinates of a site at (i, j) are:

$$\begin{aligned} x &= i \cdot 3r/2 \\ y &= (i/2 + j) \cdot r\sqrt{3} \end{aligned} \quad (\text{B-1})$$

In polar coordinates, the azimuth angle (where the x -axis represents 0° azimuth) is:

$$\mathbf{q} = \tan^{-1} \frac{1}{\sqrt{3}} \left(1 + 2 \frac{j}{i} \right) \quad (\text{B-2})$$

Cells surrounding the center cell can be grouped in “tiers”. Cells in the first tier all adjoin the center cell. Second-tier cells adjoin the first tier cells, etc. If L is the tier index, then

in the first quadrant of the i - j coordinate system, $i + j = L$. Also, there are $6L$ cells in tier L . Figure shows how the cells are indexed, for selected cells in the first two tiers.

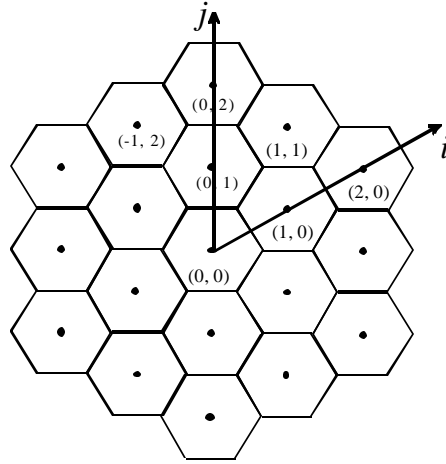


Figure B-2: Other cell indexing and tier structure

Consider the L cells within the first quadrant of the i - j coordinate system, excluding those along the j -axis. The i - j indices of those cells are (i_n, j_n) where $i_n = L - n$ and $j_n = n$, $0 \leq n \leq L - 1$; that is, $(L, 0), (L - 1, 0), \dots, (1, L - 1)$. For each element of this first group, its distance d_n and azimuth angle \mathbf{q}_n are computed from (B-1) and (B-2). By hexagonal symmetry, each element in this group has five images with azimuth angles $\{\mathbf{q}_n + m\mathbf{p}/3\}$, $1 \leq m \leq 5$. Thus, the entire tier can be constructed by adding $m\mathbf{p}/3$ to the $\{\mathbf{q}_n\}$ for each first-quadrant group member, where m runs from 1 to 5.

The Cartesian coordinates for each base station therefore are

$$\begin{aligned} x_{n,m} &= d_n \cos(\mathbf{q}_n + m\mathbf{p}/3) \\ y_{n,m} &= d_n \sin(\mathbf{q}_n + m\mathbf{p}/3) \end{aligned} \quad 0 \leq n \leq L - 1, \quad 0 \leq m \leq 5 \quad (\text{B-3})$$

If a target mobile has Cartesian coordinates (x, y) , then the total other-cell interference is

$$I_{oc}(x, y) = s_{tgt} \sum_{L=1}^{L_{\max}} \sum_{n=1}^L \sum_{m=0}^5 s_{n,m} \left[(x_{n,m} - x)^2 + (y_{n,m} - y)^2 \right]^{-g/2} \quad (\text{B-4})$$

where g is the path loss exponent and L_{\max} is the highest tier considered in the calculation. In practice, tiers beyond the second contribute little to the total other-cell interference. The $\{s_{n,m}\}$ are independent random variables which represent the effects of shadow fading, typically modeled as lognormal, and s_{tgt} represents shadow fading effect common to the paths from all base stations (local shadowing of the mobile). This approach (dividing shadow fading into a common component and a source-dependent component) is the same as is used in [11].

Figures B-3 and B-4 show the other-cell interference vs. azimuth angle for $d/r = 0.4$ and 0.8 , respectively. These parameters were selected specifically for comparison with Figs. 10.3 and 10.4 of [12] (p. 1010). The azimuth angle is offset by 30° because the cells in [12] are rotated 30° with respect to the orientation used here. The curves agree with those in [12], supporting confidence in the algorithm used here to calculate the other-cell interference.

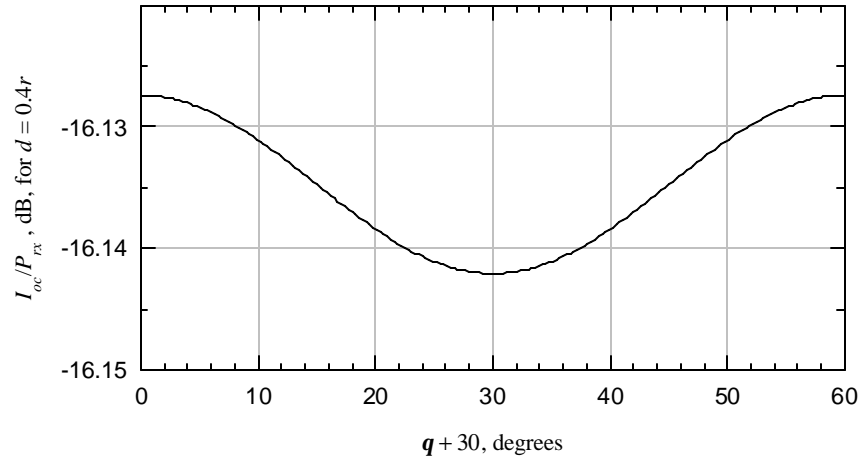


Figure B-3: Other-cell forward link interference vs. azimuth angle at a distance of $0.4r$.

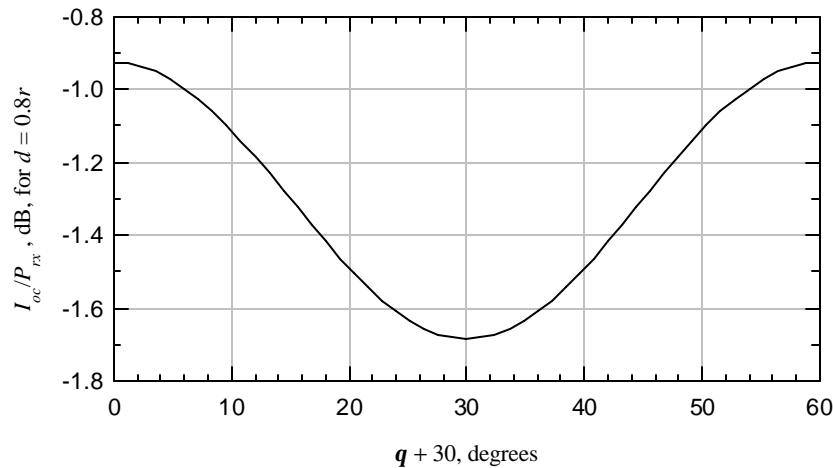


Figure B-4: Other-cell forward link interference vs. azimuth angle at a distance of $0.8r$.

The in-cell downlink power is $P_{rx}(d) = d^{-g} = (x^2 + y^2)^{-g/2}$, so the average needed for the capacity calculations is:

$$\left\langle \frac{I_{oc}}{P_{rx}} \right\rangle = \left\langle (x^2 + y^2)^{g/2} I_{oc}(x, y) \right\rangle, \quad (\text{B-5})$$

where the $\{x, y\}$ are selected to be uniformly-distributed over the area of a cell sector.

References

- [1] Federal Communications Commission, DA 02-554, released March 6, 2002; IB Docket No. 01-185; ET Docket No. 95-18.
- [2] Globalstar, "Technical Comments on Certain Proposals to Permit Flexibility in the Delivery of Communications by Mobile Satellite Service Providers in L-Band, the 2 GHz Band and the 1.6/2.4 GHz Bands," Attachment to Globalstar's "Response to FCC Public Notice DA 02-254, IB Docket No. 01-185 and ET Docket No. 95-18, March 22, 2002.
- [3] Comments of New ICO Global Communications, IB Docket No. 01-185, ET Docket No. 95-18, October, 2001.
- [4] E. C. Jordan and K. G. Balmain, *Electromagnetic Waves and Radiating Systems*, second edition, Prentice-Hall, 1968.
- [5] V. H. McDonald, "The Cellular Concept," *Bell Sys. Tech. J.*, Jan. 1979, pp. 15-40.
- [6] William Feller, *An Introduction to Probability Theory and Its Applications*, second ed., vol. II, New York: Wiley, 1971.
- [7] A. Papoulis, *Probability, Random Variables, and Stochastic Processes*, New York: McGraw-Hill, 1965.
- [8] A. Erdelyi, *et al*, *Tables of Integral Transforms*, vol. 1, New York: McGraw-Hill, 1954.
- [9] M. Abramowitz and I. E. Stegun, *Handbook of Mathematical Functions*, U. S. Department of Commerce, National Bureau of Standards, ninth printing, Nov. 1970.
- [10] E. S. Sousa and J. A. Silvester in "Optimum Transmission Ranges in a Direct-Sequence Spread-Spectrum Multihop Packet Radio Network," *IEEE J. Selected Areas Commun.*, vol. 8, no. 5, June 1990, pp. 762-771.
- [11] Andrew J. Viterbi, *CDMA – Principles of Spread Spectrum Communication*, Addison-Wesley, Reading, MA, 1995.
- [12] J. S. Lee and L. E. Miller, *CDMA Systems Engineering Handbook*, Artech House, Boston, MA, 1998.